

**A STUDY OF THE THERMAL AGEING OF CARBOXYLATED NITRILE
RUBBER LATEX THIN FILMS**

FOO YIAN TYAN

MASTER OF SCIENCE

**FACULTY OF SCIENCE
UNIVERSITI TUNKU ABDUL RAHMAN
AUGUST 2013**

**A STUDY OF THE THERMAL AGEING OF CARBOXYLATED NITRILE
RUBBER LATEX THIN FILMS**

By

FOO YIAN TYAN

A dissertation submitted to the Department of Chemical Science,

Faculty of Science,

Universiti Tunku Abdul Rahman,

in partial fulfilment of the requirements for the degree of

Master of Science

August 2013

ABSTRACT

A Study of Thermal Ageing of Carboxylated Nitrile Rubber Latex Thin Films

Foo Yian Tyan

Properties of rubbers are subject to change as a result of ageing, even during storage or during the use of rubber products. Ageing is an irreversible process, leading to a deterioration of their properties such as reduction of the tensile strength, elasticity and elongation, wear resistance, changing plasticity, and increase hardness of the rubber, eventually to the point where the material is no longer capable of fulfilling its function. Therefore, increase the resistance of rubber to ageing is of great importance for increase the reliability and performance of rubber products. In this study, the effect of accelerated ageing on the physical changes as well as the morphology changes of Carboxylated nitrile rubber (XNBR) thin film were investigated at temperature range between 60 °C and 100 °C and for times between 0.5 hours to 3360 hours. Results shown that accelerated ageing reduce the tensile strength and swelling properties of the XNBR thin film. At the end of ageing, XNBR turned to yellowish colour and the changes become more pronounce at higher temperature. Cracks are gradually observed under Scanning Electron Microscopy (SEM) as ageing in progress. On the other hand, real time ageing carried out under florescent light and in dark condition. In order to correlate accelerated ageing to real-time ageing and predict its shelf life, Arrhenius and

Time-Temperature approaches were applied. Both approaches gave a similar reading where the time estimated for the physical properties to fall to 75% retained force at break is 27 years at 25 °C for both approaches and the activation energy calculated were 81.91 kJ/mol and 81.94 kJ/mol respectively. To develop a better understanding of the chemical changes in XNBR ageing, characterization of the XNBR thin film with and without antioxidant after accelerated ageing using Fourier Transform Infrared Spectroscopy (FTIR) had been carried out. FTIR study shown that thermal oxidation of XNBR mostly generates hydroxyl and carbonyl related species.

ACKNOWLEDGEMENTS

I would like to take this opportunity to sincere gratitude to Dr. Mohammad Aminuzzaman and Dr. Chee Swee Yong for serving as the supervisor and co-supervisor throughout this research project, and for their observations regarding my work and for also providing me valuable suggestions with the insights and guidance to recognize my mistakes. I would also like to thank them for giving me adequate freedom and flexibility throughout the experimental and thesis works which have contributed to the success of this research.

I would also like to express my appreciation to the Synthomer Sdn. Bhd. for the project funding and offering scholarship for my study. I would like to express my gratitude to Mr. Tong Heam Keat and Ms. Masuzi for their supportive and warm help for this project and for sharing valuable knowledge and cooperation.

I thank to laboratory assistants, Mr. Nickolas Ooi, and other laboratory assistants for their supportive and warm help for this project.

Finally, and most of all, I would like to thank my parents and all my friends for their eternal support, love, and encouragement.

FACULTY OF SCIENCE

UNIVERSITI TUNKE ABDUL RAHMAN

Date: _____

SUBMISSION OF THESIS

It is hereby certified that **FOO YIAN TYAN** (ID No: **11ADM01677**) has completed this thesis/dissertation entitled “**A STUDY OF THERMAL AGEING OF CARBOXYLATED NITRILE RUBBER LATEX THIN FILMS**” under supervision of Assistant Prof. Dr. Mohammod Aminuzzaman (Supervisor) from the Department Chemical Science, Faculty of Science, and Assistant Prof. Dr. Chee Swee Yong (Co-Supervisor) from the Department Chemical Science, Faculty of Science.

I understand that the University will upload softcopy of my thesis/dissertation in pdf format into UTAR Institutional Repository, which may be made accessible to UTAR community and public.

Yours truly,

(**FOO YIAN TYAN**)

APPROVAL SHEET

This dissertation/thesis entitled “**A STUDY OF THERMAL AGEING OF CARBOXYLATED NITRILE RUBBER LATEX THIN FILMS**” was prepared by **FOO YIAN TYAN** and submitted as partial fulfillment of the requirements for the degree of Master of Science at Universiti Tunku Abdul Rahman.

Approved by:

(Assistant Prof. Dr. Mohammad Aminuzzaman)
Supervisor
Department of Chemical Science
Faculty of Science
Universiti Tunku Abdul Rahman

Date:.....

(Assistant Prof. Dr. Chee Swee Yong)
Co-Supervisor
Department of Chemical Science
Faculty of Science
Universiti Tunku Abdul Rahman

Date:.....

DECLARATION

I _____ hereby declare that the thesis/dissertation is based on my original work except for quotations and citations which have been duly acknowledged. I also declare that it has not been previously or concurrently submitted for any other degree at UTAR or other institutions.

(FOO YIAN TYAN)

Date:

LIST OF TABLES

Table		Page
2.1	Types of degradation agents.	24
3.1	Accelerated ageing temperature and time.	59
4.1	Time required to reach the threshold of 75% retained force.	88
4.2	Time required to reach the threshold of 70%, 75% and 80% retained force at break.	90
4.3	Arrhenius shift factor (α_T) for a reference temperature at 60 °C.	94
4.4	Arrhenius shift factor (α_T) for a reference temperature at 25 °C.	96
4.5	Lifetime and activation energies prediction according to various approach and assumption.	98
4.6	FTIR peaks assignment of XNBR latex thin film.	101

LIST OF FIGURES

Figure		Page
1.1	Vulcanized rubber in stretch and relax mode (Gupta 2010b).	3
1.2	Structure of NBR.	7
1.3	Structure of HNBR.	8
1.4	Structure of XNBR.	10
2.1.	Effects of physical ageing on polymeric materials. Top: relaxation of oriented macromolecules. Bottom: post-crystallization (Ehrenstein 2001).	20
2.2.	Effects of chemical ageing (heat and/or oxygen) on polymeric materials (Ehrenstein 2001).	21
2.3.	Random thermal degradation mechanism of poly(ethylene terephthalate).	40
2.4.	Mechanism for polymer oxidation (RH = polymer hydrocarbon).	43
2.5.	Estimating the time to reach a specified threshold. X: Time in days; Y: Initial force at break in %. 1 : 75% threshold; 2: Time to reach threshold in 60 °C.	49
2.6.	Arrhenius plot for force at break assuming a threshold of 75%. Y: $\ln t_{(75\%)}$ in years; X: $1/T$ in K^{-1} . 1: Extrapolation to 25 °C; $y = 17071x - 47.71$; $R^2 = 0.9987$.	51
2.7.	Time-temperature superposition plot. Y: Retained force at break in %. X: Time at 25 °C in years.	53
2.8.	Examples of common antioxidants: a: 2,6- <i>t</i> -butyl 4-methyl phenol (butylated hydroxy toluene); b: diphenyl- <i>p</i> -phenylene diamine.	56
3.1.	Photograph of XNBR glove sample.	58
3.2.	Photograph of tensile strength measurement.	60

3.3.	Photographs of the measurement of the diameter of the disc in solvent swell test.	61
3.4.	Chromaticity coordinates of L*, a* and b*.	63
3.5.	Photograph of the thin film sample coated with platinum.	63
3.6.	Photograph of XNBR Latex Thin Film.	65
4.1.	Changes in the relative tensile strength of XNBR thin film as a function of ageing time at various temperatures.	72
4.2.	Changes in the relative elongation at maximum of XNBR thin film as a function of ageing time at various temperatures.	73
4.3.	Changes in the relative linear swell of XNBR thin film as a function of ageing time at various temperatures.	75
4.4.	Changes in the relative total colour change (ΔE) of XNBR thin film as a function of ageing time at various temperatures.	77
4.5.	SEM images for unaged sample (a), aged at 60 °C for 1344 (b) and 3360 hours (c), aged at 70 °C for 1680 (d) and 3024 hours (e), aged at 80 °C for 1008 (f) and 1680 hours (g), aged at 90 °C for 336 (h) and 504 hours (i) and aged at 100 °C for 96 (j) and 168 hours (k).	79
4.6.	Changes in the relative tensile strength of XNBR thin film as a function of ageing time for real time ageing.	81
4.7.	Changes in the relative elongation at maximum of XNBR thin film as a function of ageing time for real time ageing.	81
4.8.	Changes in the relative linear swell of XNBR thin film as a function of ageing time for real time ageing.	82
4.9.	Changes in relative total colour change (ΔE) of XNBR thin film as a function of ageing time for real time ageing.	83

4.10.	SEM images for real time ageing under fluorescent light for 1 month (a), 3 months (b), 9 months (c) and 15 months (d) and in dark condition for 1 month (e), 3 months (f), 9 months (g) and 15 months (h).	84
4.11.	Variation of relative force at break of XNBR thin film with ageing time at various ageing temperatures.	87
4.12.	Arrhenius plot of retained force at break at 75% for XNBR thin film.	89
4.13.	Arrhenius plot of retained force at break at 70%, 75% and 80% for XNBR thin film.	91
4.14.	Arrhenius plot using empirical shift factor concept.	94
4.15.	Mastercurve for relative force at break against ageing time for XNBR thin film at reference temperature of 60 °C.	95
4.16.	Mastercurve for relative force at break against ageing time for XNBR thin film at reference temperature of 25 °C.	97
4.17.	Changes of IR spectra of XNBR thin film with antioxidant aged at 70 °C (a) combined spectra and (b) split spectra.	102
4.18.	Changes of IR spectra of XNBR thin film without antioxidant aged at 70 °C (a) combined spectra and (b) split spectra.	103
4.19.	Changes of IR spectra of XNBR thin film with antioxidant aged at 90 °C (a) combined spectra and (b) split spectra.	104
4.20.	Changes of IR spectra of XNBR thin film without antioxidant aged at 90 °C (a) combined spectra and (b) split spectra.	105
4.21.	Structure of grafted butadiene.	115
4.22.	Demonstrated reaction mechanism of intermediate product and final by-product conversion pathway of XNBR under thermal-oxidation.	117

LIST OF ABBREVIATIONS

α_T	shift factors
(ΔE)	total colour changes
A	material constant
a*	chromaticity coordinates for green-red shift
Al ₂ O ₃	aluminium (III) oxide
b*	chromaticity coordinates for blue-yellow shift
C	constant
Co	cobalt
Cr	chromium
E_a	activation energy
EPDM	ethylene propylene terpolymer rubber
Fe	ferrum
FTIR	fourier transform infrared
HNBR	hydrogenated nitrile rubber
IIR	isobutylene isoprene copolymer
Kcal/mol	kilocalorie per mole
kJ/mol	kilojoule per mole
$k(T)$	reaction rate constant
kV	kilovolt
L*	chromaticity coordinates for white-black shift
mm	millimeter
Mo	molybdenum
NBR	nitrile butadiene rubber
nPbO.PbSO ₄ .H ₂ O	poly-basic lead sulfates
Ni	nickel
NR	natural rubber
PA	polyamide
PE	polyethylene
PES	polyester
PMMA	poly(methylmethacrylate)
PO	polyolefins (po)
PS	polystyrene
Pt	platinum
PU	polyurethane
PVC	polyvinyl chloride
P α MS	poly(α -methylstyrene)
R	universal gas constant

$\text{RSn}(\text{SnR}')_3$	organo-tin mercaptide
SBR	styrene butadiene rubber
SEM	scanning electron microscopy
SiO_2	silicon dioxide
(T_g)	glass transition temperature
TiO_2	titanium dioxide
T	absolute temperature in kelvin.
t_{aged}	ageing time at reference temperature, t_{aged}
t_{ref}	ageing time at reference temperature, t_{ref}
$t_{(x\%)}$	time for the property to fall to $x\%$ of the initial value
UV	ultraviolet
XNBR	carboxylated nitrile rubber

TABLE OF CONTENTS

	Page
ABSTRACT	ii
ACKNOWLEDGEMENTS	iv
PERMISSION SHEET	v
APPROVAL SHEET	vi
DECLARATION	vii
LIST OF TABLES	viii
LIST OF FIGURES	ix
LIST OF ABBREVIATIONS	xii
CHAPTER	
1. INTRODUCTION	1
1.1. Concept of elastomer	1
1.2. Uniqueness of rubber	1
1.3. Synthetic rubber	3
1.3.1. Origin	3
1.3.2. Manufacture of synthetic rubber	4
1.3.3. Applications	5
1.3.4. NBR	6
1.3.5. HNBR	8
1.3.6. XNBR	9
1.4. Natural rubber latex and synthetic rubber latex in glove manufacture	11
1.5. Scope	12
1.6. Objective of study	15

2. LITERATURE REVIEW	16
2.1. Polymer, latex, Elastomer	16
2.2. Degradation and ageing of polymer	18
2.3. Factors affecting polymer degradation	22
2.3.1. Natural degradation agent	23
2.3.1.1. Temperature	25
2.3.1.2. Ultraviolet light	25
2.3.1.3. Ionizing radiation	26
2.3.1.4. Moisture	26
2.3.1.5. Fluids	27
2.3.1.6. Mechanical stress and electrical stress	27
2.3.1.7. Microbiological attack	28
2.3.2. Nature of polymer	29
2.3.2.1. Chemical composition	29
2.3.2.2. Polymer structure	30
2.3.2.3. Molecular weight	30
2.3.2.4. Incorporation of functional groups	31
2.3.2.5. Additives	31
2.3.2.6. Chemical bonding	32
2.3.2.7. Methods of synthesis	32
2.3.2.8. Effect of substituents	33
2.4. Types of polymer degradation	34
2.5. Thermal and thermal oxidative degradation	38
2.6. Lifetime prediction	45
2.6.1. Basic methodology	46
2.6.2. Arrhenius model for lifetime prediction	47
2.6.3. Time-temperature superposition model for lifetime prediction	51
2.7. Protection and prevention degradation	54
2.7.1. Chemical and thermal stabilizers	55
2.7.2. Ultraviolet radiation stabilizers	57

3. METHODOLOGY	58
3.1. Materials	58
3.2. Method for accelerated ageing and testing	59
3.2.1. Accelerate treatment	59
3.2.2. Tensile test	60
3.2.3. Solvent swell test	61
3.2.4. Colour test	62
3.2.5. Scanning electron microscopy (SEM)	63
3.3. Method for real time ageing	64
3.4. Mechanism study	64
3.4.1. Thin film casting	64
3.4.2. Accelerated ageing of thin film	65
3.4.3. Fourier transform infrared (FTIR) characterization	65
3.5. Lifetime prediction	66
4. RESULTS AND DISCUSSION	67
4.1. Accelerated ageing and real time ageing	67
4.1.1. Accelerated ageing	68
4.1.1.1. Tensile test	68
4.1.1.2. Solvent swell test	74
4.1.1.3. Colour measurement	76
4.1.1.4. Scanning Electron Microscopy (SEM)	78
4.1.2. Real time ageing	80
4.1.2.1. Tensile test	80
4.1.2.2. Solvent swell test	82
4.1.2.3. Colour measurement	83
4.1.2.4. Scanning Electron Microscopy (SEM)	84
4.2. Lifetime prediction	85
4.2.1. Application of the Arrhenius equation predict shelf life	85
4.2.2. Application of the time-temperature superposition method to predict shelf life	91

4.2.3. Comparison of lifetime and activation energies according to different shelf life prediction approach	98
4.3. Degradation mechanism study of XNBR	99
5. CONCLUSION	118
REFERENCES	121
APPENDIXES	134

CHAPTER 1

INTRODUCTION

1.1 Concept of elastomer

“Elastomer”, is usually used as general term for the group of polymers with some common characteristics, such as high elasticity, viscoelasticity and glass transition temperature (T_g) far below room temperature. The term is derived from elastic polymer. According to White and De (2001), the term ‘elastomer’ describes a material that exhibits quick and forcible recovery of most of its original dimensions after extension or compression and can be vulcanized. In general, rubber might be called elastomer since high elasticity is its most outstanding feature. Nevertheless, elastomer cannot be regarded as the same as that of rubber in the narrow sense, because the former refers to all the polymeric materials with high elasticity including rubber. However, by usage, it is generally admitted in a broad sense that the term “rubber” refers to elastomer (Zhang 2004).

1.2 Uniqueness of rubber

Of all the polymeric materials, rubbers are unique. In most applications for rubber products there are no alternative materials. Rubber is both elastic and viscous. It is soft with high extensible and highly elastic, which consist of relatively long polymeric chains with high molecular mass molecules that joined

into a three-dimensional network structure (Loadman 1998; Gent 2001). Vulcanization forms chemical bonds between adjacent elastomer chains and subsequently imparts dimensional stability, strength, and resilience (White and De 2001; Gupta 2010b). An unvulcanized rubber lacks structural integrity and will “flow” over a period of time.

According to Schaefer (2002), rubber has a low modulus of elasticity and is capable of sustaining a deformation of as much as 1000 per cent. As a result of an externally imposed stress, the long chains may alter their configurations, an adjustment which takes place relatively rapid because of the high chain mobility. The requirement of having the chains linked into a network structure is associated with solid like features, where the chains are prevented from flowing relative to each other under external stresses. Once the external force was removed, it rapidly recovers its original dimensions, with essentially no residual or non-recoverable strain (Erman and Mark 2005). Fig. 1.1 shows the vulcanized rubber that behaves like a spring which does not undergo a permanent change when stretched, but spring back to original shape and size after the stress is removed. Rubber is resilient and yet exhibits internal damping. As a result of these unique mechanical properties, rubber can be processed into a variety of shapes and can be adhered to metal inserts or mounting plates. It can be compounded to give widely varying properties and this has permitted the development of a huge family of materials with a wide range of properties. Rubber will not corrode and normally requires no lubrication (Schaefer 2002).

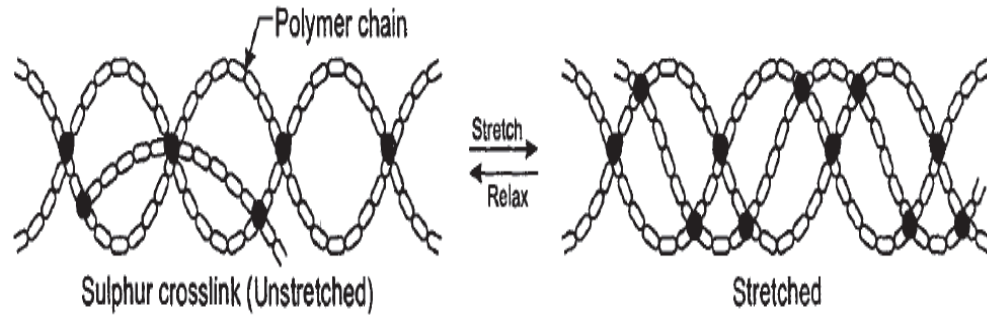


Figure 1.1: Vulcanized rubber in stretch and relax mode (Gupta 2010b).

1.3 Synthetic rubber

1.3.1 Origin

In 1927, Reimer and Tiemaun published their work on amino acids and in a short period this opened an entirely new vista for process industries (Chandrasekaran 2009). Polymer technology became a new study and research work in these avenues yielded a wide range of new materials. Chemists were actively searching for rubbery materials which could be manufactured artificially. Kuzma noted that the Russians, in 1910, prepared such a rubber, known chemically as polybutadiene. In the 1930s, the Germans began the commercial production of a synthetic rubber called Buna-S (styrene butadiene rubber), later known as SBR, which is the major material in the rubber industry today (Ciesielski 2001).

The development of polychlorobutadiene, a wholly new synthetic rubber, was announced by DuPont in 1931; it was given the name Duprene, later changed

to Neoprene (Morawets 2002; Morris 2005). Since 1934 in Germany, an oil resistant rubber called Buna-N was marketed by I.G. Farbenindustries and later as Perbunan. Its generic name is known as nitrile rubber (NBR, nitrile butadiene rubber) (White, 1995). Later in the 1940s, Butyl rubber (IIR, isobutylene isoprene copolymer) was developed, as well as Hypalon (CSM, chlorosulphonated polyethylene) and Viton (FKM, fluoroelastomer) by DuPont (now DuPont Dow Elastomers) in the 1950s and ethylene propylene terpolymer rubber (EPDM) in the 1960s (Ciesielski 2001).

The rubber that started it all, NR, has survived the onslaught of the synthetic rubbers exceptionally well and today still represents nearly one-third of all rubber in the world marketplace (Ciesielski 2001). The new awareness of our environment gives NR the added advantage of being seen as a renewable resource, because most synthetic elastomers are derived from petroleum oil based starting materials.

1.3.2 Manufacture of synthetic rubber

From the 20th century, scientists have been trying to synthesize the materials whose properties could match the NR. This has led to the production of a wide variety of synthetic elastomers. In order to produce polymer it is, of course, necessary to find ways in which small molecules, known as monomers may join together in large numbers. This process is known as polymerization (Deanin and Mead 2007); there are a number of techniques in which polymerization can be

realized, but these can all be classed under the following two main types: chain reaction polymerization and step reaction polymerization (Sperling 2006; Deanin and Mead 2007; Gupta 2010b; McMurry 2011). The simplest examples of chain reaction polymerization are the formation of polyethylene (PE) from ethylene and polyvinyl chloride (PVC) (from the corresponding monomer, the vinyl chloride (O dian 2004; McMurry 2011). Polyamide (PA), polyesters (PES), polyurethanes (PU), epoxy polymers and many others are examples of polymer obtained through step reaction processes (O dian 2004; McMurry 2011).

The versatility of polymerization resides not only in the different types of reactants (monomers) which can be polymerized, but also in the variations allowed by copolymerization, stereospecific polymerization, ring opening polymerization, etc. It is well known that the main technologies for polymer formation may be carried out with monomer alone (bulk or mass), in an organic solvent (solution), as an emulsion in water (emulsion), as droplets, with each droplets comprising an individual bulk polymerization suspended in water (suspension) and in a gas phase fluidized bed. All these techniques are commercially used (Feldman and Barbalata 1996; Deanin and Mead 2007; Slobodian 2010).

1.3.3 Applications

Most synthetic rubber is produced from two materials, styrene and butadiene. Both are currently obtained from petroleum (Brydson 1999 and Woodard and Curran 2006). Synthetic rubbers are usually developed with specific

properties for special applications. There are several synthetic polymers now in use. These include polybutadienes, SBR, acrylonitrile butadiene (nitrile rubber, a copolymer), polyisoprene, polychloroprene (neoprene), ethylene-propylene copolymer, silicone rubber, PU, polyfluorocarbon, IIR.

Tires account up to 70% of all natural and synthetic rubber used (Dunn 2002). Commonly used synthetic rubber for tyre manufacture is styrene-butadiene rubber and butadiene rubber (cloth members of the Buna family) (Chaiear and Saejiw 2010a). Butyl rubber is commonly used for inner tubes because it is gas impermeable. Due to oil resistance of nitrile rubber, it is widely used in sealing applications, roll coverings, conveyor belts, shoe soles, hose liners and plant linings. Other products containing rubber include footwear, industrial conveyor belts, car fan belts, hoses, flooring, and cables. Products such as gloves or contraceptives are made directly from rubber latex (Simpson 2002).

1.3.4 NBR

Nitrile Butadiene Rubber (NBR) is commonly called “Nitrile”, this rubber is a copolymer of butadiene and acrylonitrile (see Fig. 1.2) (Feldman and Barbalata 1996; Dunn 2002). They are produced by emulsion polymerization in batch or continuous process. The copolymer can be largely linear to highly branch depending on the conditions of polymerization. Chemically unsaturated NBR undergoes vulcanization reaction with sulphur and other vulcanizing agent. NBR under the common trade name Buna N is well known for its excellent resistances

to oils and solvent owing to its swelling property when immersed in mineral oils. NBR containing 10 to 45% of acrylonitrile (White and Kim 2008). Its chemical resistance to oils is proportional to the acrylonitrile content. The presence of acrylonitrile provides resistance to oil (petroleum hydrocarbon, mineral oils, greases, vegetable oils, animal fats) and fuel, while the butadiene provides abrasion resistance and low temperature flexibility. However, it is not resistant to strong oxidizing chemicals such as nitric acid, and it exhibits fair resistance to ozone and UV irradiation which severely embrittles it at low temperature (Hunt and Vaughan 1996; Cardarelli 2008; and Scheirs 2009).

NBR is currently the major competitor to NR in the manufacture of disposal latex gloves and are also used as textile and non-woven reinforcement, including the manufacture of synthetic leather (Dunn 2002). Common applications of NBR take advantage of the chemical resistance of the rubber. Seals, O-rings, gaskets, oil field parts, and diaphragms are the principal uses of NBR (Cardarelli 2008). Other applications include blending with phenolic and epoxy resin emulsion for adhesive and coating applications, caulks and sealants, additives for coal tar and asphalt (White and De 2001).

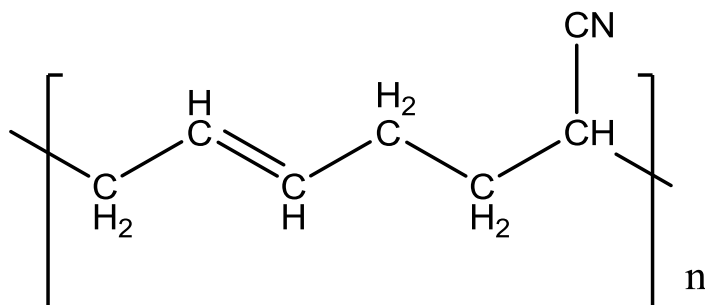


Figure 1.2: Structure of NBR.

and ageing make HNBR ideal for fuel-line hose, fuel-pump and fuel-injection components, diaphragms, as well as emission-control system (Deanin and Mead 2007). Highly unsaturated (20% unsaturated) HNBR gives good dynamic properties. They are used in rolls, belts, and oils field's parts (White and Kim 2008).

1.3.6 XNBR

Carboxylated nitrile rubber (XNBR) is chemically modified of NBR which contains one, or more, acrylic type of acid as a terpolymer. The resultant chain is similar to nitrile except for the presence of carboxyl groups (-COOH-) which occur about every 100 to 200 carbon atoms (Fig. 1.4) (White and De 2001; Simpson 2002; Gatos and Karger-Kocsis 2011). This acid group is normally encountered commercially in the form of a dispersion of the polymer in water, made by emulsion polymerization (White and De 2001).

The incorporation of carboxyl functional groups alters the polarity and colloidal stability of the dispersion, compatibility with other materials and polymer physical properties (Pinprayoon, Groves and Saunders, 2008). These acid groups provide extra “pseudo” cross-links during the vulcanisation process which are responsible for the improvement in physical properties as compared to a non-carboxylated nitrile rubber. There is enhancement in mechanical and chemical stability for latex along with improvement in wetting characteristic and adhesion to fibrous filler. Generally, the rubber shows enhance chemical resistance and

improved adhesion to other matrices. Carboxylated nitriles are, however, less flexible at low temperatures and less resilient than non-carboxylated compounds. Also, the “pseudo” crosslinks (being ionic in nature) are thermally sensitive. As temperatures increase, the ionic bonds lose strength.

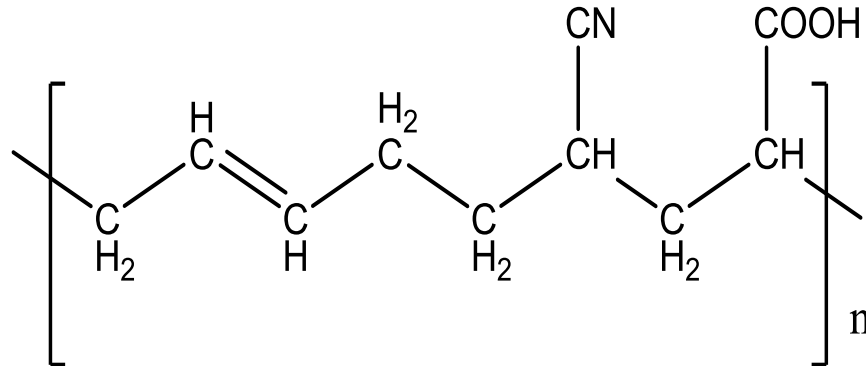


Figure 1.4: Structure of XNBR.

XNBR has better abrasion resistance than regular NBR (Gatos and Karger-Kocsis 2011). The superior resistance of XNBR to oil and solvent along with abrasion makes it suitable for industrial glove dipping (Alex 2009). Their applications in latex form include its use as a binder for paper and as a part of the coating material in coated paper as well as in the manufacturing of foam, carpet and adhesives (Pinprayoon, Groves and Saunders 2008). Other applications are automotive seals, industrial footwears, mechanical goods, textile spinning cots, packing, flat drive belting, hoses, industrial wheels, oil well specialties, and roll covers (White and Kim 2008).

1.4 Natural rubber latex and synthetic rubber latex in glove manufacture

Latex materials have been the subject of recent extensive research and development. As a result, their application areas have been expanding. NR latex products have good physical and chemical properties. The vast majority of latex gloves used by health care professionals, emergency medical technicians, police officers, and fire personnel, are made from NR latexes. The gloves are manufactured by a rubber dipping process whereby a form or mould (i.e., a model of a hand, sometimes with a forearm) is dipped into a bath containing NR latex and withdrawn, leaving a thin latex polymer coating on the form. The assembly is then dried at elevated temperatures to form the gloves, which is finally removed from the form or mould (Anderson and Daniels 2003).

NR latex has been the dominant material used to prepare disposable gloves for health care practitioners. It has an excellent barrier properties, high tensile, tear strength and elastic properties, it is soft and is comfortable to wear for extended periods of time and cost less than gloves prepared from synthetic rubber. However, the very significant downside to the use of NR latex has been the increased degree of allergic hypersensitivity in the population exposed to the NR gloves (e.g., health care professional, emergency response personnel, patients exposed to the gloves during medical and dental procedures), with estimate of allergic hypersensitivity in the order of 10% of this target population. The main routes of exposure to the proteins are direct skin contact and inhalation. Allergic reactions to the NR gloves can range from contact dermatitis, developing immediately on contact to the

gloves or several hours after exposure, to immunoglobulin E (IgE)- mediated (Type I) allergic reactions which can range from itching, rashes and congestion to life-threatening anaphylactic reactions (Chaiear 2001; Skypala and Venter 2009; Chaiear and Saejiw 2010b). To avoid allergy problems, medical field has, thus, begun to steer clear of the use of NR products in surgery and has instead leaned toward the use of synthetic rubbers. Natural latex free gloves comprised entirely of synthetic materials (e.g., vinyl nitrile, synthetic polyisoprene, SBR or carboxyl-group-containing ionomer-based elastomer such as carboxylated nitrile rubber (XNBR) gloves) are used by individuals having known allergies to natural latex rubber (Anderson and Daniels 2003; Ain and Azura 2010).

1.5 Scope

The incidence of latex protein sensitivity in NR glove give rise to various synthetic alternatives, such as vinyl, nitrile, chloroprene (neoprene). Although NBR is more superior to vinyl gloves, due to nitrile glove is highly susceptible to ozone attack (Hunt and Vaughan 1996; Cardarelli 2008; Scheirs 2009), XNBR take over NBR as the main raw material in the manufacture of nitrile glove.

Numerous studies have been published mainly focus on improving the mechanical properties of XNBR. Ain and Azura (2010) studied on the effect of types of filler and filler loading on the properties of XNBR latex films, while Mahaliang et al., (2005) investigated the effect of Zn-ion coated nanosilica filler on the cure behaviour, thermal stability and dynamic modulus and surface

morphology of XNBR. Chronska and Przepiorkowska (2008), used buffing dust as filler for XNBR, while Biswas et al., (2004), Pal et al., (2011) and Mishra, Raychowdhury and Das (2000), investigated different XNBR blends. However, little is known about the ageing of XNBR.

Storage of rubber, whether during storage or use of rubber products, is an inevitable process of ageing, leading to a deterioration of their properties. As a result of ageing, it reduced the tensile strength, elasticity and elongation, wear resistance, hysteresis and increased hardness, changing plasticity, viscosity and solubility of uncured rubber. In addition, as a result of ageing significantly reduced the duration of the exploitation of rubber products. Therefore, increasing the resistance of rubber to ageing is of great importance for increasing the reliability and performance of rubber products.

Due to the long time required to perform such tests at lower temperatures, high temperatures were typically utilized to bring the ageing time scale into a practical regime. The major objective of the current study was to utilize shorter high temperature ageing to obtain the shelf life of the samples at lower temperatures by using Arrhenius extrapolations to room temperature to.

Most of the lifetime assessments of rubbers are made by considering some measure of their performance, such as tensile strength or force at break, and specifying some lower limit for the property which is taken as the end point corresponding to when the material is no longer usable. The primary focus of this

study involves the reduction of tensile strength for the XNBR as a function of ageing time under different ageing temperatures. Although other physical parameters are important for proper parachute deployment and function, such as permeability and elasticity, tensile strength is arguably the most important and the easiest to monitor.

In the present study, the thin film samples are accelerated aged at elevated temperature range between 60 °C and 100 °C and for times between 0.5 hours to 3360 hours. The aged samples will be characterized mainly by measuring its tensile properties, linear swelling percentage, and changes in colour as well as its morphology changes with Scanning Electron Microscopy (SEM) and will be compared with unaged samples. Other techniques such as Fourier Transform Infrared (FTIR) will be used to analyse the casted thin film to develop a better understanding of the mechanism. In order to relate accelerated ageing to real-time ageing and predict its shelf life, Arrhenius equation will be used. Through extrapolation from accelerated ageing studies using Arrhenius equation, we can predict the shelf life of the samples as well as the activation energy of the samples.

1.6 Objectives of study

The objectives of this study are as follows:

- i. To study the effect of accelerated ageing on the properties changes of XNBR thin film, such as tensile strength, elongation at maximum, linear swell as well as morphological changes.
- ii. To determine the relationship between accelerated ageing and real time ageing and further to predict their shelf life as well as the activation energy using Arrhenius equation.
- iii. To study the chemistry of the ageing process in XNBR via FTIR analysis.

CHAPTER 2

LITERATURE REVIEW

2.1 Polymer, latex, elastomer

A polymer is a large molecule (macromolecule) composed of repeating structural units (monomers) typically connected by covalent chemical bonds. Polymerization is the process of covalently bonding the low molecular weight monomers into a high molecular weight polymer (Fuller 1999; Odian 2004; Speight 2010). During the polymerization process, some chemical groups may be lost from each monomer. The distinct piece of each monomer that is incorporated into the polymer is known as a repeat unit or monomer residue (Gupta 2010b).

Polymer particles (usually a few hundred nanometers in diameter) dispersed in water-based liquid or viscous state is called latex in the rubber industry and emulsion in the polymer industry (Stein et al., 1994; Wicks et al., 2007). Latex is a colloidal dispersion comprised about 50% by weight of the dispersion. Depending on the particular application, there will also be a complex mixture of pigments, surfactants, plasticizing aids and rheological modifiers. The whole dispersion is colloidally stable, meaning that it can sit on a shelf for years and remain dispersed, without sedimentation of particles making ‘sludge’ at the bottom (Routh and Keddie 2010).

Latexes may be natural or synthetic. Natural form of latex that is derived from tree (*Hevea brasiliensis*), it is essentially *cis*-isoprene emulsified by protein. Industrially and in the laboratory, latex is most often made by a reaction called 'emulsion polymerization'. Latex may be synthesized from a range of monomers, the typical ones being acrylates (methyl methacrylate, butyl acrylate, ethylhexyl acrylate), styrene, vinyl acetate and butadiene (Routh and Keddie 2010).

When the rubber particles in the latex are crosslinked, elastomer is produced. The process of crosslinking the linear chain polymers rubber is known as vulcanization. Vulcanization is a chemical process for converting rubber latex or related polymers into more durable materials via the addition of sulphur or other equivalent "curatives." These additives modify the polymer by forming crosslinking (bridges) between individual polymer chains. Vulcanization makes the rubber become more useful by reduces its stickiness at the same time increases the rubber's strength and durability and makes the rubber to retain its elasticity at a much wider range of temperatures (Coran 2005). Of course, the most common use of rubber is in automotive tires. But pencil erasers, shoes, gloves, dental dams and condoms are also made by rubber. In many products, rubber is added as a protective coating for waterproofing and roofing.

2.2 Degradation and ageing of polymer

Ageing as explained by Robert, Hastie and Morris (1993), Ehrenstein (2001), and Jones et al., (2009) is a process that occurs in polymeric materials during a specified period of time, and that usually result in changes in physical and/ or chemical structure and the values of the properties of the material. Colin, Teysseire and Fois (2011) defined that ageing as a slow and irreversible variation as a function of time (in use conditions) of a material's structure, morphology or composition leading to a detrimental change in its use properties. In polymer science and engineering, ageing is a term used when the properties of the polymer are changed over a period of time. The changes may be observed in engineering properties such as strength and toughness; in physical characteristics such as density; or in chemical characteristics such as reactivity towards aggressive chemicals (White 2006).

Changes in polymer properties due to chemical, physical or biological reactions resulting in bond scission in the backbone of macromolecules which in turn leads to the decrease in molecular weight of the polymer and subsequent chemical transformations are categorized as polymer degradation. Degradation occurs at any stage in the lifetime of a polymer. Polymer degradation results changes in polymeric material properties such as mechanical, optical or electrical characteristic in cracking, erosion, discolouration and phase separation. The changes may be undesirable, such as changes during use, or desirable, as in

biodegradation or deliberately lowering the molecular weight of a polymer (Pielichowski “ageing and Njuguna 2005; Speight 2010).

The long-term stability of polymeric materials is a matter of considerable importance, both to material scientists and to engineers. Two types of ageing occur that lead to changes in the properties of polymer: chemical and physical (Ehrenstein 2001; Cowie, McEwen and McIntyre 2003). Physical ageing processes are characterized by the thermo reversibility of the change in the material properties (Robert, Hastie and Morris 1993). During the physical ageing of a polymeric material the chemical structure remains unchanged, but the local packing of the chains is altered as a consequence of alteration of physical properties and lead to change in density, brittleness, tensile strength, glass transition temperature (T_g) and the material dimensions over extended period of time (Colin, Teyssedre and Fois 2011; Cowie and Arrighi 2011). Typical physical ageing effects are changes in morphology, such as post-crystallization, disorientation, and relaxation of internal stress as shown in Figure 2.1.

Physical ageing can also occur through evaporation or migration of volatile components or, conversely, through water absorption and swelling. It is important to distinguish between physical and chemical ageing, as both matter affect the long-term properties of a polymeric material. Unlike physical ageing, chemical ageing is non-reversible and leads to a modification of the polymer chain through processes such as chain scission, oxidation, dehalogenation, loss of pendant groups,

hydrolysis, and crosslinking, all of which are chemical reactions (Robert, Hastie and Morris 1993; Bonten and Berlich 2001; Cowie, McEwen and McIntyre 2003).

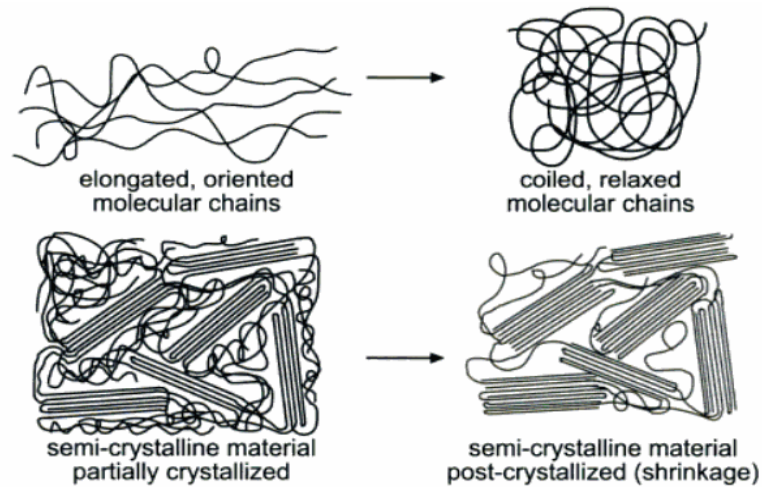


Figure 2.1: Effects of physical ageing on polymeric materials. Top: relaxation of oriented macromolecules. Bottom: post-crystallization (Ehrenstein 2001).

Chemical ageing, such as the effect of heat alone or the presence of oxygen, but also the action of chemical reagents or radiation, especially ultraviolet-rays (UV), can change the chemical structure of the polymer (Ehrenstein, 2001). The effect of heat with and without oxygen is illustrated in Figure 2.2.

The illustration in Figure 2.2 a depicts the situation where applying heat to the material causes further curing of an incompletely cured thermoset thereby changing the material properties, usually with improved results. However, all plastics will exhibit chain scission accompanied by some crosslinking when they are heated too long at high temperature as shown in Figure 2.2 b. The intermediate

effect of thermal-induced chain scission is a deterioration of the material properties.

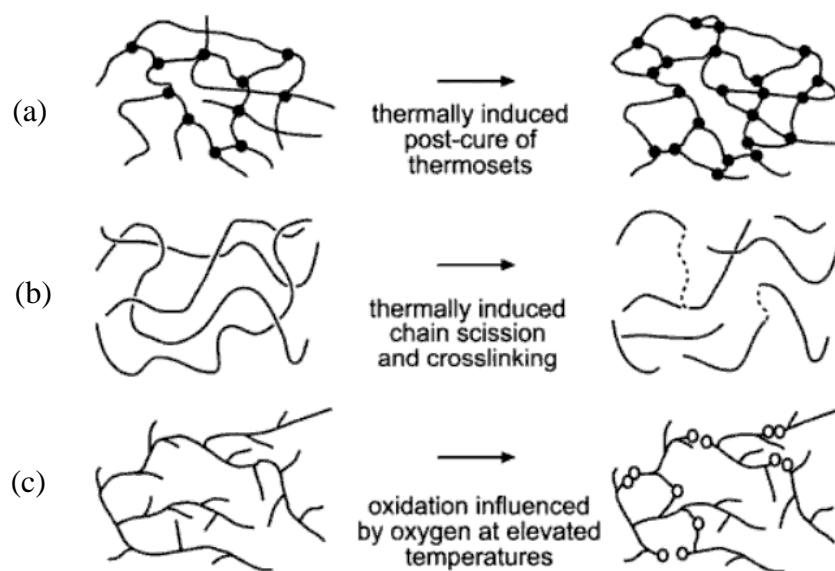


Figure 2.2: Effects of chemical ageing (heat and/or oxygen) on polymeric materials (Ehrenstein 2001).

Oxygen increases chain scission and becomes part of the macromolecules in the form of thermally unstable hydroperoxides as shown in Figure 2.2 c. UV light, ozone, and some reagents can aid and accelerate the oxidation of plastics and cause chain degradation. UV-rays, even without elevated temperatures, can cause embrittlement of impact-resistant polystyrene (PS) after several weeks in the sun. In condensation polymers, water and heat can cause a hydrolysis reaction (Ehrenstein 2001). According to Cowie, McEwen and McIntyre (2003), polymer degradation reactions can be divided into two classes,

- Main chain reactions leading to chain scission at random place and/or depolymerization;

- Substituent reaction at the side chains such as elimination of substituents.

The extent of ageing and the nature of the degradation process depend essentially on the chemical composition of the plastic, the thickness the sample being tested, and the environmental conditions. The most important, immediately noticeable, and industrially important effects of ageing are changes in the mechanical, electrical, and thermal properties, as well as changes in colour (yellowing), surface structure (cracks, voids), resistance to chemical, etc. The extent of ageing and its effects depend, apart from the inherent stability of various plastics, also on the additives present such as stabilizers, fillers, and plasticizers (Ehrenstein 2001).

2.3 Factors affecting polymer degradation

Degradation is defined as “A process which leads to a deterioration of any physical property of a polymer” by Singh and Sharma (2008). It is well accepted fact that polymeric materials are susceptible to attack by a wide variety of naturally occurring and man-made agents. In general, the degradation process affects the thermal stability, mechanical properties, crystallinity and lamellar thickness distribution and begins in the amorphous/crystalline interface (Ramis 2004).

2.3.1 Natural degradation agent

All polymeric materials are affected by outdoor weather. The outdoor weathering factors responsible for the degradation or loss of properties of the polymeric materials are listed in Table 2.1. It must be noted that ageing in the broad sense is often the consequence of several factors in combination (Brown 2002). A material is typically exposed to more than one factor during the time of outdoor usage, however, multiple outdoor weathering factors may accelerate the degradation process many times, often affect the polymer performance more severely than the effect of any single factor (Campo 2008).

Polymer degradation in broader terms includes biodegradation, oxidation, mechanical, photo, thermal and catalytic degradation. According to their chemical structure, polymers are vulnerable to harmful effects from the environment. This includes attack by chemical deteriorogens – oxygen, its active forms, humidity, harmful anthropogenic emissions and atmospheric pollutants such as nitrogen oxides, sulphur dioxide and ozone – and physical stresses such as heat, mechanical forces, radiation and ablation (Pielichowski and Njuguna 2005).

The results of exposing polymeric materials to these conditions can lead to discolouration, loss of mechanical strength, embrittlement, and loss of electrical insulation and resistance properties. The degree to which a particular material degrades depends on its susceptibility to each of the above factors (ASM International 2003).

Table 2.1: Types of degradation agents.

Degradation agent	Type of ageing or effect
Temperature	Thermo-oxidation, additive migration, crosslinking, crosslink loss (reversion)
Light	Photo-oxidation
Ionizing radiation	Radio-oxidation, crosslinking
Humidity	Hydrolysis
Fluids (gases, liquids, vapours)	Chemical degradation, swelling, additive extraction. Cracking
Bio-organisms	Decomposition, mechanical attack
Mechanical stress	Fatigue, creep, stress relaxation, set, abrasion, adhesive failure
Electrical stress	Local rupture

Two degradation agents may have a synergistic effect in that their effect, in combination, is greater or less than the sum of their individual effects. This is clearly very important when multiple agents are present. Simple examples are: perspiration in contact with elasticated garments weakening threads through swelling, which leads to more rapid ageing on cleaning; or light ageing of a stretched product causing surface relaxation, which leads to apparently improved ozone resistance (Brown, Forrest and Soulagent 2000; Brown 2001).

The rate of degradation by environmental agents is generally increased in the presence of stress. The degradation agent may be applied continuously or intermittently to give cyclic exposure. The exposure cycles may include two or more agents applied alternatively. The effects of cyclic exposure may not be the

same equivalent dose of continuous exposure (Brown, Forrest and Soulagent 2000; Brown 2001).

2.3.1.1 Temperature

Heat is also very commonly used in testing combination with other agents, notably light, liquids and gases. Low temperature (subambient) is not really a degradation agent but produces temporary physical effects on properties, such as stiffening, brittleness and recovery from strain, which may be critical in term of service performance (Brown, Forrest and Soulagent 2000; Brown 2001). Exposure to elevated temperature can result in loss of mechanical properties (embrittlement, loss of impact strength, flexibility, and elongation) and loss of electrical properties. Discolouration, cracking, chalking, loss of gloss, and flaking can also occur (ASM International 2003).

2.3.1.2 Ultraviolet light

Light includes radiation beyond the visible range, particularly in the UV region. The UV rays of solar light reaching the earth have a wavelength of 290 - 400 nm, which corresponds to the bond energy of standard organic compounds (99 - 72 Kcal/mol). Shorter wavelengths tend to have a greater effect on the surface of the material because their total energy can be absorbed within a few micrometres of the surface. Longer wavelengths tend to penetrate more deeply into a polymeric

material but have a moderate degradative effect because they are not easily absorbed (ASM International 2003).

Increasing of temperature accelerates the rate of any chemical reaction and, while most photochemical reactions are not very temperature sensitive, any subsequent chain reactions usually are temperature dependent (Brown, Forrest and Soulagent 2000; Brown 2001).

2.3.1.3 Ionizing radiation

Ionizing radiation covers X-rays, gamma rays and various subatomic particles. The intensity of ionizing radiation at the earth's surface is not high enough to significantly affect properties of rubbers and hence radiation exposure is only a consideration in connection with applications in nuclear plant and possibly where radiation is used to induce crosslinking or for sterilization. It is normally only important in specialist applications (Brown, Forrest and Soulagent 2000; Brown 2001).

2.3.1.4 Moisture

Moisture is absorbed when a polymeric material is exposed to water or humidity. Outdoor exposure to moisture can include rain, snow, humidity, and condensation. Water will cause the polymer to swell and act as a plasticizing agent with polymer material, consequently lowering its performance (Naranjo et al.,

2008). The chemical effect, known as hydrolysis, may be the major factor in the degradation of condensation polymers such as PES (Yoshioka and Grause 2008), PA (Jacques et al., 2002) and polycarbonates (Osswald and Menges 2003). Water can also attack the bonds between the polymer and an additive, such as pigment, resulting in chalking. Rain can wash away any additives, such as flame retardants, that may have bloomed or migrated to the surface as a result of sunlight or another outdoor exposure factor (ASM International 2003). There may be a synergistic effect with other agents. For example, a material resistant to UV alone or to moisture alone may fail when exposed to UV and moisture in combination (Brown, Forrest and Soulagent 2000; Brown 2001).

2.3.1.5 Fluids

Fluids encompass a whole range of chemicals, both gases and liquids, which can come into contact with the material in various ways. Fluids may be absorbed and cause swelling of the rubber, or may extract soluble constituents of the compound, or be a source of pro-oxidant materials (from water, cleaning fluids, etc.), or may have chemical effects. Ozone causes cracking of many rubbers when under strain (Brown, Forrest and Soulagent 2000; Brown 2001).

2.3.1.6 Mechanical stress and electrical stress

Fatigue failure resulting from repeated cyclic deformation is possible in many applications and can result in crack propagation or heat build-up. For seals

and similar products the set and stress relaxation which develops with prolonged deformation are critical factors to performance (Brown, Forrest and Soulagent 2000; Brown 2001).

Alternatively, under prolonged stress, creep will occur. In some applications, abrasion is clearly only an important factor in the failure of particular products but then it can be the limit to useful life, as for example in shoe soles and rubber flooring. In specialist areas, the product will be subject to electrical stress. Apart from the direct electrical stress, heating due to the current or dielectric heating will result in thermal ageing (Brown, Forrest and Soulagent 2000; Brown 2001).

2.3.1.7 Microbiological attack

Polymeric materials are generally not vulnerable to microbial attack under normal conditions. However, low molecular weight chemical additives such as plasticizers, lubricants, stabilizers, pigments and antioxidants may migrate to the surface of the polymer material and encourage the growth of microorganisms (Campo 2008). The growth of fungi and bacteria on polymeric material will result in discolouration, surface attack and loss of optical transmission (ASM International 2003). Growth rate of the microorganism strongly depends on surrounding factors such as heat, light, and humidity. Preservative additives, also known as fungicides or biocides, are added to polymeric materials to prevent the

growth of microorganisms. These additives are highly toxic to lower organism but do not affect higher organisms (ASM International 2003; Campo 2008).

2.3.2 Nature of polymer

During its lifetime a rubber can be subjected to different types of degradation from different exposure conditions. The mechanisms which produce degradation depend not only on the degradation agents present but also on the nature of the polymer and additives (Brown, Forrest and Soulagent 2000; Brown 2001).

2.3.2.1. Chemical composition

Chemical composition of the polymers plays a very important role in their degradation. The long carbon chains found in thermoplastic polyolefins (PO) makes these polymers non-susceptible to microbial degradation. However, with the incorporation of the heterogroups such as oxygen in the polymer chain makes polymers susceptible for biodegradation and thermal degradation (Singh and Sharma 2008). Presence of unsaturation in the natural rubber make it more susceptible oxidative degradation as compared to PE while linear saturated POs are resistant to oxidative degradation (Singh and Sharma 2008). As compared to crystalline areas of a polymer, amorphous regions were more labile to thermal oxidation due to the high permeability of oxygen molecule in the amorphous

regions. A polymer with unreactive methyl and phenyl groups or with no hydrogen at all shows resistance to oxidation (Singh and Sharma 2008).

2.3.2.2 Polymer structure

Natural macromolecules, such as protein, cellulose, and starch are generally degraded in biological systems by hydrolysis followed by oxidation. Thus, synthetic biodegradable polymers contain hydrolyzable linkages along the polymer chain; for example, amide enamine, ester, urea, and urethane linkages are susceptible to biodegradation by microorganisms and hydrolytic enzymes (Chandra and Rustgi 1998). The biodegradabilities of synthetic polymers are greatly affected by the hydrophilic–hydrophobic character of synthetic polymers because most of the enzyme-catalyzed reactions occur in aqueous media. A polymer containing both hydrophobic and hydrophilic segments seems to have a higher biodegradability than those polymers containing either hydrophobic or hydrophilic structures only (Chandra and Rustgi 1998).

2.3.2.3 Molecular weight

Plastics remain relatively immune to microbial attack as long as their molecular weight remains high. It has been reported that some microorganisms utilize PO with low molecular weight faster as compared to high molecular weight PO (Yamada-Onodera et al., 2001). Many plastics, such as PE, Polypropylene and PS do not support microbial growth. However, as reported by Chandra and Rustgi

(1998) and Singh and Sharma (2008), low molecular weight hydrocarbons, such as linear PO with molecular weight lower than 620 support microbial growth thus can be degraded by microbes.

2.3.2.4 Incorporation of functional groups.

Incorporation of some functional group such as carbonyl groups in PO makes these polymers susceptible to photodegradation. Rate of photodegradation increases as the number of chromophores increases due to more sites are available to absorb more photons for the photodegradation initiation reaction. According to Singh and Sharma (2008), photochemical degradation occurs when the carbonyl chromophore absorbs near-UV radiation and form radicals by the Norrish Type I, II and hydrogen-abstraction processes. Incorporation of metal-metal bond in polymer backbone induces photodegradability as the metal-metal bond cleaves homolytically on irradiation.

2.3.2.5 Additives

Non-polymeric impurities (such as residues of polymerization catalysts, transformation products of additives), fillers or pigments affect the polymer resistance to degradation. Polymer such as PVC and PS originally are not affected by sunlight, however, when presence of small amount of impurities or structural defects, which absorb light and initiate the degradation (Johanson 2009). Thermal oxidative processes of PO was accelerated by transition metal traces which

inducing hydroperoxide decomposition. For example, TiO₂ delustrant has made the PA susceptible for heat- and light induced oxidation (Singh and Sharma 2008).

2.3.2.6. Chemical bonding

Linkage affects the degree of degradation in plastic. In thermoplastic, weak points were created during addition polymerization such as head-to-head addition of monomer units and tail-to-tail addition of monomer units which make the plastic susceptible for degradation. Thermal degradation of poly(methylmethacrylate) (PMMA) is further enhanced by its head-to-head linkage of the polymer. Branching in polymer chain increases thermal degradation. Rate of photodegradation will be decreased if radical-radical combination reaction was favoured by crosslink formation locking the polymer structure and preventing lamellar unfolding because these actions prevent separation of photo-produced radicals (Singh and Sharma 2008).

2.3.2.7 Methods of synthesis

Methods of synthesis show the noteworthy effect on the stability of the polymers. Anionic polymerized PS showed more photo-stability than free radically formed polymer due to the presence of peroxide residue in the latter, which is labile for photodegradation (Pospisil et al., 2006). As compared to copolymerized PP, Ziegler-Natta catalyst and bulk polymerization of PP is more susceptible towards photodegradation (Singh and Sharma 2008).

2.3.2.8 Effect of substituents

Substituents affect the degradation processes in many polymers containing labile α -hydrogen in the repeating units and modify the reaction course profoundly even if the main chain scission reactions prevail. Chain-end scission reactions are predominant for ethylene and 1-substituted ethylene by producing either little or up to 50% monomer as volatiles. Ghosh (1990) found that 1,1-disubstituted ethylene with chlorine as substituents did not favour chain end degradation route, whereas repeated units apparently favoured 100% monomer yield. Thermal stability of a polymer decrease with increases the number of substituents on polymer backbone. For the same reason, PP and polyisobutylene are less thermal stable as compared to PE. The effect of substituent groups on the stability of the backbone C-C bond is apparent from the comparison of the bond dissociation energies for C-C bond (in kJ/mol), $\text{CH}_3\text{-CH}_3 = 368$, $\text{CH}_3\text{CH}_2\text{CH}_3 = 356$, $(\text{CH}_3)_3\text{CCH}_3 = 335$ and $\text{C}_6\text{H}_5\text{CH}_2\text{CH}_3 = 293$ (Singh and Sharma 2008).

Contrary to this, presence of aromatic groups in a polymeric backbone will increase the thermal stability of the polymer. Presence of electronegative groups such as fluorine in teflon will also increases the thermal stability of the polymer due to high dissociation energy (452 kJ/mol) of C-F bond (Singh and Sharma 2008).

2.4 Types of polymer degradation

Polymer degradation is generally indicates the irreversible change of chemical or physical properties which is caused by the chemical and/or physical action of agents. Degradation includes the deterioration of macromolecules caused by bond scissions in the polymer backbone, intermolecular crosslinking with formation of new chemical bonds between adjacent molecules and chemical reactions at the side chains (Brown 2001; Ha-Anh and Vu-Khanh 2005). There can also be changes to ingredients such as extraction of plasticisers or attack of fillers by acids. Depending upon the nature of the causing agents stated above, polymer degradation has been classified as photo-oxidative degradation, thermal degradation, ozone-induced degradation, mechanochemical degradation, catalytic degradation and biodegradation.

Photo-oxidative degradation is the process of decomposition of the material by the action of light. When the light is irradiated on a polymer, some of the atoms within the polymer become excited by absorb the energy of the photons. The absorbed photon energy can be sufficient for atoms to spontaneously dissociate from the position of the polymer resulting in degradation phenomena such as chain scission (ASM International 2003). Photodegradation changes the physical and optical properties of the polymer. The most damaging effects are the visual effect (yellowing), the chalking effect, the loss of physical and mechanical properties of the polymers, the changes in molecular weight and the molecular weight distribution (Ghaffar, Scott and Scott 1976; Nishimura and Osawa 1981;

Nagai et al., 1999; Martin, Chin and Nguyen 2003; Abadal et al., 2006; Marek et al., 2006; Rosu, Rosu and Cascaval 2009).

Under normal conditions, photochemical and thermal degradations are similar and are classified as oxidative degradation. The main difference between the two is the sequence of initiation steps leading to auto-oxidation cycle. Other difference includes that photochemical reactions occur only on the surface of the polymer, whereas thermal reactions occur throughout the bulk of the polymer (Singh and Sharma 2008). The basic categories of thermal degradation process are side group elimination, random chain scission, and depolymerization where the polymer reverts to its original monomers (Pielichowski and Njuguna 2005; Johanson 2009; Batchelor, Loh and Chandrasekaran 2010). Thermal degradation also occurs in an auto-catalytic process, at lower temperatures, when oxygen is present in the environment (ASM International 2003). This oxidative degradation of polymers is catalysed by heavy metals, such as copper, which undergo a reduction-oxidation reaction in the presence of oxygen (ASM International 2003). Complex reactions occurring in thermal degradation of polymers depend on various factors like reaction medium, heating rate, reactor geometry and pressure. High viscosity polymers make the process become complicated by impeding heat and mass transfer (Singh and Sharma 2008).

Atmospheric ozone usually causes the degradation of polymers under conditions that may be considered as normal; when other oxidative ageing processes are very slow and the polymer retains its properties for a rather longer

time (Cataldo 1998a; Cataldo 1998b; Cataldo, Ricci and Crescenzi 2000). The presence of ozone in the air, even in very small concentration, markedly accelerates the degradation of polymeric materials (Kefeli, Razumovskii and Zaikov 1971). Ozone reaction is electrophilic and therefore attacks where the electron density in a polymer chain is high (e.g. at double bond site). The rate of degradation depends slightly on temperature and is decreased in the presence of electron-withdrawing substituents at the double bonds. It is also dependent on the olefin configuration, the *trans*-isomers being more reactive by about 10 fold than the *cis*-isomers (Brown 2001; Rakovsky and Zaikov 2004). In saturated polymers, this process is accompanied by the intensive formation of oxygen containing compounds, by the changing in molecular weight and by the impairment of the mechanical and electrical properties of the specimens (Andrady 1998).

Mechanochemical degradation of polymers involves the degradation of polymer by strong ultrasonic irradiations and under mechanical stress (Li, Guo and Li, 2006). Breakdown of molecular chains by mechanical force or under shear is often aided by oxidation which is known as mechanochemical degradation. This type of degradation is common in machining process such as mastication, grinding and ball milling (Mitchell 2003). Example of mechanochemical degradation is rubber mastication which leads to chain breakage and development of plasticity under shear. Mastication of rubber in the atmosphere of nitrogen at ordinary temperature does not change the plasticity and molecular weight appreciably, but with the presence of oxygen, degradation occurs immediately and rapidly. Under mechanical shear, the rubber molecules break into radicals and react with oxygen

in the atmosphere leading to permanent chain breakage. In nitrogen, however, the primary radicals formed under shear immediately recombine to give no effective chain breakage (Gosh 2001).

Catalytic transformation of waste polymers into hydrocarbons with higher commercial value is a field of great interest. POs can be catalytically or thermally degraded into gases and oils. The most common catalysts used are acidic solids, mainly alumina, amorphous silica-alumina and zeolites. Catalytic activity and product selectivity are strongly affected by their textural and acid properties (Aguado and Serrano 1999). For polymer degradation, different types of catalysts have been reported in the literature which include Pt-Co and Pt-Mo supported over SiO_2 (Gimouhopoulos et al., 2000), transition metal catalysts (Cr, Ni, Mo, Co, Fe) on the support (Al_2O_3 , SiO_2) (Williams and Bagri 2003), zirconium hydride (Singh and Sharma 2008), zeolite catalysts (Jong-Ryeol et al., 2004) and non-zeolite catalysts (Lin and Yen 2006).

Biodegradation is a natural process by which organic compounds in the environment are converted to simpler compounds, mineralized and redistributed through element cycles (carbon, nitrogen and sulphur). Biodegradation can only occur within the biosphere as microorganisms play a central role in the biodegradation process. Biodegradable polymer involves cleavage of hydrolytically or enzymatically sensitive bonds in the polymer leading to polymer erosion (Wei et al., 2011). Mineralization of organic compounds yields methane and carbon dioxide under anaerobic conditions, and carbon dioxide and water

under aerobic conditions. Abiotic hydrolysis, photo-oxidation and physical disintegration of polymers may enhance biodegradation of polymers by reducing molecular weight to increases their surface area for microbial colonization (Palmisano and Pettigrew 1992).

2.5 Thermal and thermal oxidative degradation

There are different types of bonds that can be branched in a polymer. The bonds that tend to break first are the ones that form the weakest links in the chain. Depending upon the presence of oxygen, temperature and the structure of the polymer, degradation reactions will occur. Saturated hydrocarbons for example are much more stable than PE in the absence of oxygen as are chloroalkanes when compared with PVC (Allen and Edge 1992). In thermal degradation, degradation of polymers can follow three major pathways: side group elimination, random scission and depolymerization.

Side group elimination takes place generally in two steps. The first step is the elimination of side groups attached to a back bone of the polymer. When the side group is removed, the remaining unstable polyene macromolecule then undergoes further reaction, including the formation of aromatic molecules, scission into smaller fragments, or the formation of char (Pielichowski and Njuguna 2005). Examples are the elimination of hydrogen chloride from PVC to leave a polyene structure (Flynn 2002; Pielichowski and Njuguna 2005; Batchelor Loh and Chandrasekaran 2010) and the elimination of isobutylene from poly(*t*-

butyl methacrylate) to leave polyacrylic acid (Flynn 2002). Thermal dehydrochlorination of PVC begins with internal allylic chloride and tertiary chloride structural defects formed during polymerization. During thermal degradation, ordinary monomer units are converted into internal allylic chloride defects by a mechanism that may include the abstraction of hydrogen by triplet cation diradicals derived from polyene intermediates. Cyclization reactions seem likely to contribute to the termination of polyene growth (Starnes 2002).

Random scission involves the formation of free radical at some point on the polymer backbone, producing small repeating series of oligomers usually differing in chain length by the number of carbons (Pielichowski and Njuguna 2005). This is a reverse process of polycondensation where lower molecular weight fragments were produced but practically no monomer is liberated (Feldman 1990). The molecular weight falls rapidly from the start, only after the process has continued for a long time are there many molecules small enough to be volatile (Flynn 2002). For random degradation to occur, the polymer chain does not require necessarily to carry any active site (Singh and Sharma 2008). PES undergoes hydrolytic degradation resulting in chain scission. PE also undergoes random degradation through migration of a hydrogen atom from one carbon to another thus degraded into two fragments (Singh and Sharma 2008). Other polymers that typically degraded by the random chain scission process are generally vinyl polymers such as PS, poly(acrylonitrile), etc. The yield of monomer of such polymers is usually low, and the pyrolyzed fragments are ordinarily larger than corresponding monomer unit (Feldman 1990). For example,

poly(ethylene terephthalate) follows random thermal degradation route (Figure 2.3); the initial step resulting in scissions leads to carboxyl and vinyl groups.

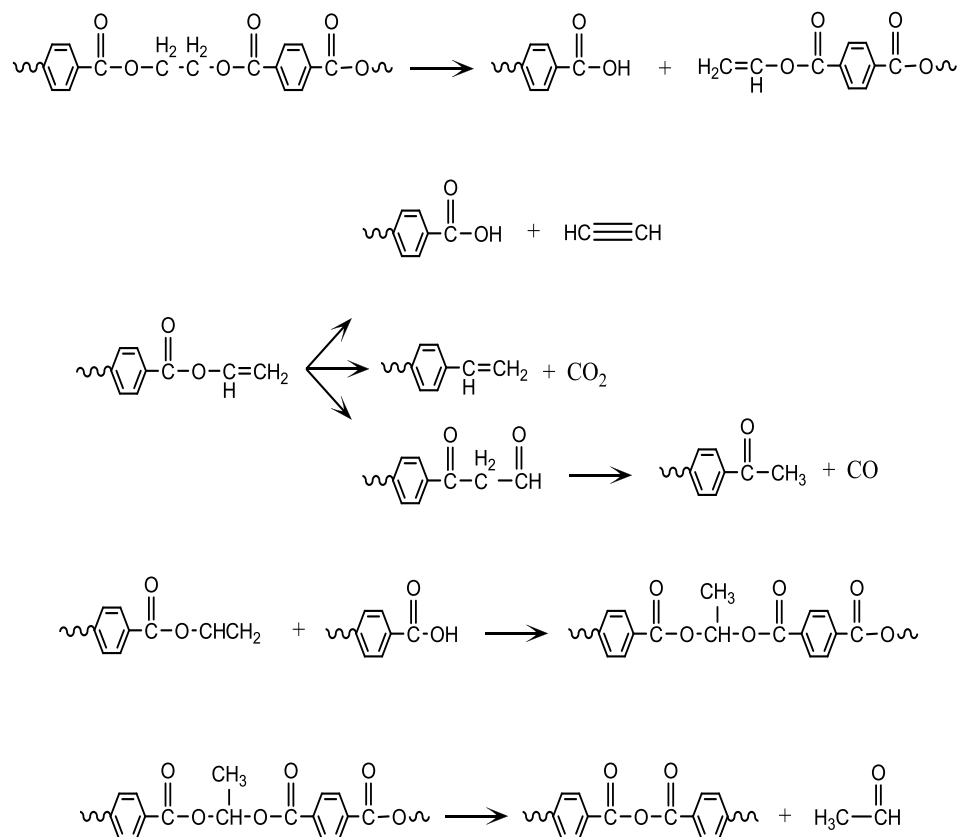


Figure 2.3: Random thermal degradation mechanism of poly(ethylene terephthalate)

Thermal degradation of the polymers follows either random degradation route (Equation 2.1) or chain end degradation (also known as unzipping route) (Equations 2.2 and 2.3) as shown below:





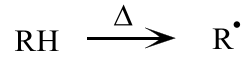
The chain end degradation also known as depolymerization reaction, starts from the end of the chain and successively releases the monomer units (Feldman 1990). Depolymerization reaction is the opposite of the propagation step in addition polymerization occurs through free radical mechanism. In this type of degradation, molecular weight of the polymer decreases slowly and large quantity of the monomer is liberated simultaneously (Singh and Sharma 2008). The depolymerization reaction in thermal degradation need not be initiated at terminal end of the macromolecule, instead, imperfections in the chain structure (initiator fragment or a peroxide or ether link) form a weak link from where depolymerization starts (Rawe 2000). A large number of addition polymers depolymerize at elevated temperature, for example, PS, PMMA and polyaldehyde are prone to converted almost quantitatively back to the monomer while PE suffers random chain scission and decomposed into longer olefinic fragments and actually producing little monomer (Daraboina and Madras 2008; Singh and Sharma 2008; Batchelor, Loh and Chandrasekaran 2010).

In general, chain end degradation occurs when the backbone bonds are weaker than the bonds of the side groups and only with polymer molecules, carrying active chain ends with a free radical, cation, anion, etc. Chain end degradation most frequently occurs when the polymer backbone contains a tertiary carbon atom, such as, PMMA, poly(α -methylstyrene) (P α MS), PS, PP, polytetrafluoroethylene and poly α -methylacrylonitrile (PMCN) (Feldman 1990).

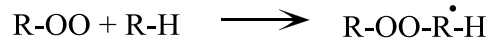
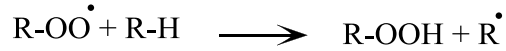
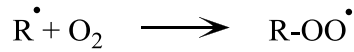
For example, P α MS synthesized through anionic mechanism upon heating from -70 °C to +60 °C undergoes degradation from the chain end carrying the active carbanion in such a manner that at 60 °C, the entire polymer gets converted into the monomer (Singh and Sharma 2008). The major degradation products for fluorinated polyacrylate are monomer, dimer, trimer, saturated diester and corresponding methacrylate along with remarkable amounts of alcohol (Budrugaec 2000; Zuev et al., 2006).

Unlike thermal degradation, where polymer scission can occur randomly and/or at the chain end, oxidative degradation is characterized by random scission in the polymer backbone ((Pielichowski and Njuguna 2005). According to Johanson (2009), thermal oxidation, like photo-oxidation, is caused by autoxidation, the difference merely being that the radical formation from hydroperoxide is now activated by heat. At temperatures from ambient to over 100 °C, these hydroperoxide groups will be slowly generated in the presence of oxygen at labile groups and linkages on the polymer chain. For example, tertiary carbon atoms are more susceptible to autoxidation than secondary, which are, in turn, more easily attacked than CH₃ groups. Unsaturated linkages and ether groups are easily attacked and aldehydes are more susceptible than ketones. The presence of residual metals and other catalysts in the polymeric material also may initiate the hydroperoxide group formation (Flynn 2002). The typical chemical equations for polymer oxidation involving free radical chain mechanism are shown in Figure 2.4.

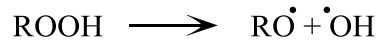
Initiation



Propagation



Branching



Termination

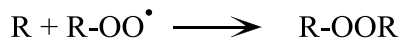
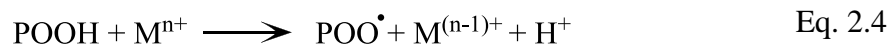


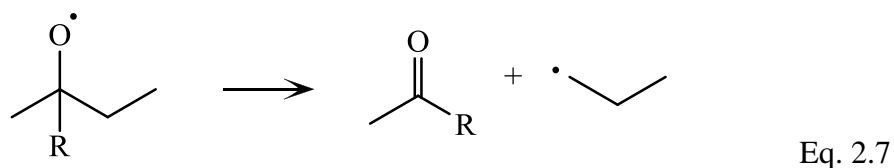
Figure 2.4: Mechanism for polymer oxidation (RH = polymer hydrocarbon).

The initial step in thermal degradation is the cleavage of the weakest bonds present in the polymer. The critical bond is the aliphatic CH, which permits a number of the facile radical reactions that lead to cross linking or chain degradation (ASM Internaional 2003). Hydroperoxide builds up as the reaction proceeds and later, thermal decomposition of hydroperoxide groups becomes the main source of the free radical formation by branching reaction (Flynn 2002). Presence of the metal ion (transition metal based pigment) may also catalyses the

decomposition of hydroperoxide group in the polymer into radicals by the following reactions (Scheirs 2000):



Termination achieved by combining free radicals into inert product. Peroxyl radicals eventually terminate by reaction with other radicals to give dialkyl peroxides, carbonyl species or alcohols (Singh and Sharma 2008). The most important side reaction that could decrease the mechanical properties of polymeric product is the chain cleavage reaction caused by β -scission reaction of alkoxy radicals (Equation 2.7) (Gijssman 2011).



Thermal degradation above 200 °C leads to chain scission and largely depends on impurities like head-to-head units, unsaturation sites, and other defectives (Ramis et al., 2004). POs are known to be sensitive to thermal oxidation, due to the impurities generated during their manufacture at high temperatures (Khabbaz, Albertsson and Karlsson 1999). Compounds formed by

thermo-oxidative degradation of PES are formaldehyde, acetaldehyde, formic acid, acetic acid, carbon dioxide and water in large quantities while hydroxyaldehydes, hydroxyacids, aldehyde acids are also identified in small quantities (Singh and Sharma 2008).

Drago, Vera and Davorka (1995) have studied thermally stimulated oxidative degradation of high impact PS with nitric acid. Mechanism of oxidation and nitration depends upon temperature and leads to the molecular and chemical heterogeneity and also lowering in mechanical properties of the polymer. PS thermally gets degraded into organic compounds such as quinone, phenol, diphenylamine and naphthalene at the experimental temperature of 350 - 450 °C (Karaduman et al., 2001; Faravelli et al., 2003; Kiran, Ekinici and Srape 2004; Bortoluzzi et al., 2006).

2.6 Lifetime prediction

Predictions of the long-term behaviour of polymers are based on methodologies that have already been tested by Laboratory for Research and Control of Rubber and Plastics (LRCCP) for various industrial sectors: civil engineering (Channel Tunnel), construction, aeronautics and spatial, offshore, fluid transport, nuclear and marine (Huy and Evrard 1998). Most assessments of lifetime of rubbers are made by considering some measure of performance, such as tensile strength, and specifying some lower limit for the property which is taken as

the end point corresponding to when the material is no longer usable (Brown, Forrest and Soulagent 2000; Brown 2001).

Ageing is a difficult problem to study in practice, because it usually proceeds slowly in service conditions of materials and lifetime reaches typically several tens of years. Therefore, it is not advisable to test and qualify materials for a given application on a natural ageing basis as it is usually time consuming. Therefore accelerated laboratory test are highly valuable and frequently used to study polymer durability (Manceau, Rivaton and Gardette 2012). Simulation and modelling of long-term behaviour are only possible on the basis of accelerated artificial ageing tests under the most representative conditions of the real environment (Huy and Evrard 1998). Accelerated ageing test is then performed in laboratories by increasing the level of the degradation agent such as temperature or the intensity of radiation to speed up the normal ageing processes of items. It is used to help determining the long term effects of expected levels of stress within a shorter time and estimate the useful lifespan of a product when actual lifespan data is unavailable (Brown 2001).

2.6.1 Basic methodology

The principle of the method consists in accelerating the physico-chemical change of the material by raising the temperature to simulate its long-term state, and then measuring the relevant properties in this thermo-activated state. This method thus assumes that, where the other parameters do not change, the same

state of the material is attained after both a long period of exposure to the working temperature and a shorter period of exposure to a higher temperature. Experimental procedures based on known kinetic models (particularly Williams-Landell-Ferry model and Arrhenius model) make it possible to characterize this equivalence between time and temperature, in other words, to establish the law of change of the material's properties in relation to these parameters. The resulting property values can then be estimated far in excess of the experimentally accessible time scale. The method remains applicable so long as the rise in temperature does not change the mechanisms involved and it is also valid when considering properties over very short periods of time. The choice of temperatures, the interval between each temperature and the temperature range under consideration are determined step by step, comparing the fitting of the results to the model (Huy and Evrard 1998).

2.6.2 Arrhenius model for lifetime prediction

The Arrhenius model has been used for many years to predict polymer lifetimes in various application equations (Huy and Evrard 1998; Lundquist et al., 2000; Gillen, Celina and Bernstein 2003; Gillen, Bernstein and Celina 2005a; Roland 2009; Choudhury, Bhowmick and Soddemann 2010; Kahlen, Wallner and Lang 2010; Woo and Park 2011). Most degradation processes are temperature activated, and they were best represented by the classic Arrhenius reaction rate. Arrhenius approach has been utilized to analyse shorter-term high temperature accelerated ageing exposures and then to extrapolate these results to make long-

term predictions at the much lower ambient temperature of interest (Lundquist et al., 2001; Gillen, Bernstein and Celian 2005a). The shelf life of a rubber product is predicted based on the Arrhenius principle of chemical reaction rates. Chemical processes generally accelerate exponentially as the temperature is increased and in many cases change in rate with temperature can be described by the well-known Arrhenius relationship (Potter 2006). The Arrhenius equation has the basic form:

$$k(T) = A \times e^{\frac{-E_a}{RT}} \quad \text{Eq. 2.8}$$

where $k(T)$ is reaction rate constant for the process, A is the material constant, E_a is the activation energy, R is the universal gas constant and T is the absolute temperature in Kelvin.

In order to apply the Arrhenius equation to the ageing of rubber products, it is assumed that the time required for a specific physical property, such as force at break, to deteriorate to a specified threshold value, is directly proportional to the extent of chemical reaction that has occurred. In turn it can be shown that the time for the chemical reaction to reach a specified extent is inversely proportional to the rate constant, $k(T)$. The Arrhenius equation can be rearranged as follow:

$$\frac{C}{t_{(x\%)}} = A \times e^{\frac{-E_a}{RT}} \quad \text{Eq. 2.9}$$

or taking natural logarithm of both sides and rearranging Eq. 2.8 becomes;

$$\ln t_{(x\%)} = \frac{E_a}{RT} - \ln \frac{A}{C} \quad \text{Eq. 2.10}$$

Where $t_{(x\%)}$ is the time for the property to fall to $x\%$ of the initial value and C is a constant.

In the example shown in Figure 2.5, the property parameter has been plotted against ageing time at five different temperatures, and the reaction rate taken as the time for the property to reach a predetermined threshold value or end of life criterion. . According to British Standards Institution 2009, median of force at break and threshold value of 75% of the original value was chosen. Figure 2.5 illustrates how this done assuming a threshold value of 75% retained force at break.

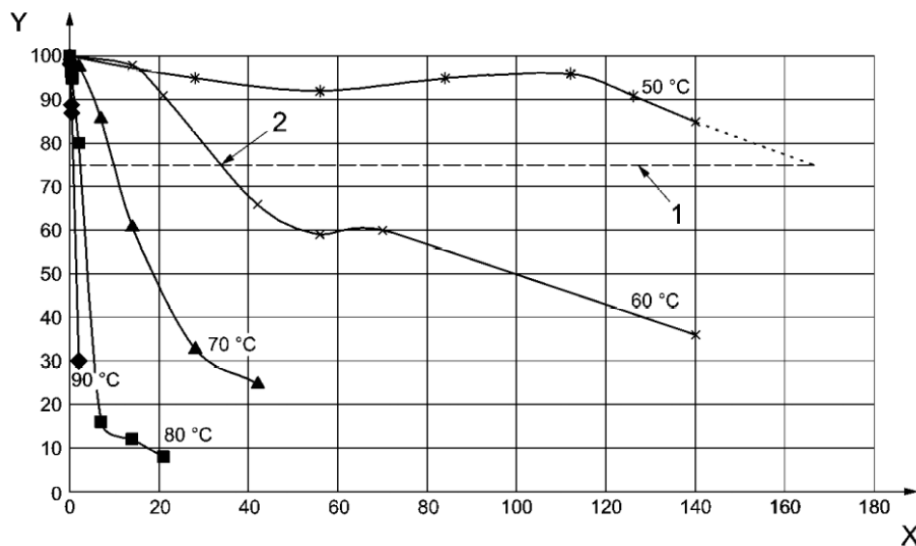


Figure 2.5: Estimating the time to reach a specified threshold. X: Time in days; Y: Initial force at break in %. 1: 75% threshold; 2: Time to reach threshold in 60 °C.

Basically the time required to a specific property to fall to a defined threshold value are determined in a series of different temperatures and the natural logarithms of these times are plotted against the reciprocals of the absolute temperatures. If the Arrhenius relationship is followed then, a straight line graph will be obtained (Lundquist et al., 2001; Potter 2006; British Standards Institution 2009). A linear extrapolation of the straight line allows prediction of the life at lower temperature. The slope of the line provides the activation energy of the property change. Typical activation energies for many chemical reactions average 83 kJ/mol although the actual values found in practice way vary widely. Mott and Roland (2001) found the activation energies of ageing of natural rubber in air and seawater are 90 ± 4 and 63 ± 3 kJ/mol, respectively. The best fit to the Arrhenius plot can be found by the least squares method and extrapolated to find the time to the threshold value at a temperature of interest. The application of such a model is shown in Figure 2.6.

One of the most critical aspects of this type of analysis is the ability to draw a straight line through the various data point. However, the relation describes a simple chemical reaction whereas in practice the reactions are likely to be complex. It is assumed that the reactions at the service temperature are the same as those at the testing temperatures, that the activation energy is independent of temperature and that the chemical changes relate directly to the physical properties measured (Huy and Evrard 1998; Brown 2001). Beside the straight line, a discontinuation in the linear also gives us a lot of information. Once the discontinuation is realized, this can be translated into a change of mechanism

within the chemical kinetics phenomena. If there is a discontinuation, there may be two or more events or mechanism occurring (Harvey 2005).

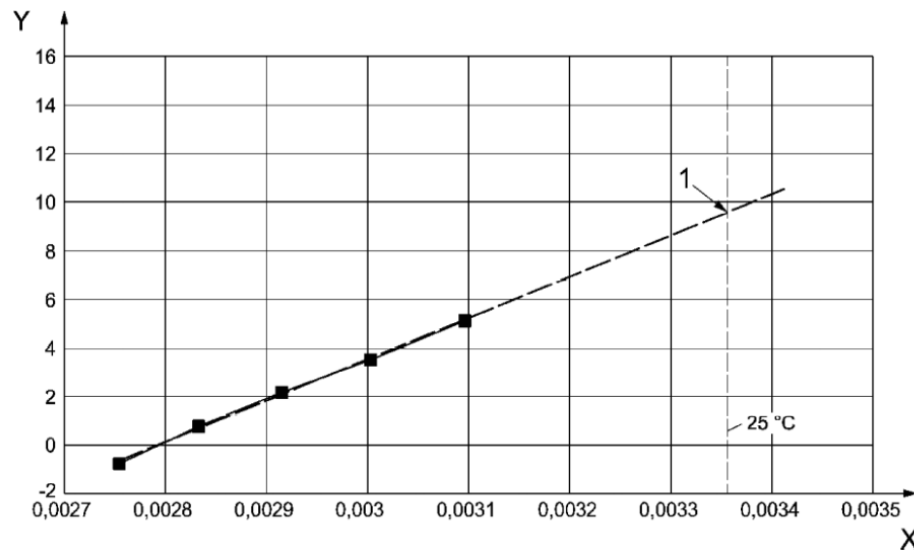


Figure 2.6: Arrhenius plot for force at break assuming a threshold of 75%. Y: $\ln t_{(75\%)}$ in years; X: $1/T$ in K^{-1} . 1: Extrapolation to 25 °C; $y = 17071x - 47.71$; $R^2 = 0.9987$.

Note: The time estimated for the physical properties to fall to 75% from Figure 2.6 is 39 years at 25 °C. The activation energy is calculated as 141.9 kJ/mol.

2.6.3 Time-temperature superposition model for lifetime prediction

An alternative method of presenting accelerated ageing data is to use the time-temperature superposition plot described by Wise, Gillen and Clough (1995); Gillen, Celina and Keenan (2000), Gillen, Bernstein and Derzen (2005b); British Standards Institution (2009); Kahlen, Wallner and Lang (2010) and others. This method is based on the Arrhenius equation and is widely used in the scientific

literature to present accelerated ageing data on polymeric materials. Time-temperature model is based on the application of the time temperature equivalency. As compare to the Arrhenius model, this model does not need a prior require the definition of a failure criterion. This approach defines the extension or reduction of lifetimes at temperatures other than the reference temperature, as multiplying factors to the lifetime at a given temperature, may be based on any type of failure criterion.

An important prerequisite for the applicability of this approach is the fulfilment of the self-similarity criterion (Gillen et al., 1996; Gillen, Celina and Keenan 2000; Ha-Annh and Vu-Khanh 2005; Kahlen, Wallner and Lang 2010). A superposition of data generated for various ageing temperatures is obtained by shifting the various ageing curves horizontally along the time axes, so that one single mastercurve is obtained. In this procedure the time values at each temperature are transformed to equivalent times at a common reference temperature by multiplying them by the Arrhenius shift factor, α_T , which is derived from the Arrhenius equation:

$$\ln \alpha_T = \ln \frac{t_{T_{ref}}}{t_{T_{aged}}} = \frac{E_a}{R} \times \left(\frac{1}{T_{ref}} - \frac{1}{T_{aged}} \right) \quad \text{Eq. 2.11}$$

where $t_{T_{ref}}$ and $t_{T_{aged}}$ are the respective ageing time at reference temperature, T_{ref} and ageing temperature T_{aged} in Kelvin, respectively, E_a is the activation energy, R the universal gas constant and T the absolute temperature in Kelvin.

The physical properties obtained at the various ageing temperatures are plotted against the respective transformed times on a common graph. The activation energy for the specific material under consideration may be estimated as described in 2.6.2 or obtained from the scientific literature (British Standards Institution 2009; Roland 2009). If the ageing properties transform according to the Arrhenius equation and the correct value is used for the activation energy then a single master curve is obtained. The properties of the polymer material after any period of ageing at the reference temperature can be readily read off the resulting curve. An example of a time-temperature superposition plot (based in data given in Figure 2.5) is given in Figure 2.7.

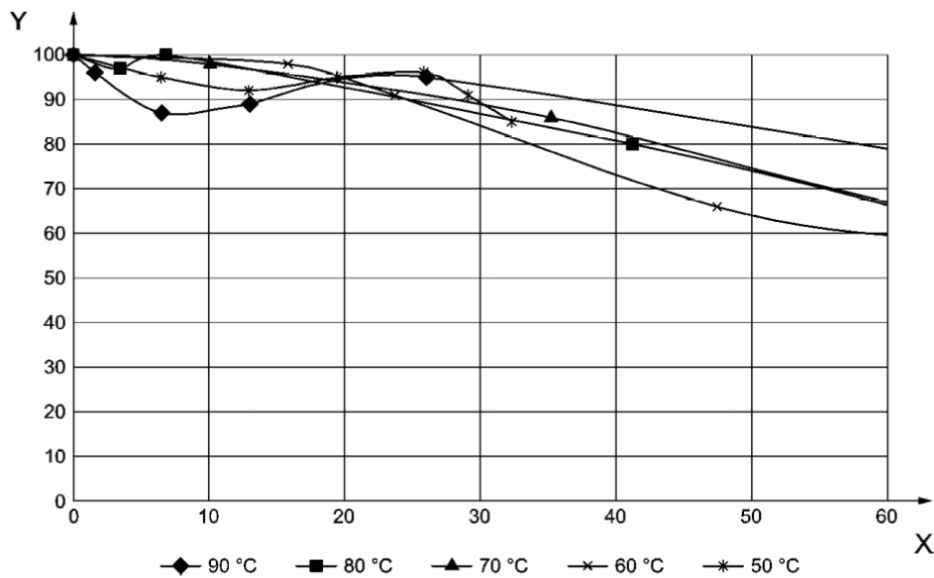


Figure 2.7: Time-temperature superposition plot. Y: Retained force at break in %. X: Time at 25 °C in years.

Note: If 25% of decline in force at break can be tolerated before the polymeric material is at risk of failing the specified requirement then the shelf life will be 38 years.

2.7 Protection and prevention of degradation

Many plastics available can be differentiate from each other by molecular parameters such as (co-) monomer composition, molecular weight, molecular weight distribution, chain branching and end groups, added fillers (e.g., glass, nano-clay, talcum), pigments, and other inherent properties improving additives. All these factors during polymerization and processing are well controlled to produce materials with desired properties. However, once these plastics are exposed to shear stress, heat, light, air, water, radiation, or mechanical loading, chemical reactions can be initiated that lead to changes in molecular weight and chemical composition. In practice this might result in an undesired change (degradation) in appearance (e.g., gloss, texture, and colour) and mechanical properties (e.g., tensile, flexural, or impact strength) (Gijsman 2011).

To protect the polymer against degradation, blends of stabilizers will be used at various stages throughout the polymer life cycle. Stabilizer comes in three varieties based on the type of degradation they prevent: chemical stabilizers (typically antioxidants), thermal stabilizers, and UV radiation stabilizers (Peacock and Calhoun 2006). According to Peacock and Calhoun (2006), the first two act by removing the reactive species during the initiation step. They are radical scavengers that react with radicals to either create a less reactive species or to create a termination reaction, thereby eliminating the radical species. UV radiation stabilizers interact with the photons which may cause degradation of the polymer. They either block the photons from reaching the polymer or absorb the high

energy radiation and emit a lower frequency of light, which does not have the energy necessary to initiate bond cleavage.

2.7.1 Chemical and thermal stabilizers

Chemical and thermal stabilizers both deactivate the by-products of degradation processes, preventing them from causing further damage to the polymer. Their chemical structure and mobility define their effectiveness in any given polymeric system. The most common type of chemical and thermal stabilizers is antioxidants.

Primary antioxidants are radical scavengers such as hindered phenols antioxidants and aromatic amines (Rauwendaal 2002; Peacock and Calhoun 2006; Gupta 2010a; Gijsman 2011; Palmer, 2011). They act by interrupting in the oxidative degradation cycle by scavenging radicals. Primary antioxidants function by donating their reactive hydrogen to the peroxy free radicals so that the propagation of subsequent free radicals does not occur (Palmer, 2011). Their main use is as processing or long-term heat stabilizer. Secondary antioxidants are used in conjunction with primary antioxidants to provide added stability to the polymer. They act against oxidative degradation by decomposing hydroperoxide to form nonreactive product (Peacock and Calhoun 2006; Palmer, 2011). Important classes of secondary antioxidants are phosphites and thioethers (Rauwendaal 2002; Gijsman 2011). Against degradation during processing, mainly phosphites are used, while as long-term heat stabilizer thioethers as well as phosphites are used. However, the effectiveness of the antioxidants depends on which types of polymer

are used (Gijssman 2011). The level of antioxidant used in a polymer system depends on the expected lifetime of the final part, the environment in which the part will be used, and the susceptibility of the polymer to oxidation. Figure 2.8 shows two common antioxidants used in PO.

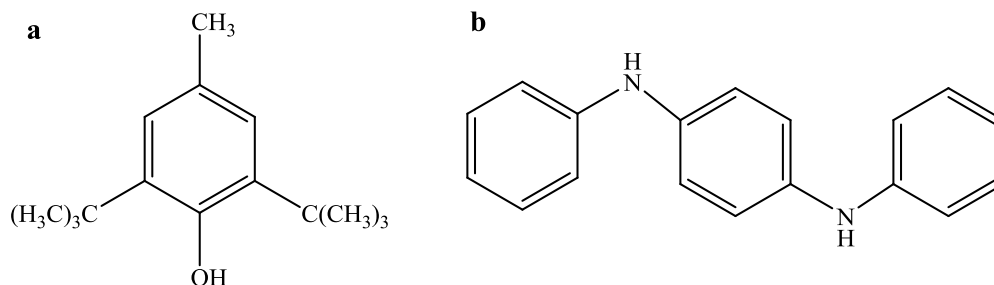


Figure 2.8: Examples of common antioxidants: a: 2,6-*t*-butyl 4-methyl phenol (butylated hydroxy toluene); b: diphenyl-*p*-phenylene diamine.

Certain polymers are particularly unstable during processing and use. The most notorious of these is PVC. The highly reactive chlorine atom easily forms radicals under high shear and heat conditions and can then migrate through the polymer, abstracting a proton and forming hydrogen chloride. The process is autocatalytic, so it is essential to eliminate the radicals before the evolution of hydrogen chloride that damages the processing equipment and degrades the resin further. Different types of stabilizers are used to accomplish this, but all act to remove the radicals. Examples of the thermal stabilizers used in PVC include members of the organo-tin mercaptide family which have a general structure of (RSn(SnR')₃) where R and R' represent organic functional groups (Wirth and Andreas 1977; Bilgic 1998). Lead oxides, and poly-basic lead sulfates (nPbO.PbSO₄.H₂O) are also used as thermal stabilizers (Bilgic 1998; Peacock and

Calhoun 2006). In addition, some bases have been incorporated in PVC formulations to react with the hydrogen chloride produced (Peacock and Calhoun 2006).

2.7.2 Ultraviolet radiation stabilizers

UV radiation stabilizers are chemicals which reduce or inhibit degradation of polymers resulting from UV radiation. It can either block the light from reaching most of the polymer or can absorb the light and then release it as heat. An example of an UV radiation blocker is carbon black (Bilgic, 1998; Shah 2002; Peacock and Calhoun 2006; Gugumus 2009). This material blocks the UV radiation light from penetrating far into the polymer by physically blocking the radiation (Peacock and Calhoun 2006). Carbon black stabilizers are often used in conjunction with UV radiation absorbers. An example of an UV radiation absorber is benzotriazole (Bilgic 1998; Peacock and Calhoun 2006). This molecule act as screen absorbs UV radiation light in the range of 250 to 400 nm and then reemits the energy at a longer frequency and lower energy before they cause damage to the polymer. Blocking stabilizers are typically pigments that can absorb UV radiation to a certain extent and provide some degree of protection (Shah 2002; ASM International 2003). The presence of pigments prevents the light from penetrating far into the polymeric part so that degradation will only occur near the surface. UV radiation stabilizers that absorb the radiation contain strong chromophores, which dissipate the energy they absorb to the surroundings as heat (Peacock and Calhoun 2006).

CHAPTER 3

MATERIALS AND METHODS

3.1 Materials

Non-sterile nitrile medical examination gloves made by polymerizing butadiene, acrylonitrile and methyl acrylate acid are provided by Synthomer Sdn. Bhd. XNBR glove samples are in medium size and blue in colour as shown in Figure 3.1. XNBR latex (coded as 6322) with and without antioxidant are also provided by Synthomer Sdn. Bhd. Analytical grade cyclohexanone used in swelling test was from Merck, Germany.



Figure 3.1: Photograph of XNBR glove sample.

3.2 Method for accelerated ageing and testing

3.2.1 Accelerated treatment

Glove samples with thickness range about 0.085 mm to 0.100 mm were first cut into dumbbell (die C), circle (25 mm in diameter) and square shape (150 mm x 80 mm) before being subjected for accelerated ageing. Accelerated ageing was carried out in air circulated oven at various temperatures between 60°C and 100°C and for duration of between 0.5 and 4000 hours as tabulated in Table 3.1. After accelerated ageing, samples were conditioned in desiccator for at least 16 hours to allow them to reach an equilibrium state before testing. Following the ageing treatment, tensile properties, swelling in cyclohexanone, colour and surface morphology of the samples were tested after ageing and compared to results obtained from the unaged thin film.

Table 3.1: Accelerated ageing temperature and time.

Ageing Temperature (°C)	Ageing Time (day)
60	0, 7, 14, 21, 42, 56, 70, 105, 140.
70	0, 2, 7, 14, 28, 42, 70, 98, 126.
80	0, 0.16667, 0.33333, 2, 7, 14, 28, 42, 56, 70.
90	0, 0.02083, 0.08333, 0.16667, 0.33333, 1, 7, 14, 21.
100	0, 0.02083, 0.04167, 0.08333, 0.16667, 0.33333, 1, 2, 4, 7.

3.2.2 Tensile test

Tensile properties of 13 samples for each batch of glove sample were determined using a Tinius Olsen H10KS tensiometer (Tinius Olsen Limited., United Kingdom) equipped with an extensometer at room temperature (25 ± 2 °C). The distance between upper and lower clamps was set at 60.00 ± 5 mm with a crosshead speed was 500 mm/min. Dumbbell specimens were prepared using a type C die according to ASTM Standard D 412 for tensile properties of elastomers. The thickness of each specimen was taken as an average value of three different positions on the narrow section of the specimen by electronic micrometer, which was 6 mm wide. Two lines 25 mm apart were marked on the narrow section. When the specimen was stretched, the change in the separation of the two lines was recorded by the extensometer (Figure 3.2). The tensile properties of the samples such as tensile strength, force at break and elongation at break were calculated from 13 measured quantities.



Figure 3.2: Photograph of tensile strength measurement.

3.2.3 Solvent swell test

Two disc films with a diameter of 25 mm were prepared for solvent swell test. 20 ml of cyclohexanone was poured into a petri dish using measuring a cylinder. The sample disc film was ensured to be properly soaked into cyclohexanone in petri dish for 30 minutes. The diameter of the films was measured at 5 min, 10 min, 15 min and 30 min respectively by putting the petri dish above a graph paper (Figure 3.3). The results were taken as the average of 2 disc films in percentage of linear swell of dipped films which was calculated using the equation below:

$$\text{Percentage linear swell (\%)} = \frac{(x - 25 \text{ mm})}{25 \text{ mm}} \times 100 \quad \text{Eq. 3.1}$$

* x = diameter of dipped film after a certain period of time

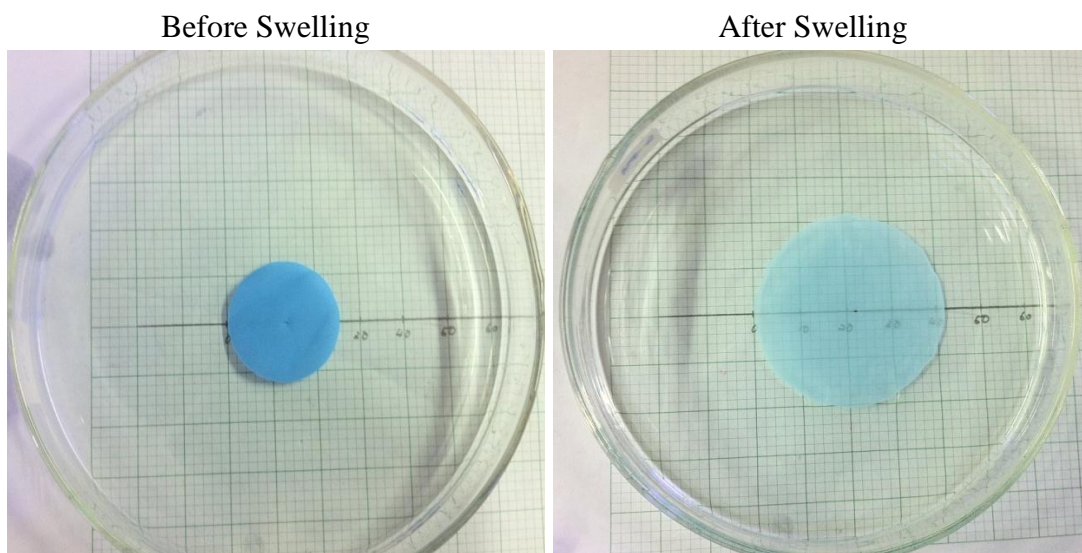


Figure 3.3: Photographs of the measurement of the diameter of the disc in solvent swell test.

3.2.4 Colour test

The colour changes of the samples were measured using Colour Reader Konica Minolta CR-10 (Konica Minolta Sensing Americans, America). The device was calibrated against white standard tile. Colour changes of the samples during accelerated ageing was measured using the L^* , a^* , b^* coordinates of the CIEL*a*b* (Commission International de l'e'clairage) 1967 colour space as shown in Fig. 3.4 (Rosu, Rosu and Cascaval 2009). The total colour changes (ΔE) as a function of the accelerated ageing treatment were calculated with Equation 3.2, using the corresponding untreated material as reference:

$$\Delta E = \sqrt{(L_2^* - L_1^*)^2 + (a_2^* - a_1^*)^2 + (b_2^* - b_1^*)^2} \quad \text{Eq. 3.2}$$

where subscript 1 denotes the values before ageing and subscript 2 denotes the values after ageing, L^* represents the grey value, which varies between 0 (black) and 100 (white), positive values of $(a_2^* - a_1^*)$ describe a red shift, negative values of $(a_2^* - a_1^*)$ describe a green shift, positive values of $(b_2^* - b_1^*)$ describe a yellow shift and negative values of $(b_2^* - b_1^*)$ describe a blue shift. Each colour difference reported is the average of two samples, with an average of three measurements of each sample.

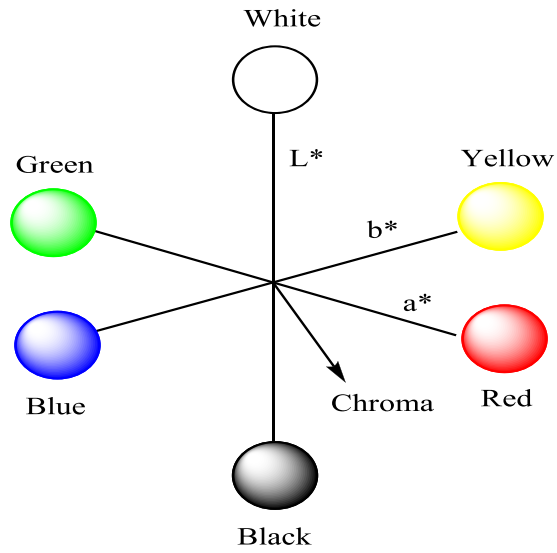


Figure 3.4: Chromaticity coordinates of L^* , a^* and b^* .

3.2.5 Scanning electron microscopy (SEM)

The surface morphology of the specimens was observed by SEM (JSM-6701F, JEOL Limited, Japan) at a tension of 2 kV in secondary electron mode, magnification at X2500. SEM scanning was carried out for unaged and aged samples. The specimens were sputter coated with platinum to minimize charge accumulation and beam damage (Figure 3.5).

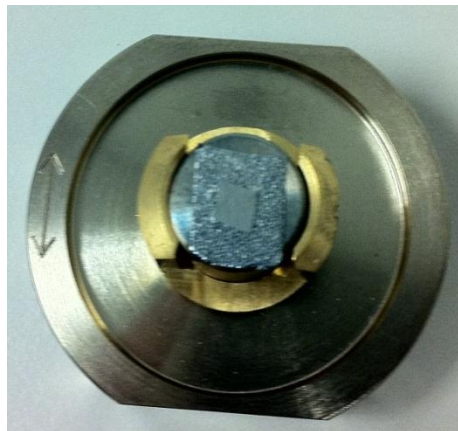


Figure 3.5: Photograph of the thin film sample coated with platinum.

3.3 Method for real time ageing

Real time ageing was carried out by storing the fresh gloves in laboratory at about 26 °C in commercial packaging and humidity about 65%, both in ambient light (or under fluorescent lamp, 36 watt) with a distance of 2 meter above and in dark condition (inside a drawer). Both of the samples in ambient light and in dark condition were tested after 1 month, 2 months, 3 months, 6 months, 9 months, 12 months and 15 months for the four tests stated in Part 3.2.2 to 3.2.5 (Tensile test, solvent swell test, colour test and SEM scanning).

3.4 Mechanism study

3.4.1 Thin film casting

Thin films were casted using XNBR Latex 6322 diluting in a beaker using distilled water in a ratio of 5:1. Diluted latex was properly dropped on the surface of a glass sheet using a dropper. Bubbles were removed and excess latex was drained back to the beaker. Cast thin film was then dried in an oven at 60 °C for 30 minutes. After dried, the casted thin film was immersed in distilled water for 5 minutes in order to ease peeling. Thin film was placed on a card holder followed by drying in an oven for another 10 minutes (Figure 3.6). Thickness for cast film was measured by electronic micrometer which is around 0.020um.



Figure 3.6: Photograph of XNBR Latex Thin Film.

3.4.2 Accelerated ageing of thin film

Accelerated ageing treatment was carried out at 70 °C for 12 weeks and 90 °C for 4 weeks in an air circulated oven. After accelerated ageing, samples were conditioned in desiccator for at least 16 hours to bring them into an equilibrium state before FTIR characterization.

3.4.3 Fourier transform infrared (FTIR) characterization

Chemical changes were detected by FTIR Spectrometer Spectrum RX 1 (Perkin Elmer Incorporated, America) during the ageing of the samples. FTIR characterization was carried out for the cast film samples aged at temperatures 70 °C and 90 °C at a week intervals. For comparison, FTIR characterization was also performed for unaged cast film samples, which corresponded to the original state of the polymer cast films.

3.5 Lifetime prediction

For lifetime prediction, two models applied in this study, the first was based on BS EN 455:4 (2009), which aims at the determination of the time required to reach a specified threshold for a specific physical property of polymers in general. This model is based on a direct application of the force at break criterion to the Arrhenius relationship. The advantage of this approach is that it is rather simple and straight forward and easy to apply to the experimental data directly. In comparison to British Standards, the second model does not need a prior definition of a failure criterion. Time-temperature superposition method proposed by Wise, Gillen and Clough (1995) and Gillen, Celina and Keenan (2000) is based on the superposition of ageing curves at different temperatures to a master curve by a horizontal shifting procedure by applying application of the time temperature equivalency. The shift factors obtained are then analysed in term of Arrhenius relationship.

CHAPTER 4

RESULTS AND DISCUSSION

4.1 Accelerated ageing and real time ageing

In general, short term effects are physical and reversible when the temperature is returned to ambient, whilst the long term effects at elevated temperature are mostly chemical and not reversible. The long term chemical effects are usually referred to as the results of ageing.

Thermal ageing of rubber is taken to mean the effect of elevated temperatures for prolonged periods but heat ageing treatments are carried out for two distinct purposes. First, it can be intended to measure changes in the rubber at the (elevated) service temperature or, secondly, it can be used as an accelerated test to estimate the degree of change which would take place over much longer times at normal ambient temperature.

In order to investigate the effect of thermal ageing on the physico-mechanical properties of XNBR thin film, accelerated ageing were carried out in air circulated oven at various temperatures between 60 °C and 100 °C and for duration between 0.5 and 4000 hours. Real time ageing was carried out under two conditions; under the fluorescent light and in dark condition for fifteen months at room temperature (26 °C). Changes in tensile strength, linear swell, colour and

surface morphology after the ageing treatment were compared with the unaged thin film.

4.1.1 Accelerated ageing

4.1.1.1 Tensile test

During thermal ageing, main chain scission, crosslink formation and crosslink breakage can take place. If crosslinking dominates during ageing, the elastomer hardens and embrittles resulting in increases in tensile stress at a given elongation, increases in hardness, and decreases in ultimate elongation. This is the general behaviour of butadiene-based material such as polybutadiene, styrene-butadiene rubber, and acrylonitrile-butadiene rubber (Tung 2007).

It is also noticed that the rubber became rigid after high temperature ageing and losing all elasticity which can be associated with both crosslinking reactions and lubricant loss (Delor-Jestin et al., 2000). The tensile strength and elongation at break are related to the crosslinking density of the rubber vulcanisates. These changes are directly associated with changes in the original crosslink structure, such as main chain scission and crosslink modifications (Yahya, Azura and Ahmad 2011).

The dependence of the tensile strength and elongation at break on thermal ageing is shown in terms of relative tensile strength values and relative elongation at break values (defined as the ratio of tensile strength values or elongation at

break values in aged and the unaged reference state in %) in Figure 4.1 and 4.2. Each data point typically represents the average result of thirteen identically aged samples. Thickness of the samples range from 0.085 mm to 0.100 mm.

For all the temperatures tested in Figure 4.1, the relative tensile strength demonstrates a trend which increases at the beginning to a maximum peak at a given ageing time before it decreases with prolonged ageing time. A more steady decrease is observed after the maximum for the lower temperatures. The test at 100 °C show more dramatic decrease after the maximum peak for tensile strength as compared to other temperatures. As the temperature increases from 60 °C to 100 °C, the time to obtain the maximum is also decreases during the accelerated ageing. For instance, at 60 °C and 100 °C, the characteristic times to reach the maximum are around 70 days and 2 days respectively. The drop for tensile strength is more pronounced at higher ageing temperatures.

The relative elongation at maximum property for XNBR thin film samples after thermal ageing at temperature between 60 °C and 100 °C for different duration of time is shown graphically in Figure 4.2. The elongation at maximum data have a relatively large standard deviation makes it difficult to define clear trends. This large standard deviation might cause by the impurities or defects on the manufacturing of the film. However, it is clear that thermal ageing caused gradually decreases of the elongation for all temperatures from the beginning of until the end of the experiment, which means that ageing steadily takes away its

rubber-likier property. Higher the thermal ageing temperature will decrease the elongation at maximum in faster speed.

Instead of look into the singe data point, a broad view of the data will be preferred. During the earlier stages of thermal ageing, crosslink scissions and the formation of new crosslinks into the stable networks affected these properties. Fluctuations of some of the points probably are cause by the balancing between the crosslink scission and the crosslink formation in the polymer. In fact, both crosslink scission and crosslink formation occur simultaneously, and these reactions occur all the time in the ageing treatment. The thermal ageing of XNBR results in an increase in the tensile strength and decrease in the elongation at break indicating that crosslinking dominates during the early stage of ageing.

Additional network chains due to crosslinking increase the molecular weight and create branched molecules. It is more difficult for these branched molecules to disentangle and so, strength is enhanced (Ratnam, Chantara and Mohd 2006; Tung 2007). However, the initial increase of the relative tensile strength values might be also due to the incomplete crosslink in the cured rubber system.

The tensile strength increases rapidly to give a maximum peak for all temperatures, probably from an optimized balance between the strength enhancement from additional crosslink formation during the ageing treatment and the capability of the crosslinked network to dissipating strain energy. On further

ageing after the characteristic time, crosslink scission become dominant as compare to crosslink formation which results in main chain degradation. Thus, caused a drastic reduction of both tensile strength and elongation properties at the ending stage of the ageing treatment (Ha-Anh and Vu-Khanh, 2005; Choudhury, Bhowmick and Soddemann 2010).

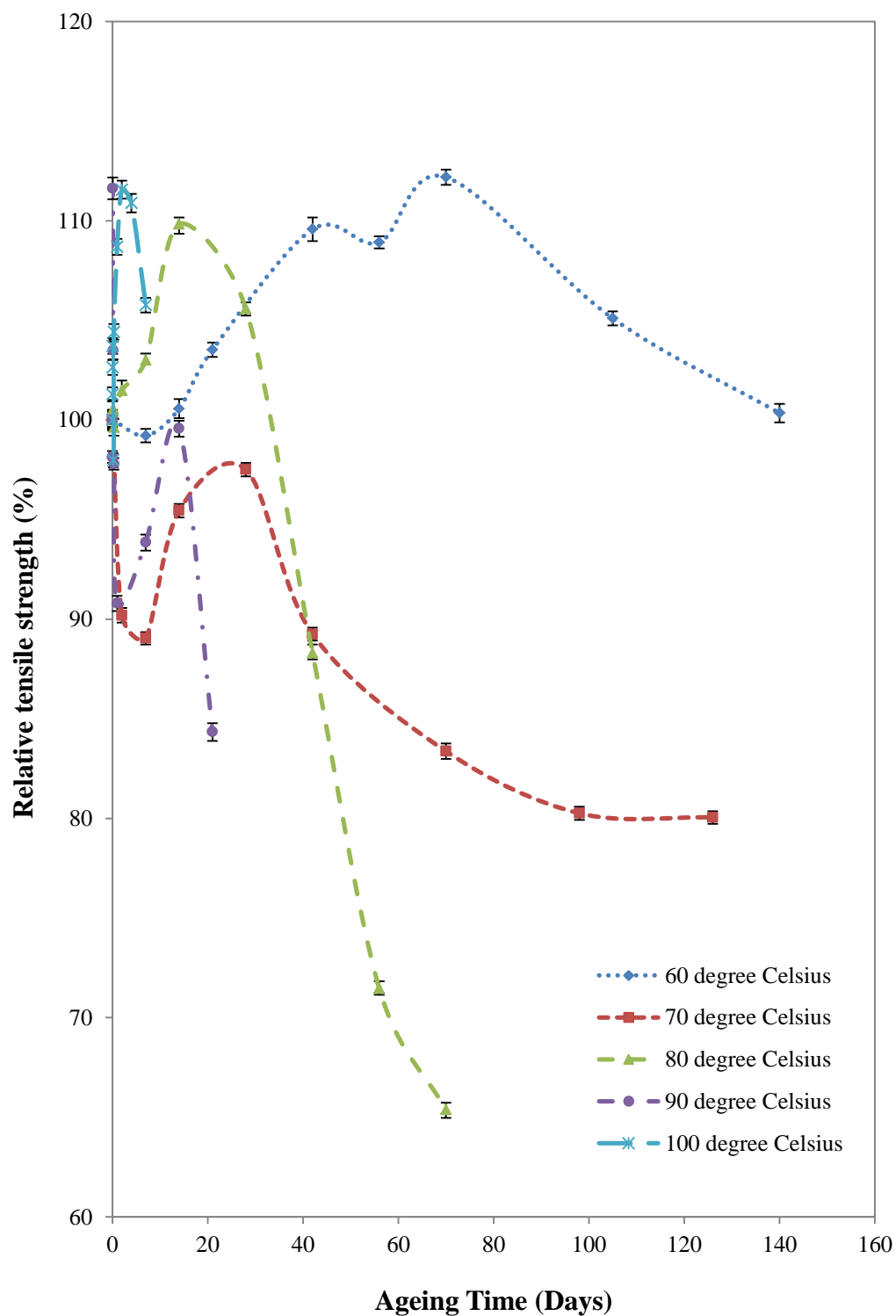


Figure 4.1: Changes in the relative tensile strength of XNBR thin film as a function of ageing time at various temperatures.

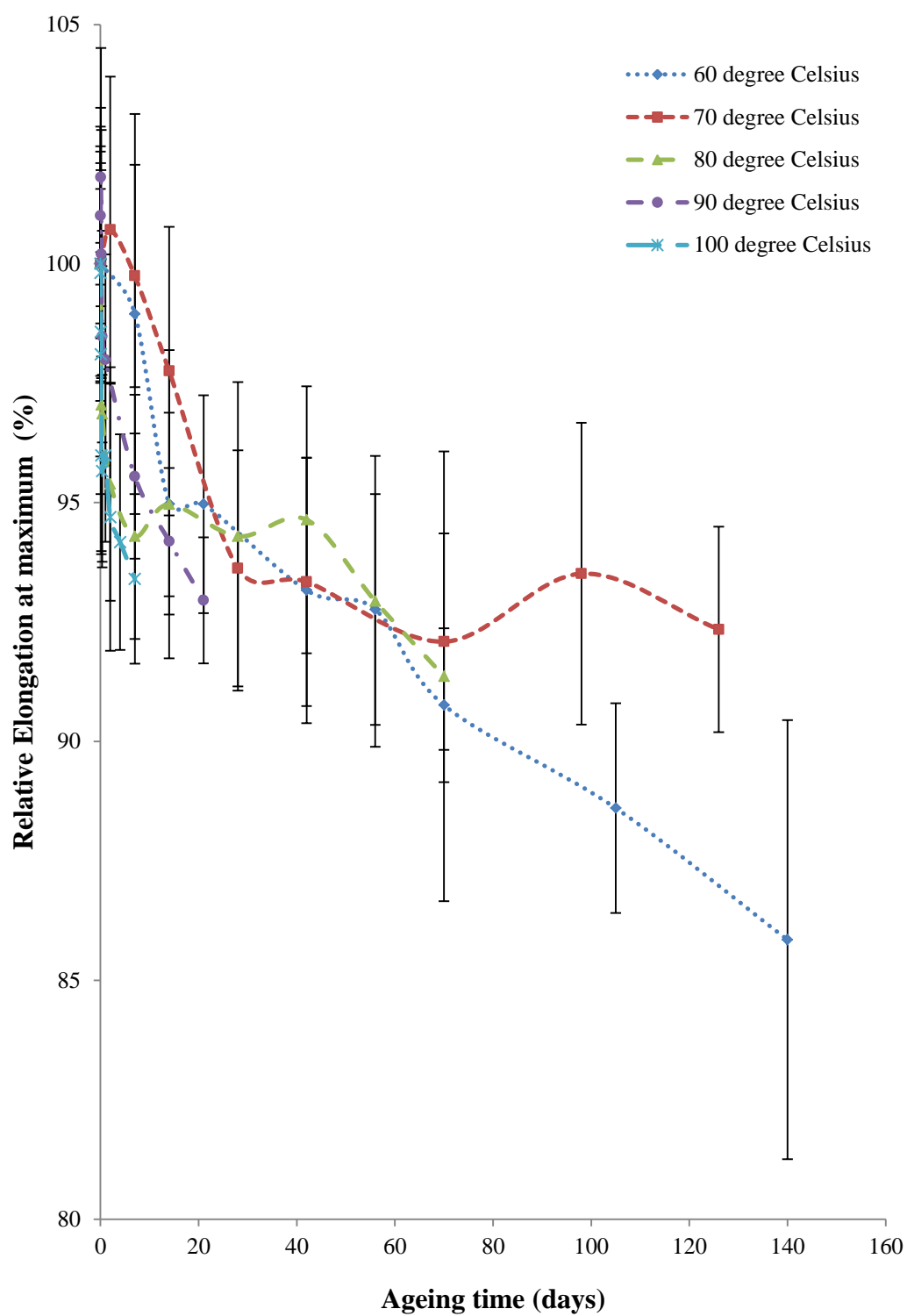


Figure 4.2: Changes in the relative elongation at maximum of XNBR thin film as a function of ageing time at various temperatures.

4.1.1.2 Solvent swell test

Figure 4.3 shows the relative linear swell (defined as the ratio of linear swelling percentage values in aged and the unaged reference state in %) of the XNBR thin film over various ageing periods at different temperature.

The results show that before ageing treatment, the relative linear swell is 80% for all the temperature range. Upon accelerated ageing, the linear swell shows decreasing pattern for all temperatures but the changes are more pronounced as the temperature was increased from 60 °C to 100 °C. The relative linear swell decrease more rapidly as the temperature increased. The relative linear swell starts to decrease to 78% and 74% after ageing for 168 hours at 60 °C and 4 hours at 100 °C. The linear swell is related to the crosslink density of the elastomers. The early stage of decreases can be explained by the formation of crosslink is dominant over main chain scission and crosslink breakage. Increase of crosslinking in the rubber, resulted in an increase in the network elasticity contribution. As explained by Ha-Anh and Vu-Khanh (2005), higher crosslink density results in closer molecular chains and thus an increase in intermolecular forces. These crosslinks restricted the extensibility of the elastomer chains induced by swelling and made it more difficult for the solvent to diffuse between the gaps of the elastomer molecules. This decreased swelling of the sample and, thus, countered any tendency for dissolution. Therefore, the linear swell decreased with increasing network. However, the relative linear swell reached a constant value at around 60% of swelling. The decreases to a constant value may be caused by chain scission of the

backbone resulted by prolonged ageing. Loss of lubricant and embrittlement of the sample may be also one of the factors causing the decrease on its swelling property.

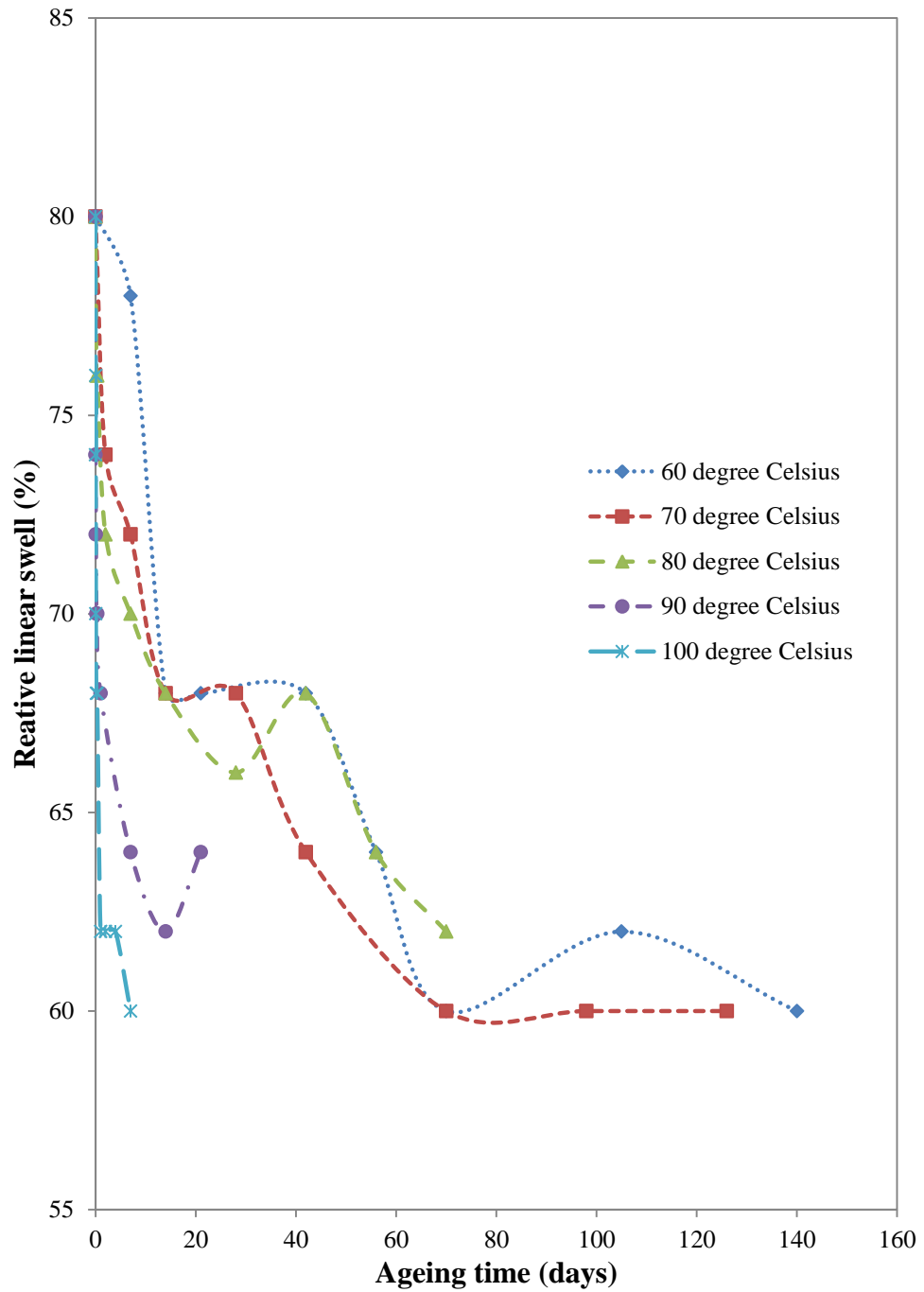


Figure 4.3: Changes in the relative linear swell of XNBR thin film as a function of ageing time at various temperatures.

4.1.1.3 Colour measurement

Aged samples suffer an intense and irreversible colour change during the thermal ageing treatment basically due to the formation of chromophores. The observed colour change is strongly dependent on temperature. At lower temperature, a noticeable yellowing is observed only after 3000 hours of ageing at 60 °C; however, at 100 °C the samples appear clearly more yellow after 24 hours of ageing and brown materials are observed at the end of ageing (7 days at 100 °C). Figure 4.4 shows the total colour differences (ΔE) of the samples measured before and after thermal ageing at different temperatures for various duration of time. The total colour differences (ΔE) values in Figure 4.4 confirmed that both the final colour and discolouration rate are depending on temperature. Higher temperature accelerates the chemical reaction in ageing, speed up the formation of chromophores and yellowing is observed much earlier as compared to lower temperature.

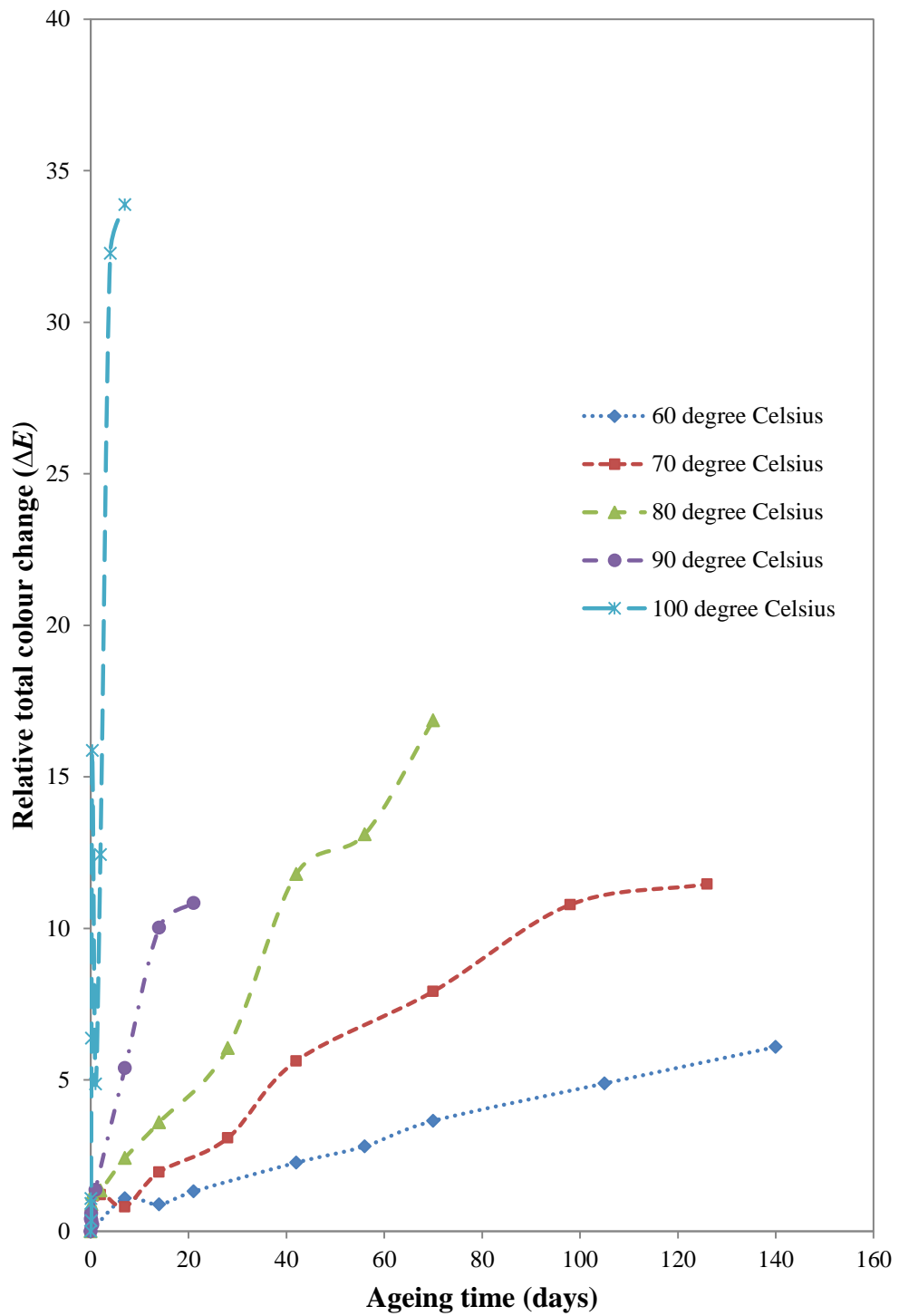


Figure 4.4: Changes in the relative total colour change (ΔE) of XNBR thin film as a function of ageing time at various temperatures.

4.1.1.4 Scanning Electron Microscopy (SEM)

The surface morphology of the XNBR thin films were investigated using SEM. The SEM image for unaged sample presented in Figure 4.5a shows a homogeneous morphology without cracking. The SEM images of samples exposed to accelerated ageing at 60 °C (56 and 140 days), 70 °C (70 and 126 days), 80 °C (42 and 70 days), 90 °C (14 and 21 days) and 100 °C (4 and 7 days) are shown in Figure 4.5b – 4.5g respectively. The first microcrack detected on the film surface were 56, 70, 42, 14 and 4 hours for the samples aged at 60 °C, 70 °C, 80 °C, 90 °C and 100 °C respectively. The number of microcraks increased upon prolonged ageing period and at higher ageing temperature.

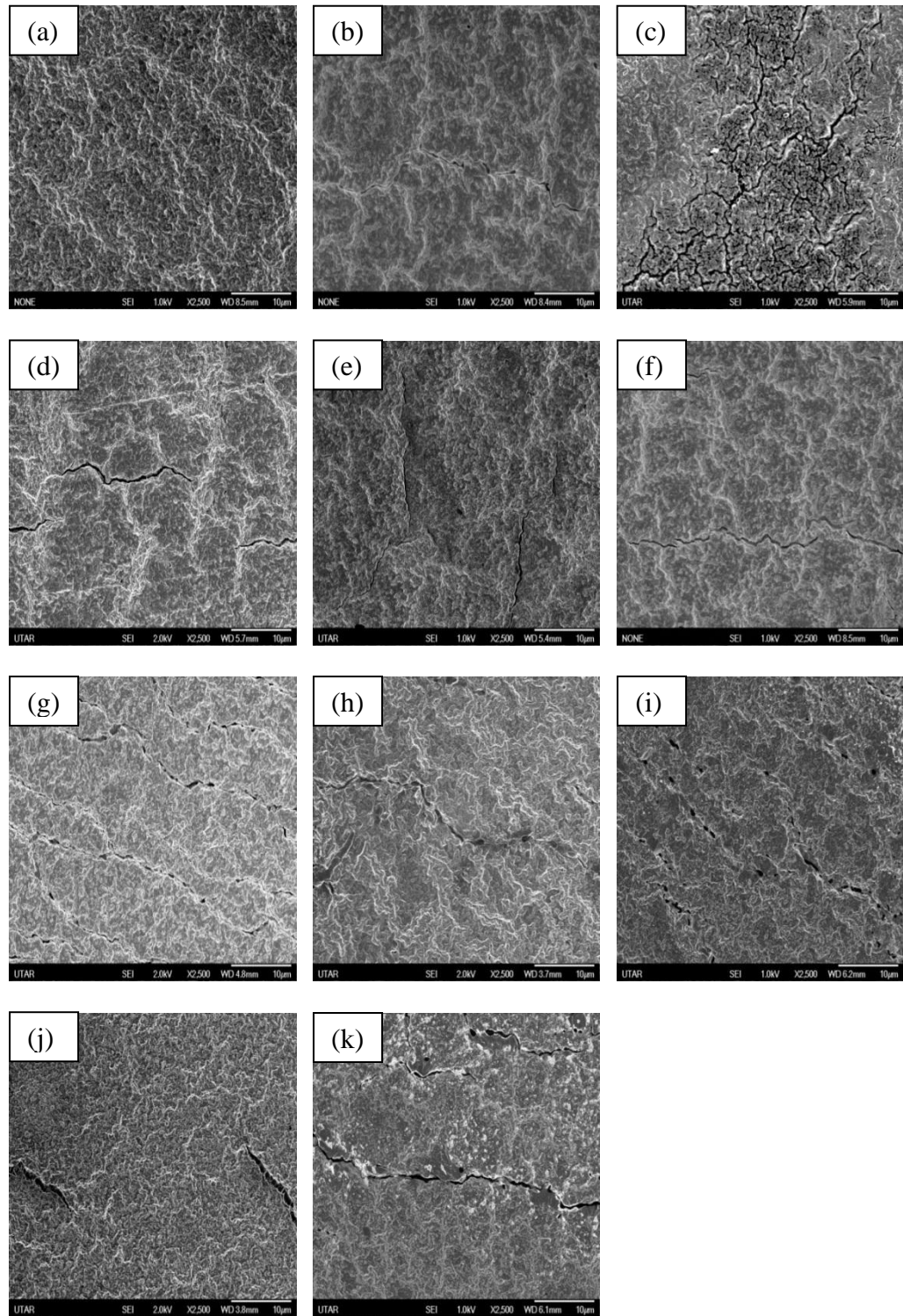


Figure 4.5: SEM images for unaged sample (a), aged at 60 °C for 56 (b) and 140 days (c), aged at 70 °C for 70 (d) and 126 days (e), aged at 80 °C for 42 (f) and 70 days (g), aged at 90 °C for 14 (h) and 21 days (i) and aged at 100 °C for 4 (j) and 7 days (k).

4.1.2 Real time ageing

4.1.2.1 Tensile Test

Effect of real time ageing on tensile strength and elongation at maximum were shown in Figures 4.6 and 4.7. During the ageing, crosslink formation and crosslink scission were taken place simultaneously. The fluctuation at the early stage of the ageing is due to the stability enhancement between the crosslink formation and crosslink scission until a maximum was reached. In broad view, both tensile strength and elongation at maximum are decreases when increases ageing time. As compared to accelerated ageing, the decrease of these properties upon real time ageing is much slower, however, their trends are similar. The lowest value for tensile strength and elongation at maximum is not more than 80% of retained strength and elongation after fifteen months of ageing. In generally, the effect of real time ageing under florescent light is more pronounce than in dark condition. In fact, UV is one of the potential degradation agents.

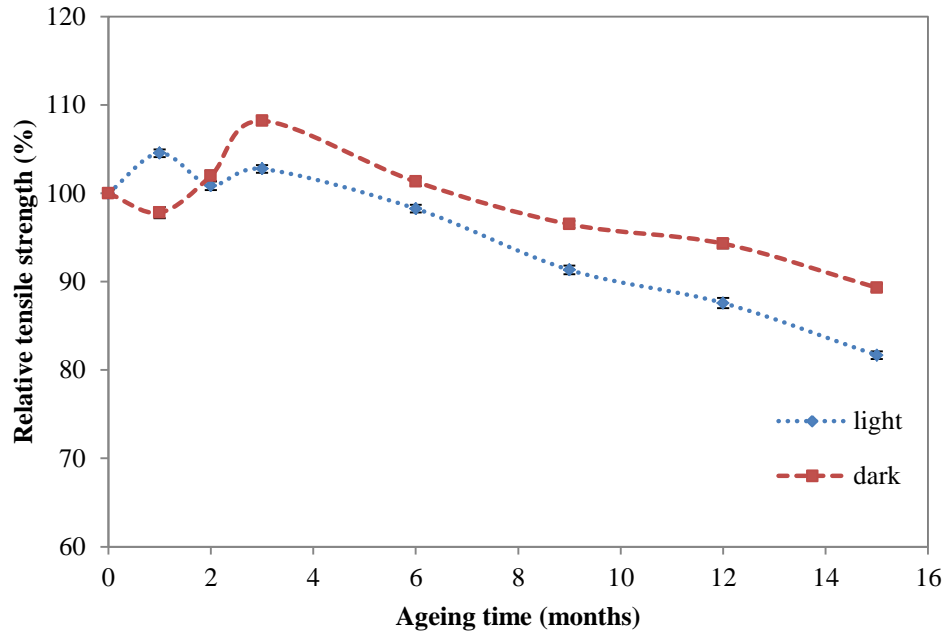


Figure 4.6: Changes in the relative tensile strength of XNBR thin film as a function of ageing time for real time ageing.

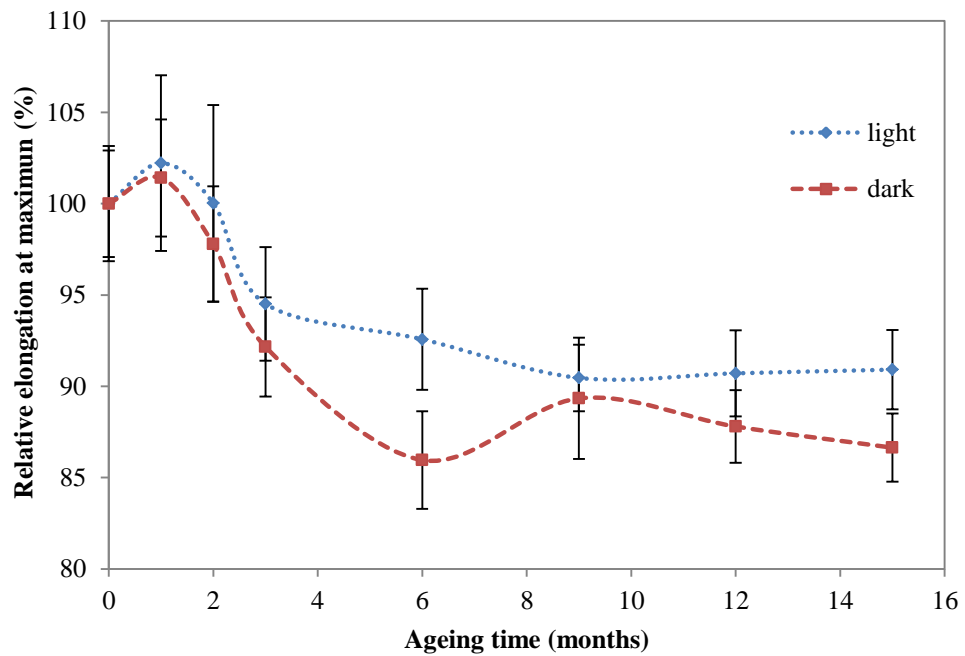


Figure 4.7: Changes in the relative elongation at maximum of XNBR thin film as a function of ageing time for real time ageing.

4.1.2.2 Solvent swell test

Results of solvent swell test were shown in Figure 4.8. Solvent swell for samples at real time ageing shows a decrease at the early stage and reach a constant at around 60% of the swelling percentage as in accelerated ageing, but in a slower rate. The trends for both conditions (under florescent light and dark condition) are similar. In fact, there is a difference between light condition and dark condition at month twelfth about 2% differences, however this difference is not significant enough to make any judgment. In real time ageing, it took fifteen months to reach 66% of swelling percentage. However, in accelerated ageing it only took ten weeks at temperature 60 °C, and only took one week at higher temperature (100 °C).

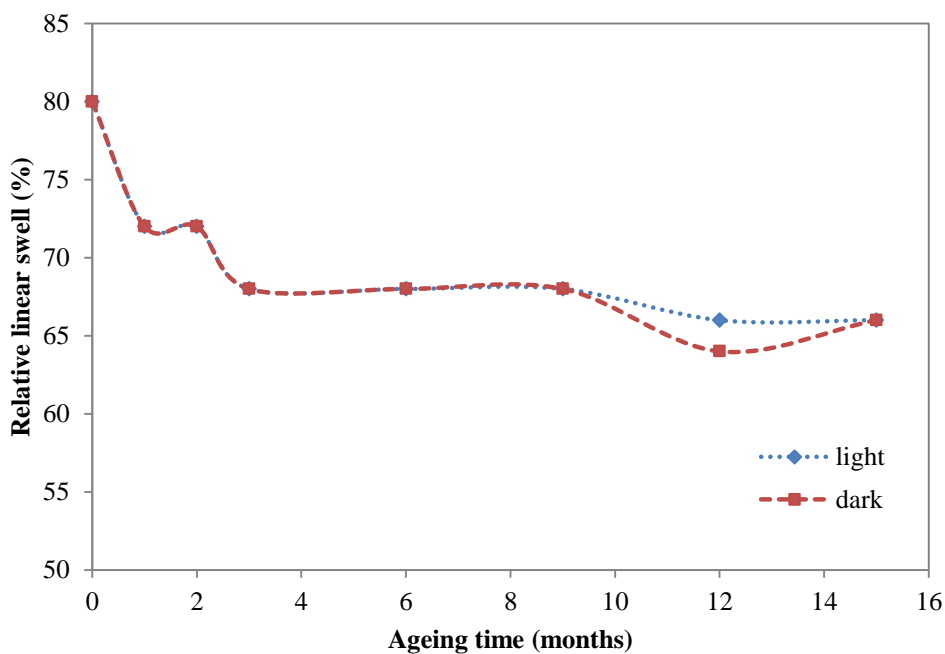


Figure 4.8: Changes in the relative linear swell of XNBR thin film as a function of ageing time for real time ageing.

4.1.2.3 Colour measurement

After fifteen months of real time ageing, no yellowing was observed and the samples retained its original colour which is blue. As shown in Figure. 4.9, the total colour change (ΔE) is inconsistent and the highest value for total colour change (ΔE) is 1.3 for real time ageing under fluorescent light. This value is much lower than that found in accelerating ageing, and the changes of the colour cannot be observed by visible eyes. This low intensity of the total colour change (ΔE) value is most probably caused by the background noise and it is not significant enough to conclude that there is colour change on the samples cause by real time ageing.

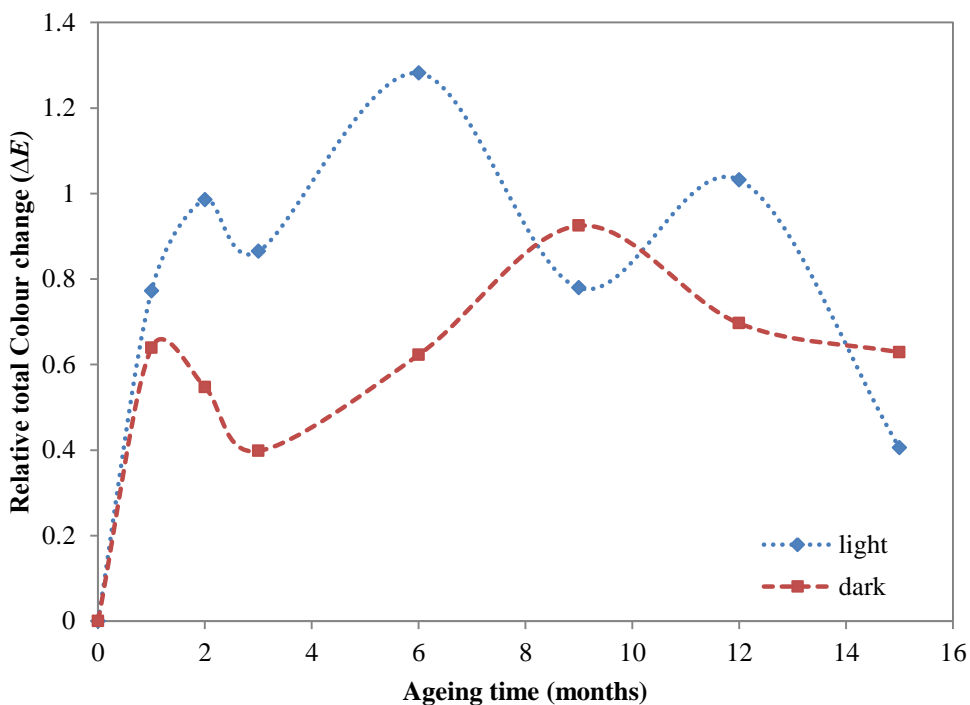


Figure 4.9: Changes in relative total colour change (ΔE) of XNBR thin film as a function of ageing time for real time ageing.

4.1.2.4 Scanning Electron Microscopy (SEM)

For morphology study, the first crack was observed at the ninth month of ageing under fluorescent light while for samples in the dark condition, no crack was observed after fifteen month of ageing treatment (Figure 4.10).

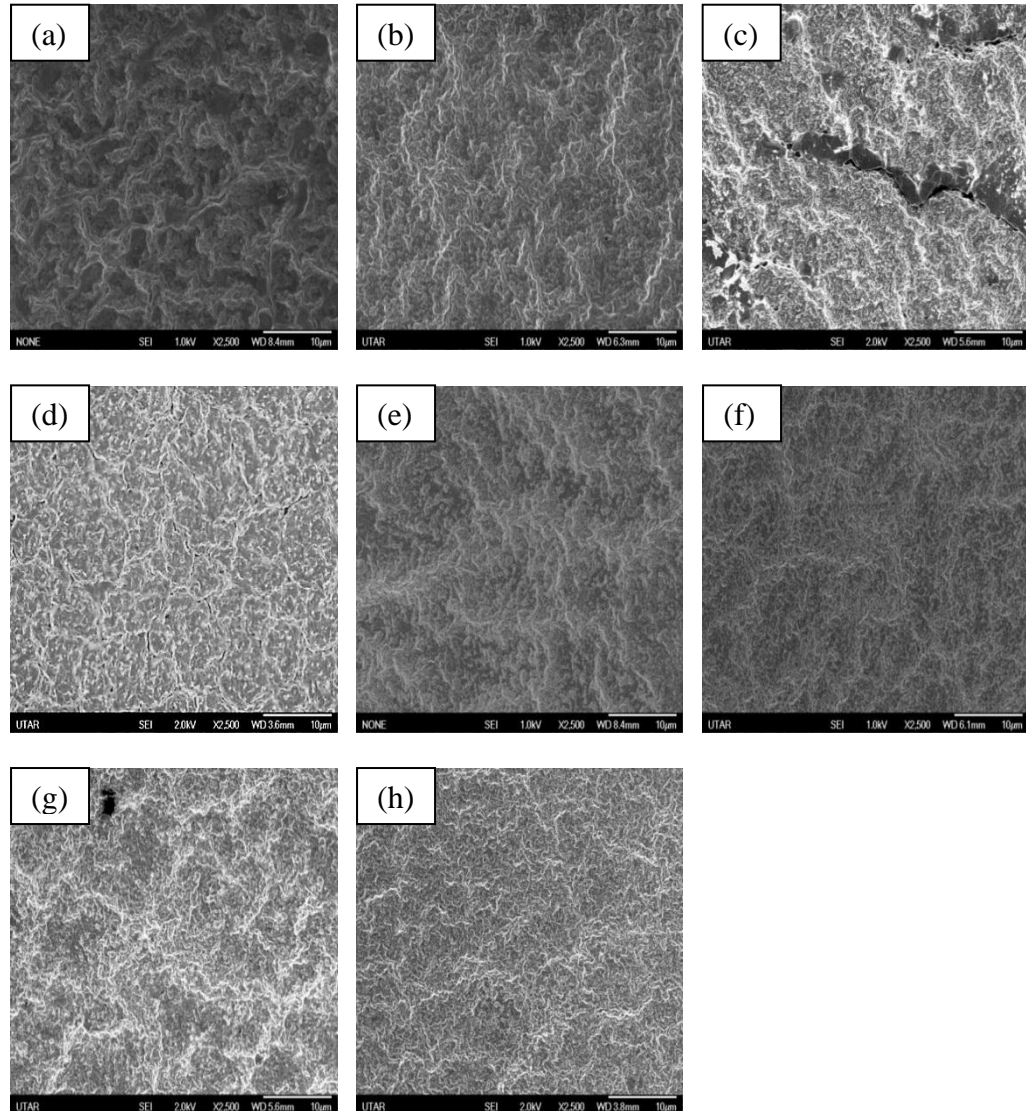


Figure 4.10: SEM images for real time ageing under fluorescent light for 1 month (a), 3 months (b), 9 months (c) and 15 months (d) and in dark condition for 1 month (e), 3 months (f), 9 months (g) and 15 months (h).

4.2 Lifetime prediction

4.2.1 Application of the Arrhenius equation to predicting shelf life

Generally, the useful life of a rubber component is governed by its susceptibility to failure by either mechanical or chemical deterioration. In a laboratory study chemical degradation can be accelerated by ageing the compound at temperatures higher than the intended service temperatures. Such accelerated testing has a long history in the rubber industry (Morrell, Patel and Skinner 2003, Woo and Park 2011). The short time, high temperature degradation behaviour is extrapolated to yield predictions of the property deterioration expected for long time, lower temperature exposure, with quantitative predictions of lifetimes obtained through the use of the Arrhenius relation (Roland 2009).

The shelf life of a rubber product is predicted based on the Arrhenius principle of chemical reaction rates. Chemical processes generally accelerate exponentially as the temperature is increased and in many case the change in rate with temperature can be described by the well-known Arrhenius relationship. A typical Arrhenius approach has been utilized to analyse shorter-term high temperature accelerated ageing exposures and then to extrapolate these results to make long-term predictions at the much lower ambient temperature of interest. This approach is based on the assumption that the degradation involves an activated chemical process whose rate is proportional to $\exp(-E_a/RT)$ where E_a is

the activation energy, R is the universal gas constant and T is the absolute temperature in Kelvin.

$$K(T) = A e^{-E_a/RT} \quad \text{Eq. 4.1}$$

Once an E_a value is obtained empirically from the accelerated experimental results at high temperatures, it can be used to make extrapolated predictions at lower temperatures with the assumption that E_a remains constant over the extrapolated temperature range (Gillen, Bernstein and Celian 2005a). If the overall degradation mechanism remains unchanged throughout the experimental temperature range, the logarithm of the time to a given amount of degradation (property change) should be linearly related to the inverse absolute temperature, yielding Arrhenius behaviour (Gillen et al., 1996; Kahlen, Wallner and Lang 2010).

Implicit in this approach, it is assumed that the reactions at the service temperature are the same as those at the testing temperatures, that the activation energy is independent of temperature and that the chemical changes relate directly to the physical properties measured (Wise, Celina and Clough 1995; Huy and Evrard 1998; Brown 2001). The widely recognized inherent weakness of the Arrhenius approach is the quality of the latter assumption which is not known in prior, and may depend on many factors, for example, competition either between multiple oxidation mechanisms within a material or between oxygen reaction and diffusion could lead to temperature dependent activation energies (Wise, Gillen and Clough 1995).

In order to predict the service lifetime, accelerated ageing was carried out with air-circulated oven at the temperature ranging from 60 °C to 100 °C for a period ranging from 30 minutes to 140 days. Figure 4.11 shows in terms of relative median of retained force at break (defined as the ratio of median of retained force at break in aged and the unaged reference state in %) for five different temperatures.

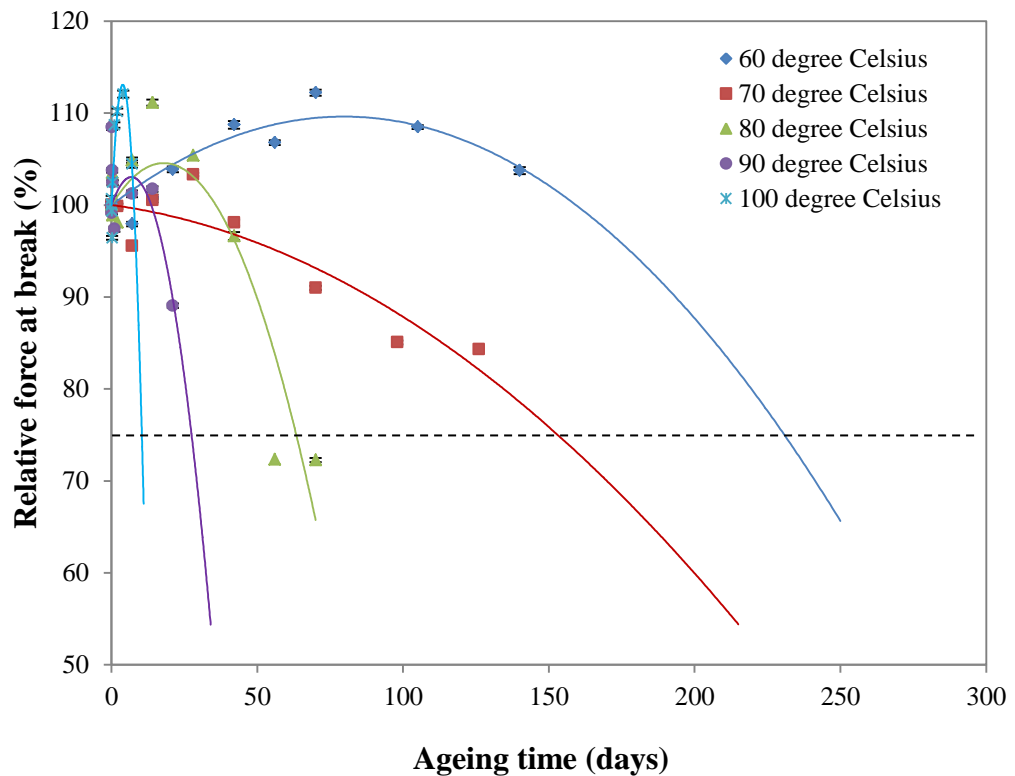


Figure 4.11: Variation of relative force at break of XNBR thin film with ageing time at various ageing temperatures.

According to British Standards Institution (2009), to construct an Arrhenius plot, a specific physical property and a predetermined threshold is requested. A median of force at break and threshold value of 75% retained force at break of the original value was chosen. From Figure 4.11, the time required for each temperature to reach the threshold of 75% retained force was tabulated in Table 4.1 below:

Table 4.1: Time required to reach the threshold of 75% retained force.

Temperature (°C)	1/T (K ⁻¹)	Time (days)
60	0.00300	230.80877
70	0.00292	153.06729
80	0.00283	63.36035
90	0.00275	27.44257
100	0.00268	10.38562

For data analysis and extrapolation, British Standards Institution 2009 recommends applying the method of least squares to the experimental data. The graphical application of the above relationship to the existing experimental data generated for XNBR thin film after accelerated ageing in air-circulated oven along with extrapolations to lower temperatures for the criterion of force at break is shown in Figure 4.12. Also indicated in the figures is the quality of the linear fit in terms of regression coefficients which is equal to 0.9754.

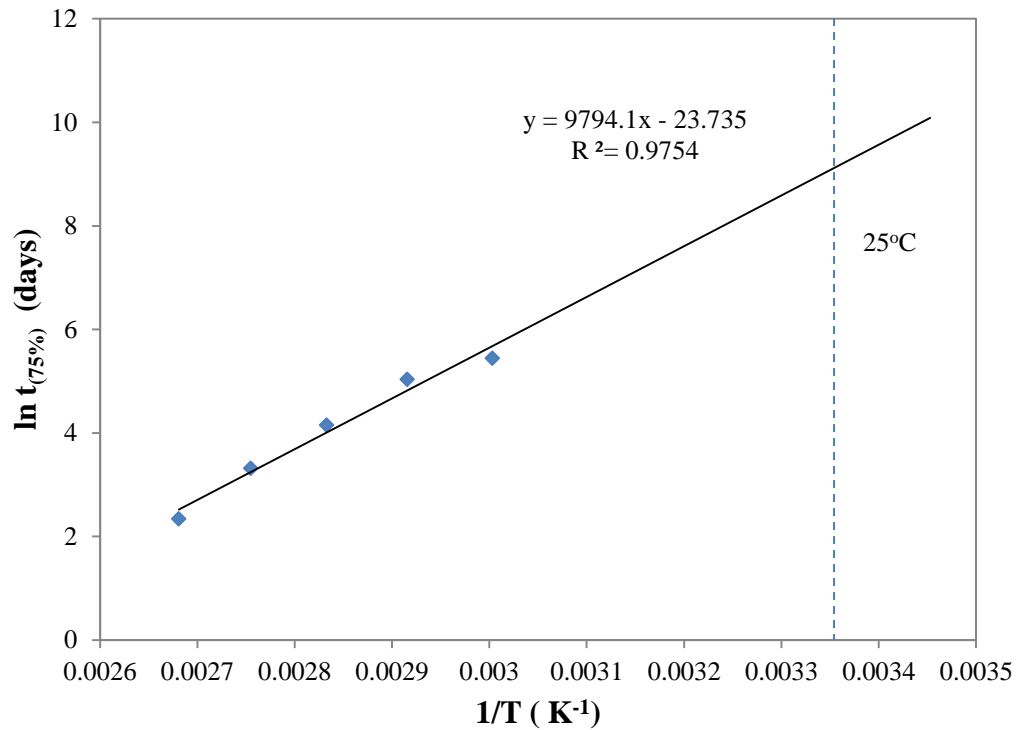


Figure 4.12: Arrhenius plot of retained force at break at 75% for XNBR thin film.

Using Equation 2.10 in Chapter 2, the activation energy and the time for the property to reach the specific threshold at 25 °C can be easily calculated. From Figure 4.12, the time estimated for the physical properties to fall to 75% is 25 years at 25 °C. From the slope of the straight line, activation energy of 81.43 kJ/mol is obtained using Equation 2.10 in Chapter 2. Typical activation energies for many chemical reactions are an average of 83 kJ/mol although the actual values found in practice vary widely (British Standards Institution 2009). Mott and Roland (2001) found the activation energies of ageing of natural rubber in air and seawater are 90 ± 4 and 63 ± 3 kJ/mol, respectively.

Huy and Evrard (1998) stated that ageing is a complex mechanism resulting from a combination of several elementary processes that may have different activation energies. Choosing the 70%, 75% and 80% of the retained force at break of XNBR thin film as failure criteria, the corresponding time to reach these limits are presented in Table 4.2. The linear and parallel plots of the natural logarithm of time for physical properties to fall to 70%, 75% and 80% with various ageing temperatures of XNBR thin film is shown in Fig. 4.13 which suggests that the effective activation energy may remain unchanged throughout the experimental temperature range and the change in force at break during ageing is controlled by Arrhenius behaviour. In another word, it has constant activation energy in the range of experimental test. Average slope of these straight lines gave global activation energy of 81.33 kJ/mol.

Table 4.2: Time required to reach the threshold of 70%, 75% and 80% retained force at break.

Temperature (°C)	1/T (K⁻¹)	Time (days) at 70%	Time (days) at 75%	Time (days) at 80%
60	0.00300	241.35721	230.80877	219.46707
70	0.00292	169.90428	153.06729	134.48708
80	0.00283	67.05799	63.36035	59.33429
90	0.00275	29.20718	27.44257	25.51224
100	0.00268	10.80226	10.38562	9.94060

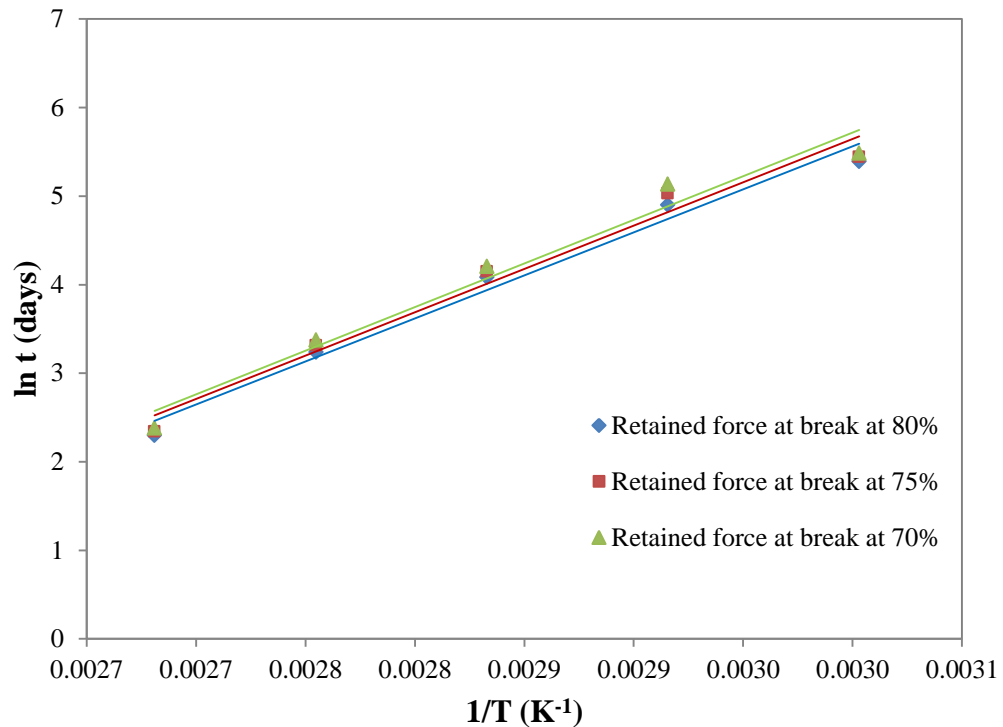


Figure 4.13: Arrhenius plot of retained force at break at 70%, 75% and 80% for XNBR thin film.

4.2.2 Application of the time-temperature superposition method to predict shelf life

Time-temperature superposition approach according to Wise, Gillen and Clough 1995; Gillen, Celina and Keenan 2000, Gillen, Bernstein and Derzon 2005b; British Standards Institution 2009; Kahlen, Wallner and Lang 2010 and others is based on the application of the time temperature equivalency principle. In comparison to the Arrhenius model this model does not require to define a failure criterion in advance. This approach defines the extension or reduction of lifetimes at temperatures other than the reference temperature, as multiplicative

factors to the lifetime at a given temperature, which may be based on any type of failure criterion.

An important prerequisite for the applicability of this approach is the fulfilment of the self-similarity criterion (i.e., the shape of the characteristic ageing curves is similar for different temperatures) (Wise, Gillen and Clough 1995, Kahlen, Wallner and Lang 2010). The data in Figure 4.11 are plotted against the ageing time since this allows us to visually determine how the shapes of the curves compare as a function of temperature. When raising the ageing temperature in order to accelerate degradation, the fundamental underlying assumption is that all reactions are accelerated equally. This constant acceleration (independent of the level of degradation) assumption implies that the degradation curves at differing ageing temperatures will have the same shape when plotted versus the ageing time. As shown in Figure 4.11, the prerequisite of self-similar ageing curve and assumption are reasonably fulfilled for the investigated XNBR thin film in accelerated ageing.

Using time-temperature superposition approach, the raw data in Figure 4.11 will be shifted to a selected reference temperature, T_{ref} , to obtain a mastercurve as in Figure 4.15 with a reference temperature at 60 °C. This is accomplished by multiplying the times appropriate to experiments at temperature T by a shift factor of a_T . The shift factors, a_T , are chosen empirically to give the best superposition of the data. If the data adhere to an Arrhenius relation, the set of shift factors a_T , will be related to the Arrhenius energy, E_a , by the following expression:

$$\ln \alpha_T = \ln \frac{t_{T_{ref}}}{t_{T_{aged}}} = \frac{E_a}{R} \times \left(\frac{1}{T_{ref}} - \frac{1}{T_{age}} \right) \quad \text{Eq. 4.2}$$

where $t_{T_{ref}}$ and $t_{T_{aged}}$ are the respective ageing time at reference temperature, T_{ref} and ageing temperature T_{aged} in Kelvin, respectively, E_a is the activation energy, R the universal gas constant and T the absolute temperature in Kelvin.

In this study, the lowest temperature was always chosen for which data in a given set are available which is 60 °C. Note that although the quality of the superposition is independent of the T_{ref} , the use of a T_{ref} below the lowest temperature for which data is available requires an assumption regarding the temperature dependence of shift factor (α_T) below the lowest experimental temperature.

An Arrhenius plot of the natural logarithmic values of the empirically determined shift factors (α_T) for the accelerated ageing is plotted as a function of reciprocal temperature in Figure 4.14. As shown in Figure 4.14, these data give a straight line and display excellent Arrhenius behaviour which gives an activation energy of 81.43 kJ/mol and a lifetime of 25 years at 25 °C. Again, the data reasonably fit the relationship of Equation 4.2, with regression coefficients value equal to 0.9754 for the least square linear fit of the experimental data.

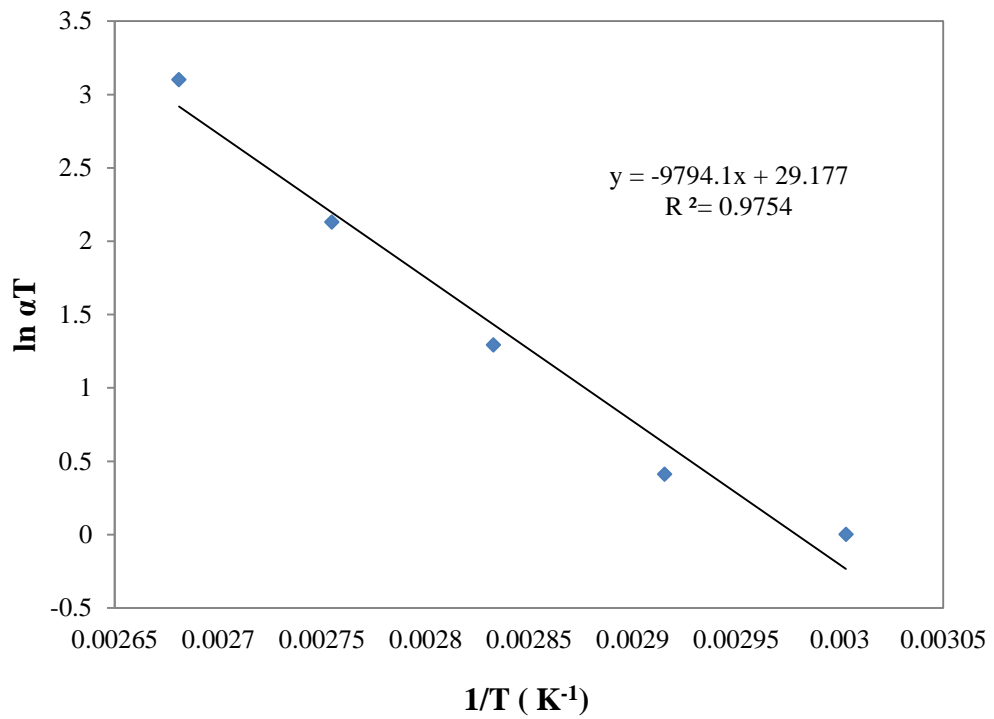


Figure 4.14: Arrhenius plot using empirical shift factor concept.

Table 4.3: Arrhenius shift factor (α_T) for a reference temperature at 60 °C.

Temperature (°C)	Arrhenius shift factor, α_T
60	1.0000
70	1.5079
80	3.6428
90	8.4106
100	22.2239

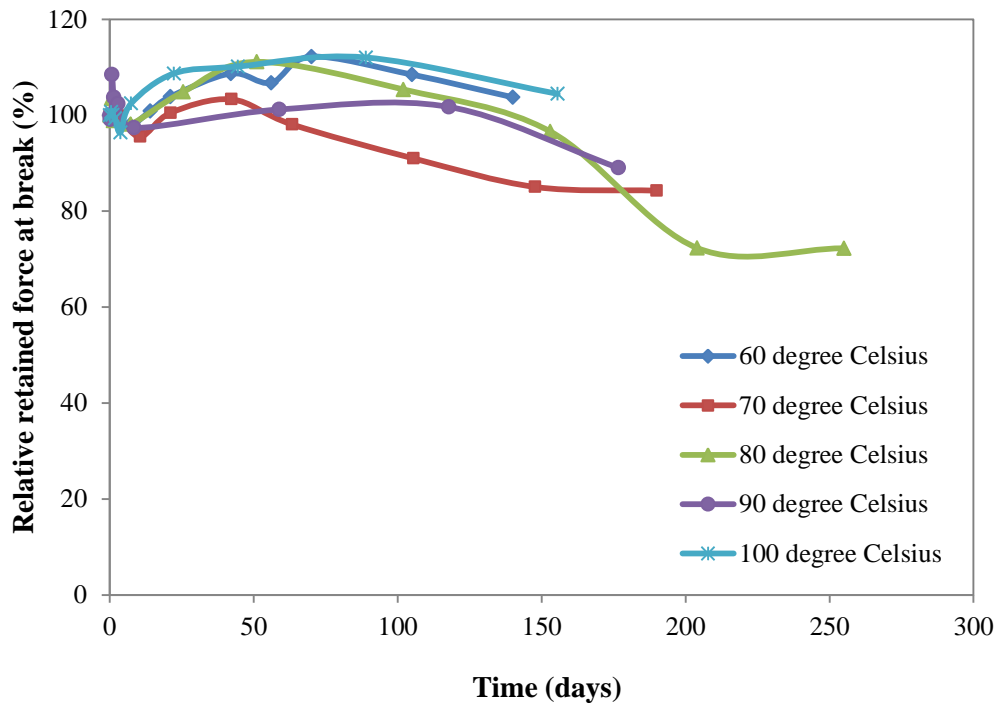


Figure 4.15: Mastercurve for relative force at break against ageing time for XNBR thin film at reference temperature of 60 °C.

The best time-temperature superposition of the ageing curve of force at break data in Figure 4.11 to a mastercurve for XNBR thin film at reference temperature of 60 °C is depicted in Figure 4.15; whereas the shift factors are shown in Table 4.3. The superposition is excellent as expected given the similarities in curve shapes observed for the five ageing temperatures (Fig. 4.15).

An alternative way to get a mastercurve is by applying Equation 4.2 using the activation energy estimated earlier in Arrhenius approach or in early part in Time-temperature superposition approach or from the scientific literature. Since both approaches are giving the same activation energy value, the shift factor were

calculated by using 81.43 kJ/mol as the activation energy and 25 °C as the reference temperature as tabulated in Table 4.4. Figure 4.16 is the mastercurve with 25 °C as the reference temperature. The properties of the thin film sample after any period of ageing at the reference temperature can be readily read off in the resulting mastercurve. From Figure 4.16, the estimation for the physical properties to fall to 75% retained force at break is 24 years at 25 °C.

Table 4.4: Arrhenius shift factor (a_T) for a reference temperature at 25 °C.

Temperature (°C)	Arrhenius shift factor, a_T
60	31.6317
70	74.58058
80	167.46624
90	359.64442
100	741.34555

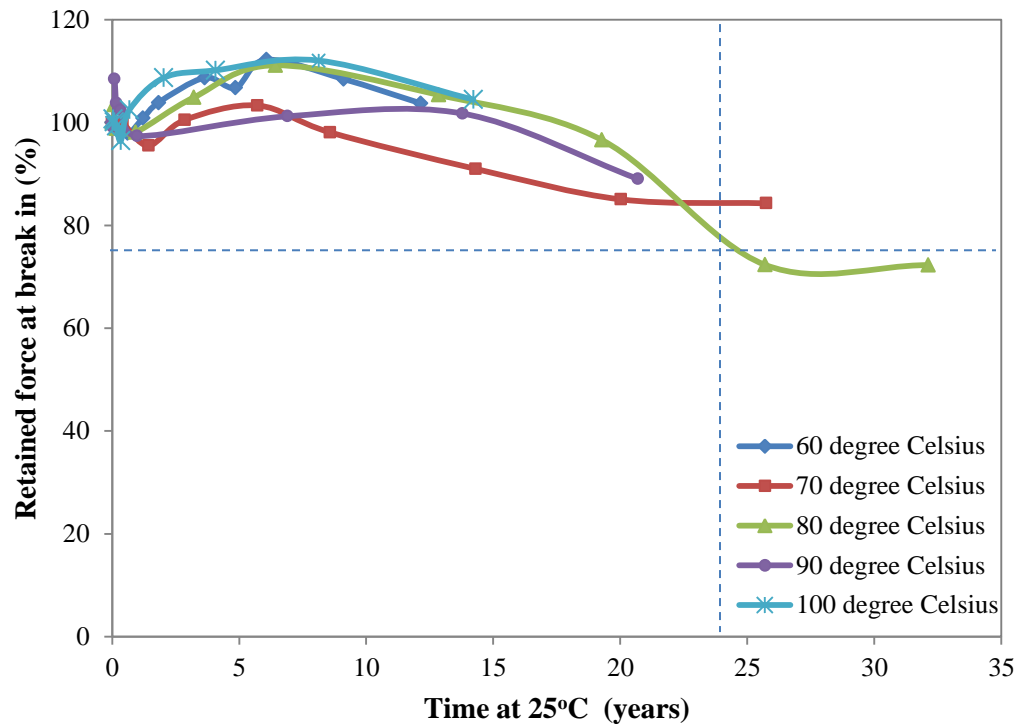


Figure 4.16: Mastercurve for relative force at break against ageing time for XNBR thin film at reference temperature of 25 °C.

4.2.3 Comparison of lifetime and activation energies according to different shelf life prediction approach

A comparison of the activation energies derived from applying the various approaches described above is summarised in Table 4.5. For both approaches, the calculated lifetime and activation energies are rather similar when using Arrhenius plot, while when using the application of activation energy to construct the mastercurve, the lifetime is slightly lower. According to British Standards Institution 2009, typical activation energies for many chemical reactions are an average 83 of kJ/mol although the actual values found in practice vary widely.

Table 4.5: Lifetime and activation energies prediction according to various approach and assumption.

	Arrhenius approach	Time-Temperature superposition approach	Time-Temperature superposition approach (using the activation energy obtained)
Lifetime (year)	25 years	25 years	24 years
Activation Energy (kJ/mol)	81.43	81.43	-

4.3 Degradation mechanism study of XNBR

Synthetic polymers are degraded in processes which involve breaking of main valence bonds in the backbone of the chains or in side groups. Ranby (1989) explained then formation of free radicals is because splitting of electron pairs into two unpaired electrons in most cases the most favourable basic reaction considering the energy required for breaking a chemical bond. Degradation of polymers is a general phenomenon which can also be initiated in several other ways, e.g. by photo, thermal, mechanical, chemical or biological (enzymatic) effects. Degradation and oxidation of the polymers have several serious effects on the physical properties such as on the molecular weight (molar mass) and the molecular weight distribution, on the mechanical properties (tensile strength, modulus, impact strength, creep, etc.) and on elasticity, softening point and surface hardness. Various types of stabilizers are therefore added to many polymeric materials to slow down the rate of degradation and prolong the useful lifetime of the rubber product (Ranby 1989).

To study the mechanism of ageing, thin films were cast using XNBR latex with and without antioxidant and subjected to thermal ageing at 70 °C and 90 °C. Accelerated ageing of the thin film at both temperatures give a similar spectrum. At the end of the ageing, the films without antioxidant turned yellowish, while the films contained antioxidant remained colourless, and it occurred to both temperatures (70 °C and 90 °C). We used conventional techniques, FTIR

spectroscopy, to identify the chemical changes of these XNBR thin films through thermal ageing.

Thermal ageing leads to significant changes in the FTIR absorption spectra. The major by-product resulting from oxidation is carbonyl and hydroxyl species. For thin film contain antioxidant (Figure 4.17 and 4.19), the only changes is on the intensity of carbonyl region ($1800 - 1600 \text{ cm}^{-1}$), no significant increase in the hydroxyl region ($3600 - 3200 \text{ cm}^{-1}$) or decrease in the nitrile group (2237 cm^{-1}) as well as in butadiene group (970 cm^{-1}). In the case of XNBR without antioxidant (Figure 4.18 and 4.20), hydroxylated (3400 cm^{-1}) as well as carbonylated (1720 cm^{-1}) species are observed. Figure 4.17 – 4.20 shows FTIR spectra of XNBR thin films with and without antioxidant for different exposure times through thermal ageing at $70 \text{ }^\circ\text{C}$ and $90 \text{ }^\circ\text{C}$. Table 4.6 shows the assignment of some characteristic peaks of XNBR thin film. FTIR spectra for thin film without antioxidant aged at $90 \text{ }^\circ\text{C}$ have a similar pattern as those aged at $70 \text{ }^\circ\text{C}$. However, the rate of the degradation is higher at $90 \text{ }^\circ\text{C}$ compared to $70 \text{ }^\circ\text{C}$.

Table 4.6: FTIR peaks assignment of XNBR latex thin film.

Stretching (cm^{-1})	Assignments
3528	hydroxyl group (OH) stretching region
3074	=CH stretch
2925	Asymmetric stretching of the methylene group (CH_2)
2849	Symmetric stretching of the methylene group (CH_2)
2237	Stretching of nitrile triple bonds ($\text{C}\equiv\text{N}$)
1730	Carboxyl group (for free COOH group)
1698	Hydrogen bonded carbonyl
1639	$\text{C}=\text{C}$ stretching
1541,1534	Carbonyl stretching vibration of zinc carboxylate salt
1448	In-plane deformation of the methylene group (C-H)
1380,1350,1307,	C-C stretching vibration
1230~1000	C-O stretching
970	Out-of-plane vibration of the hydrogen atom of the 1,4-trans component
918	Out-of-plane vibration of the methylene hydrogen atom of the vinyl group
690	C-H bond (disubstituted) $(\text{CH})_{n>4}$

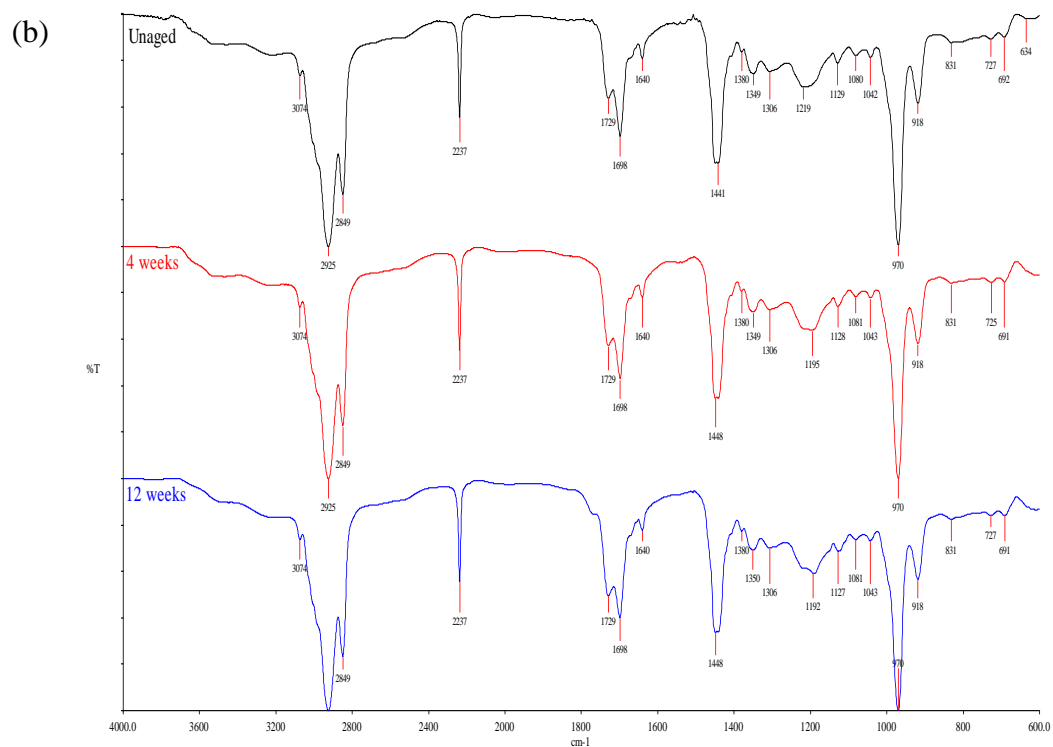
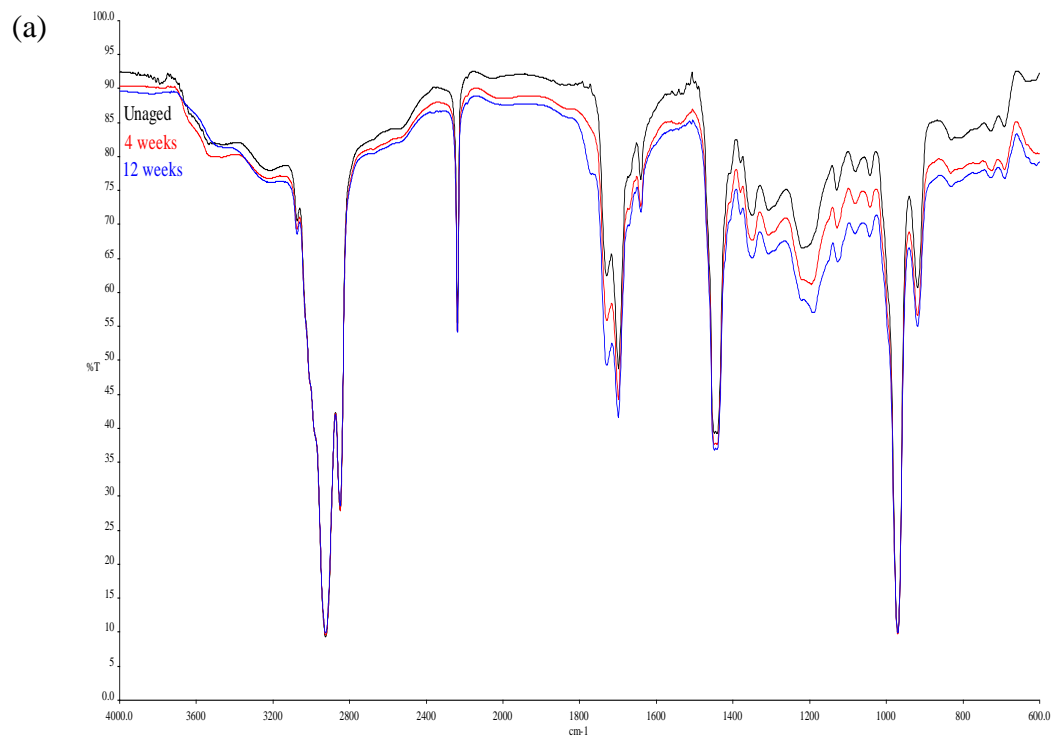


Figure 4.17: IR spectra of XNBR thin film with antioxidant aged at 70 °C (a) combined spectra and (b) split spectra.

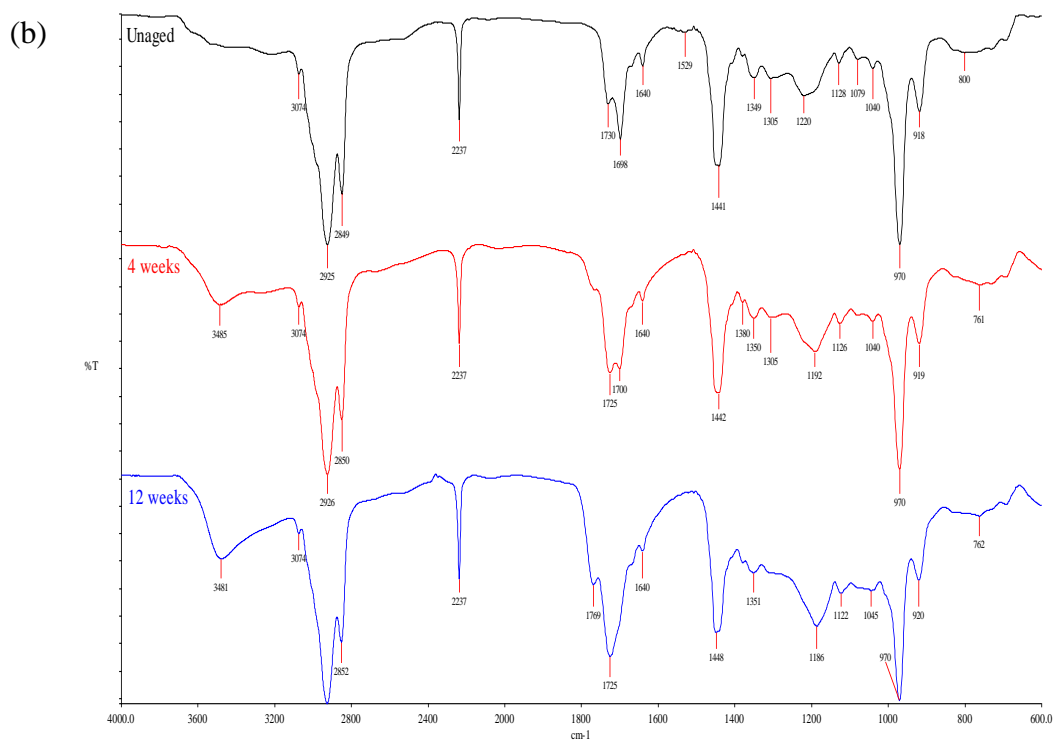
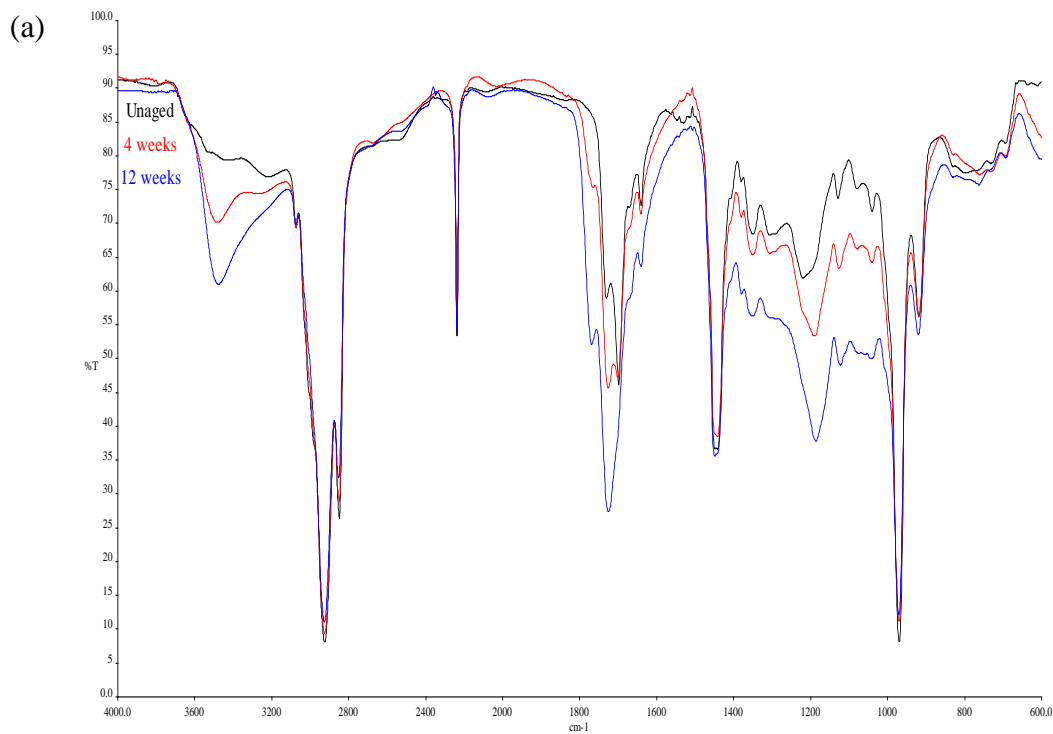


Figure 4.18: IR spectra of XNBR thin film without antioxidant aged at 70 °C (a) combined spectra and (b) split spectra.

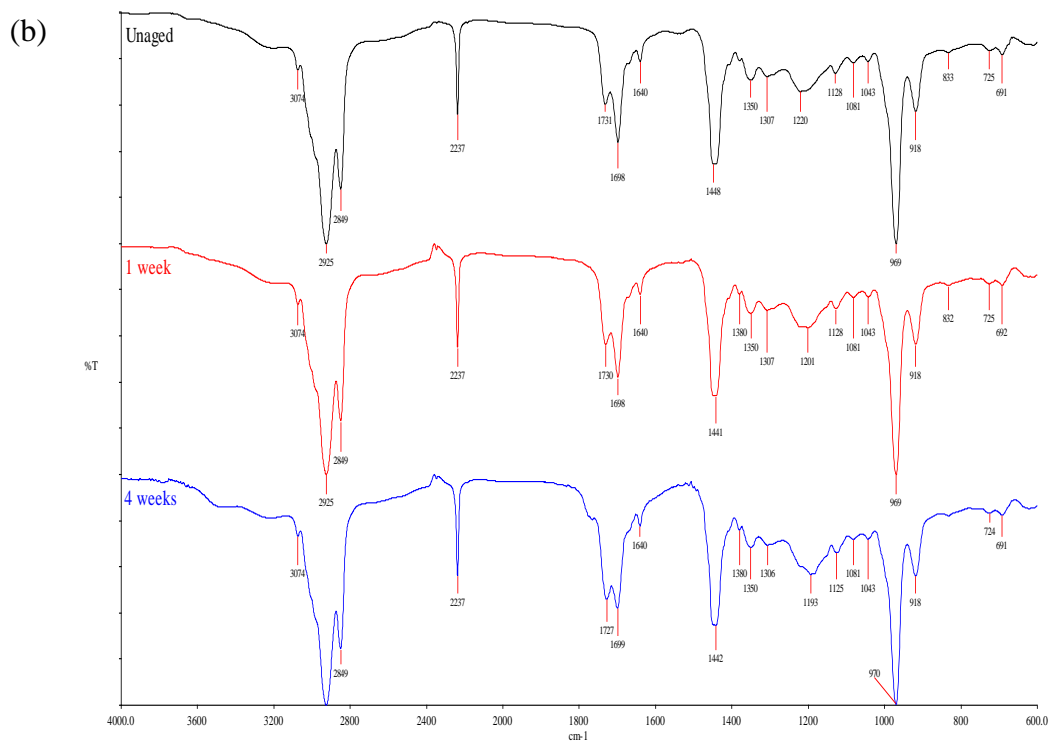
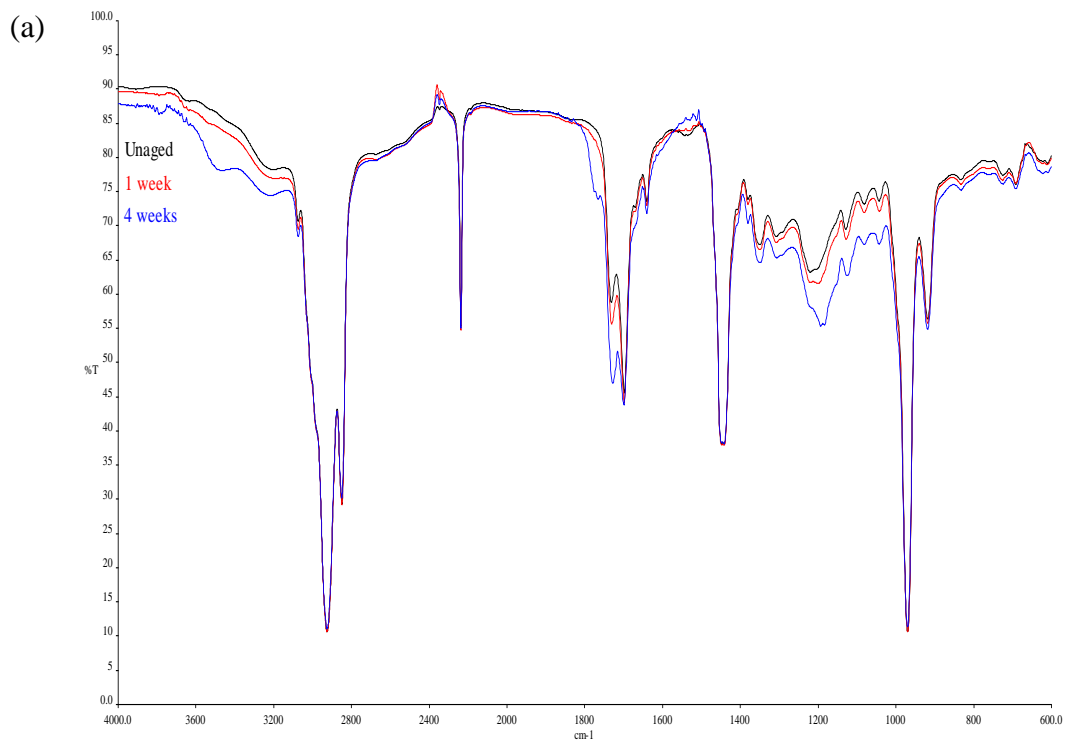


Figure 4.19: IR spectra of XNBR thin film with antioxidant aged at 90 °C (a) combined spectra and (b) split spectra.

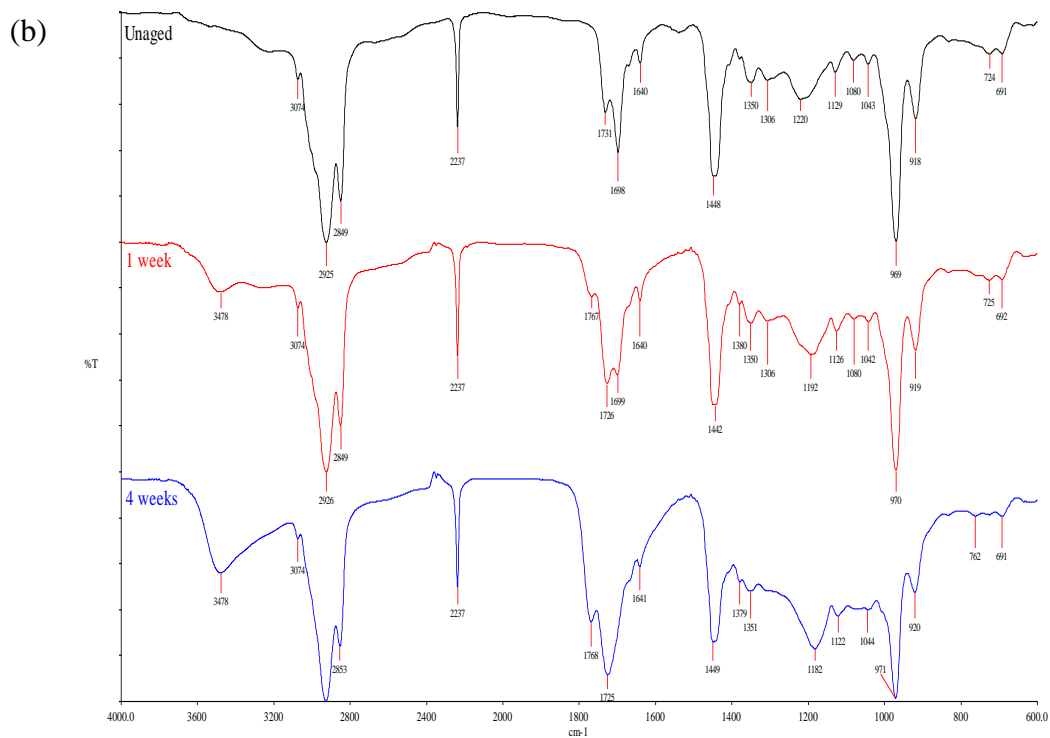
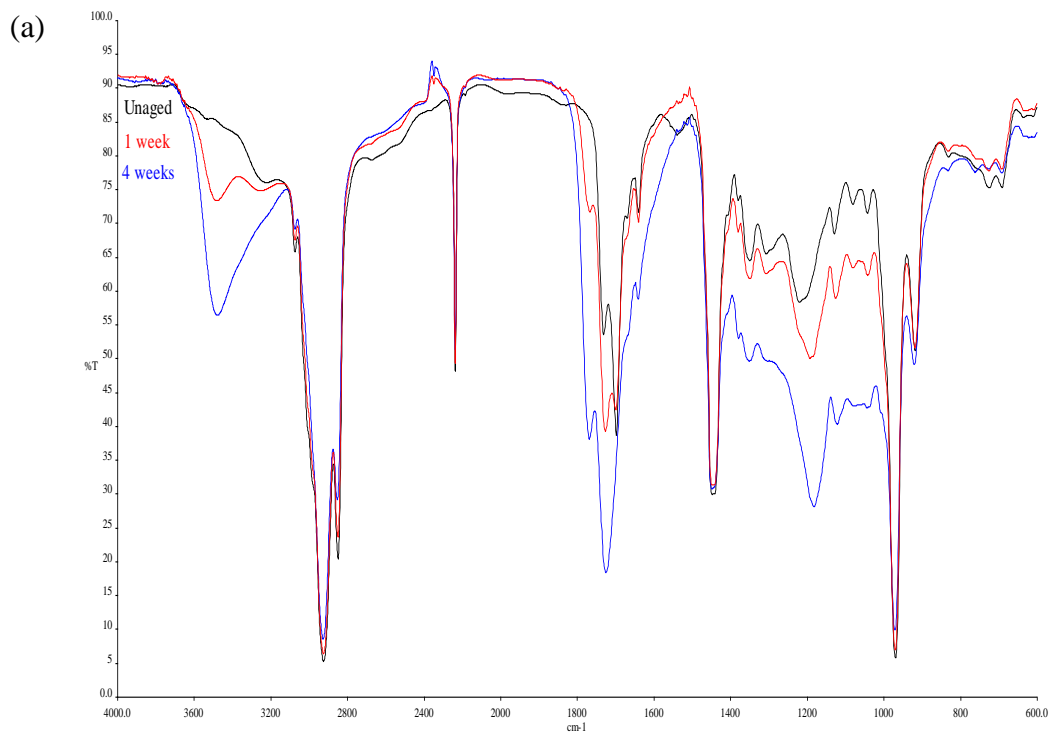


Figure 4.20: IR spectra of XNBR thin film without antioxidant aged at 90 °C (a) combined spectra and (b) split spectra.

Broad absorption bands corresponding to oxidation products, such as carbonyl functional groups (C=O) in the region 1660 - 1800 cm^{-1} , and hydroxyl functional groups (O-H) in the region 3200 - 3400 cm^{-1} , increase progressively with increasing ageing time. These bands were observed in both thin film without antioxidant aged at 70 °C and 90 °C.

In the region of hydroxyl stretching vibrations (3600 - 3200 cm^{-1}) shown in Figure 4.18, a broad absorption bands at 3485 cm^{-1} appeared in the earliest stage of thermal-oxidation ($t < 4$ weeks). The intensity of the band continuously increased and shifted to 3481 cm^{-1} . According to Adam, Lacoste and Lemaire (1989a, 1990) and Delor-Jestin et al. (2000), this band can be ascribed to associated hydroperoxides and alcohols. Shift of the band may be caused by hydrogen bonding which occurs between the alcoholic group and acrylonitrile units (Adam, Lacoste and Lemaire 1990).

The region of carbonyl stretching vibrations (1800-1600 cm^{-1}), illustrated in Figure 4.18, showed two absorption bands at 1698 cm^{-1} and 1730 cm^{-1} in the initial stage of the thermal-oxidation. As thermal oxidation proceeds, the intensity of this latter band increases and the bands at 1730 cm^{-1} was shifted to 1725 cm^{-1} whilst the band at 1690 cm^{-1} shifted to 1700 cm^{-1} and became constant after 4 weeks of ageing and difficult to be observe in the FTIR spectrum. Furthermore, a shoulder peak was detected at 1769 cm^{-1} . The bands at 1698 and 1730 cm^{-1} are corresponding to the C=O stretching of saturated, unsaturated acids and ketones according to Delor-Jestin et al., (2000), while the band at 1769 cm^{-1} usually

interpreted as the formation of unsaturated anhydride, γ -lactone and perester according to Piton and Raviton (1996a) and Piton and Raviton (1996b).

In the complex regions of $1500 - 1300 \text{ cm}^{-1}$ and $1300 - 1000 \text{ cm}^{-1}$ an important increase of absorbance is observed correspond to $-\text{CH}_2$ deformation and C-O stretching vibrations. Several peaks are noted in the spectrum at 1349, 1305, 1220, 1128, 1079, and 1040 cm^{-1} . Especially significant increases at peaks 1220 cm^{-1} shifted to 1186 cm^{-1} as after 12 weeks of ageing. This band was assigned to lactone structure according to Piton and Raviton (1996a) and Piton and Raviton (1996b).

In the region of the deformation vibrations ($1000 \text{ cm}^{-1} - 600 \text{ cm}^{-1}$), shown in Figure 4.17, the out-of-plane vibrations of the C-H bond linked to unsaturation can be observed (1-4 *trans* unsaturation at 970 cm^{-1} , 1-2 vinyl at 918 cm^{-1}), this band is characteristic of the structure of the butadiene part. While in the region of 2925 cm^{-1} and 2850 cm^{-1} corresponding to the aliphatic CH_2 asymmetrical and symmetrical stretching in the polymer backbone. These bands show decreases, indicating chemical changes in these regions, probably attributed to crosslinking or saturations in reactions. The susceptibility of these bands to attack is attributed to their proximity to inherently reactive double bonds and the aliphatic chain.

The nitrile band at 2237 cm^{-1} shows no significant change and the decrease of the double bonds during oxidation was detected (970 cm^{-1}); these results confirm the preferential attack on butadiene units.

From the previous studies on butadiene based polymer, the observed changes in FTIR spectrum on photo-oxidation of NBR (Adam, Lacoste and Lemaire 1990) were almost the same as those described for butadiene rubber (BR) (Adam, Lacoste and Lemaire 1989a), styrene butadiene rubber (SBR) (Adam, Lacoste and Lemaire 1989b) exposed in identical experimental conditions. A typical band observed in the hydroxyl region was characteristic of hydroperoxides and alcohols groups. While the carbonyl region which was characteristic of acids and ketones (saturated and unsaturated) were detected. In the deformation vibration region reported results have shown a decrease of unsaturation bands. The nitrile absorption band at 2240 cm^{-1} has shown no significant change indicate that the acrylonitrile units are not acting as preponderant reactive sites during photo-oxidation. Low temperature thermal-oxidation of NBR (Delor-Jestin et al., 2000; Adam, Lacoste and Lemaire 1990) gave a lot of similarities between the shapes of spectra in photo-oxidation, especially in the hydroxyl and the carbonyl regions.

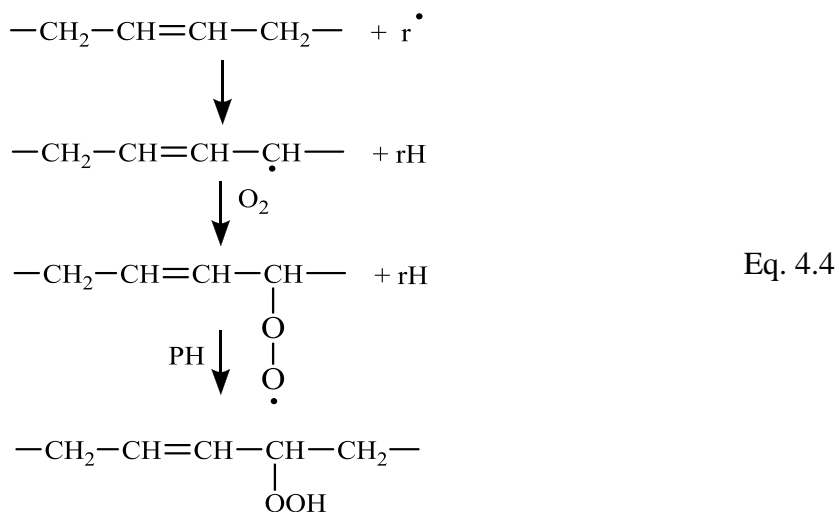
Same changes were also observed in thermo-oxidation of XNBR in this study. It is believed that butadiene based polymer would have a similar oxidation mechanism during thermal ageing. The thermal-oxidation of XNBR was characterized with FTIR by the appearance of hydroxyl bands (hydroperoxides and alcohols) and carbonyl bands (saturated, unsaturated acids and ketones) whilst the characteristic bands for butadiene were decreased.

As proposed in the literature (Adam, Lacoste and Lemaire 1989a; 1989b; 1990; Piton and Rivaton 1996a, 1996b; Delor-Jestin et al., 2000; Pielichowski and

Njuguna 2005; Johanson 2009), the first step in the oxidation process is usually the loss of hydrogen atom from the polymer chain due to energy input, and in this case, is by heat energy.

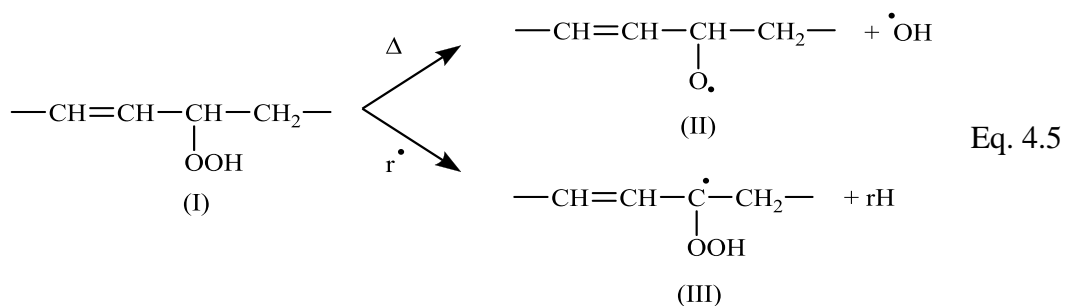


Researchers found that the thermal ageing of butadiene based polymer is closely associated with the unsaturated bond of the polymer. The thermal oxidation mechanism of butadiene based polymer is assumed to involve primary radical (r^{\bullet}) attack on the methylene group in the α -position to the double bond. Subsequent oxygen addition followed by hydrogen abstraction results in the formation of α,β -unsaturated hydroperoxides according to:



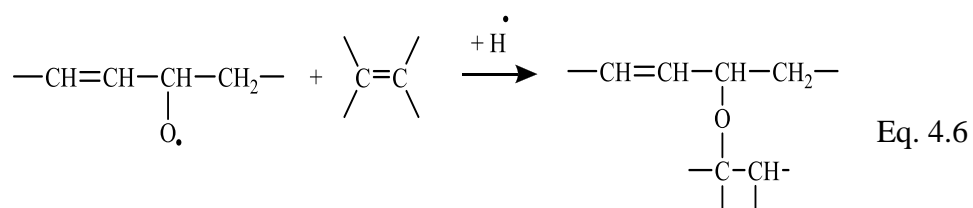
Homolysis of thermal unstable hydroperoxides (I) (Eq. 4.5) will lead to the formation of radicals (II) (Eq. 4.5) by scission of the CO-OH bond and radical (III)

(Eq. 4.5) by radical attack of the secondary hydrogen of the hydroperoxide according to the Equation 4.5 below:

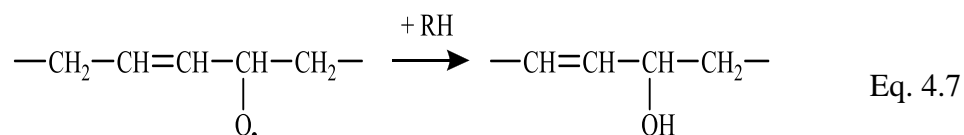


Radicals (II) (Eq. 4.5) and (III) (Eq. 4.5) so formed are the precursor for various saturated and unsaturated products under thermal oxidation. The alkoxy radical (II) (Eq. 4.5) may react in different pathways:

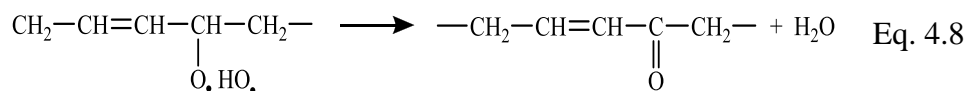
1. The alkoxy radical (II) (Eq. 4.5) attack on the neighbouring unsaturation in the polymer chain to produce crosslink via ether bonds. Hydroperoxides formed on carbon atoms in the α -position to the ether bonds are known to be converted into formates, esters and hemiacetals (Piton and Rivaton 1996a). The absorption at $1230 - 1000 \text{ cm}^{-1}$ can be ascribed to the C-O deformation of ether linkage or unsaturated alcohol formed below:



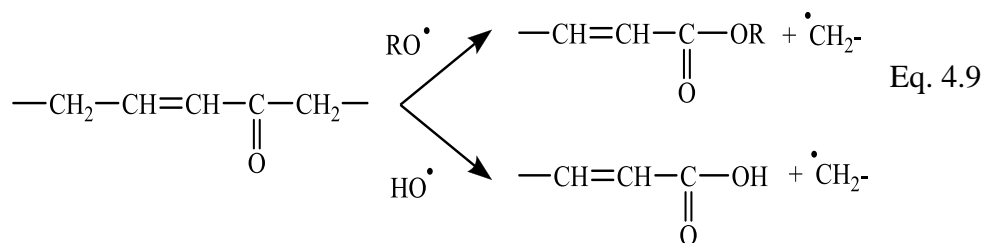
2. Hydrogen abstraction by alkoxy radicals (II) (Eq. 4.5) lead to the formation of α,β -unsaturated alcohols give rise to the absorption in hydroxyl region ($3600 - 3200 \text{ cm}^{-1}$).



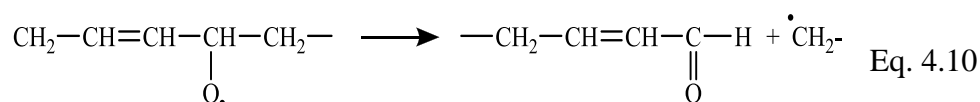
3. α,β -unsaturated ketones, detected in carbonyl region ($1800 - 1600 \text{ cm}^{-1}$) are may obtained from the cage reaction of the alkoxy radicals (II) (Eq. 4.5). The increase of the yellowing observed during the thermal oxidation has been attributed to the *cis/trans* isomerization of the α,β -unsaturated ketones (Piton and Rivaton 1996a).



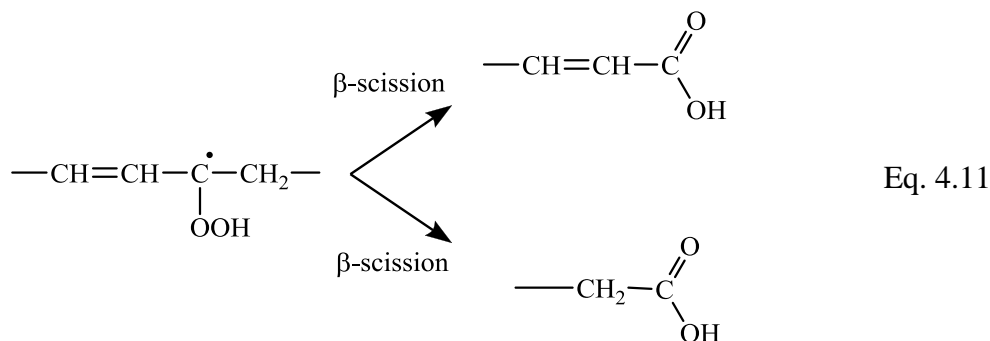
Radical attack of ketonics groups by $\text{RO}\cdot$ and $\text{OH}\cdot$ produced α,β -unsaturated ester and acid.



4. Decomposition of the alkoxy radical (II) (Eq. 4.5) through β -scission reaction produced unsaturated aldehydic products. However, the characteristic absorption for aldehydic structure ($\sim 2730\text{ cm}^{-1}$) was not detected in this study. This may be due to the rapid oxidation of the aldehydic product to saturated acids.



β -scission of the tertiary radical (III) (Eq. 4.5) leads to the formation of carboxylic structure.

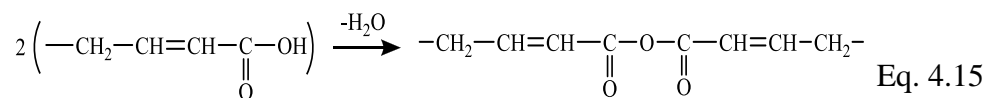


Subsequent reactions of the α,β -unsaturated products are reported below:

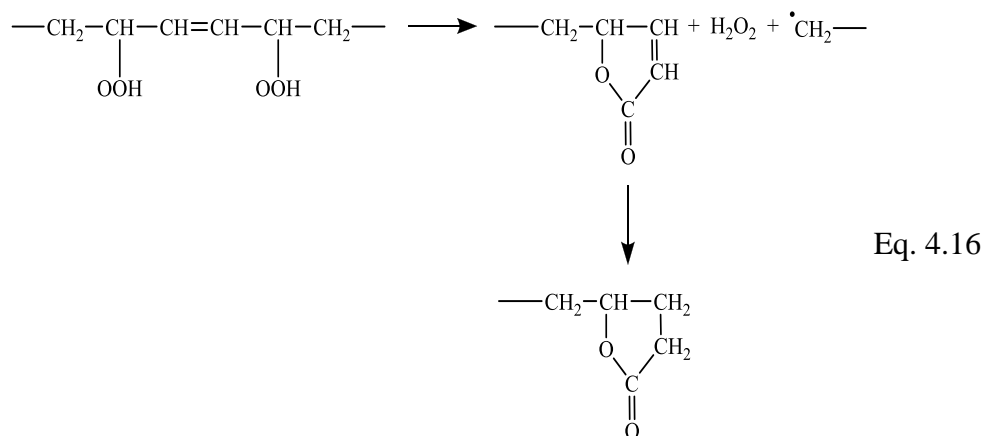
1. Saturation reaction of α,β -unsaturated products may occur via crosslinking resulting the formation of the saturated alcohols, ketones, aldehydes and acids.

Unsaturated anhydride, γ -lactone, and perester can be formed as shown in mechanisms below:

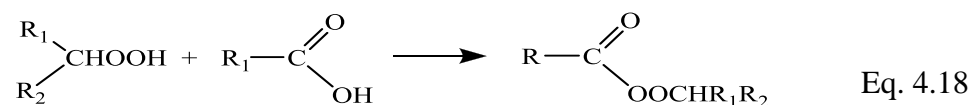
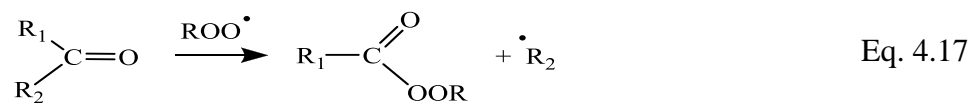
1. α,β -unsaturated anhydrides could be obtained through the dehydration of two α,β -unsaturated carboxylic acid units.



2. γ -lactone are formed by cyclization of two hydroperoxide groups in α -position to the double bond.



3. Perester could be formed in one or two reactions



Grafted butadiene (Figure 4.21) containing tertiary allylic carbon atoms (A), are preferentially oxidized in the first stages as compared to secondary allylic carbons atoms (B).

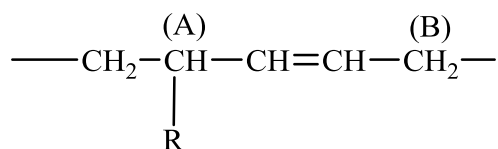
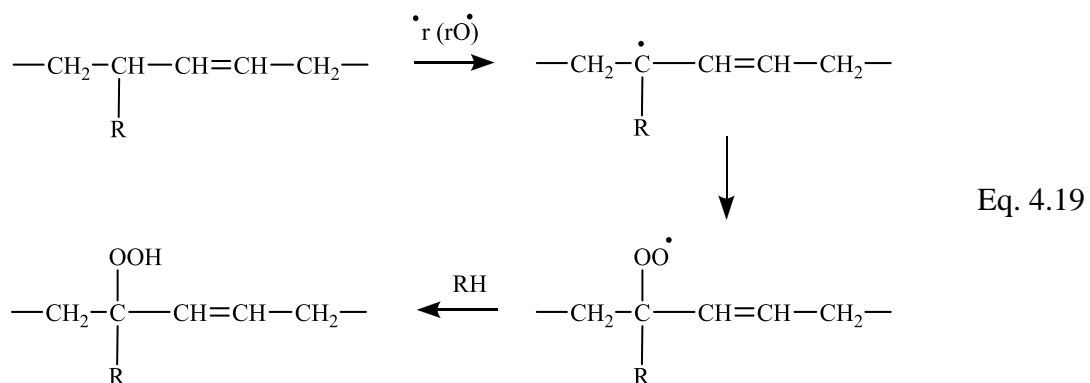
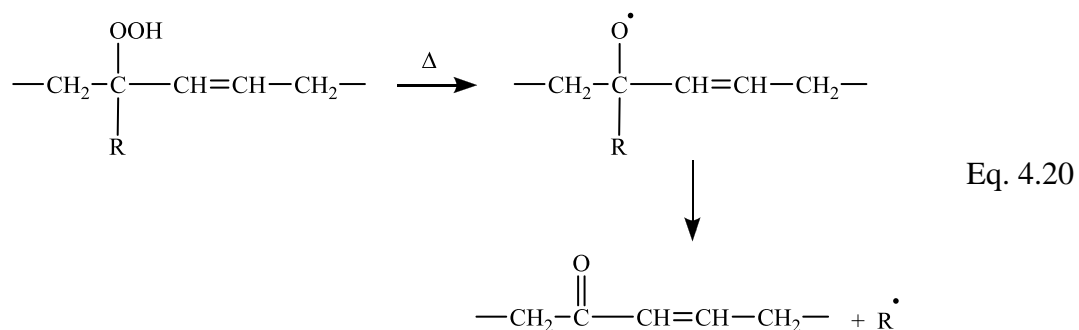


Figure 4.21: Structure of grafted butadiene.

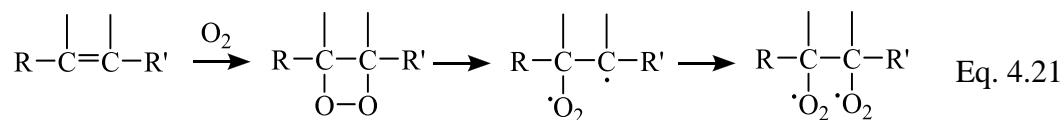
Tertiary hydroperoxides are formed according to:



Thermal homolysis of tertiary hydroperoxides leads to the formation of macroradicals. Breakage of grafted butadiene and formation of α,β -unsaturated ketones through β -scission of alkoxy macroradicals may occur.



The disappearance of bands typical of 1-4 *trans* and 1-2 vinyl unsaturation of butadiene part was also reported (Adam, Lacoste and Lemaire 1989a; Adam, Lacoste and Lemaire 1989b; Adam, Lacoste and Lemaire 1990; Piton and Rivaton 1996a, Piton and Rivaton 1996b; Delor-Jestin et al., 2000). This may be due to the fact that in butadiene based polymer there is electron withdrawal from the α -methylene carbon by the double bond which makes it more susceptible to be attacked by O_2 with the generation of hydroperoxide radicals. Figure 4.21 demonstrated the reaction mechanism of the intermediate product and the final by-product conversion pathway of XNBR under thermal-oxidation.



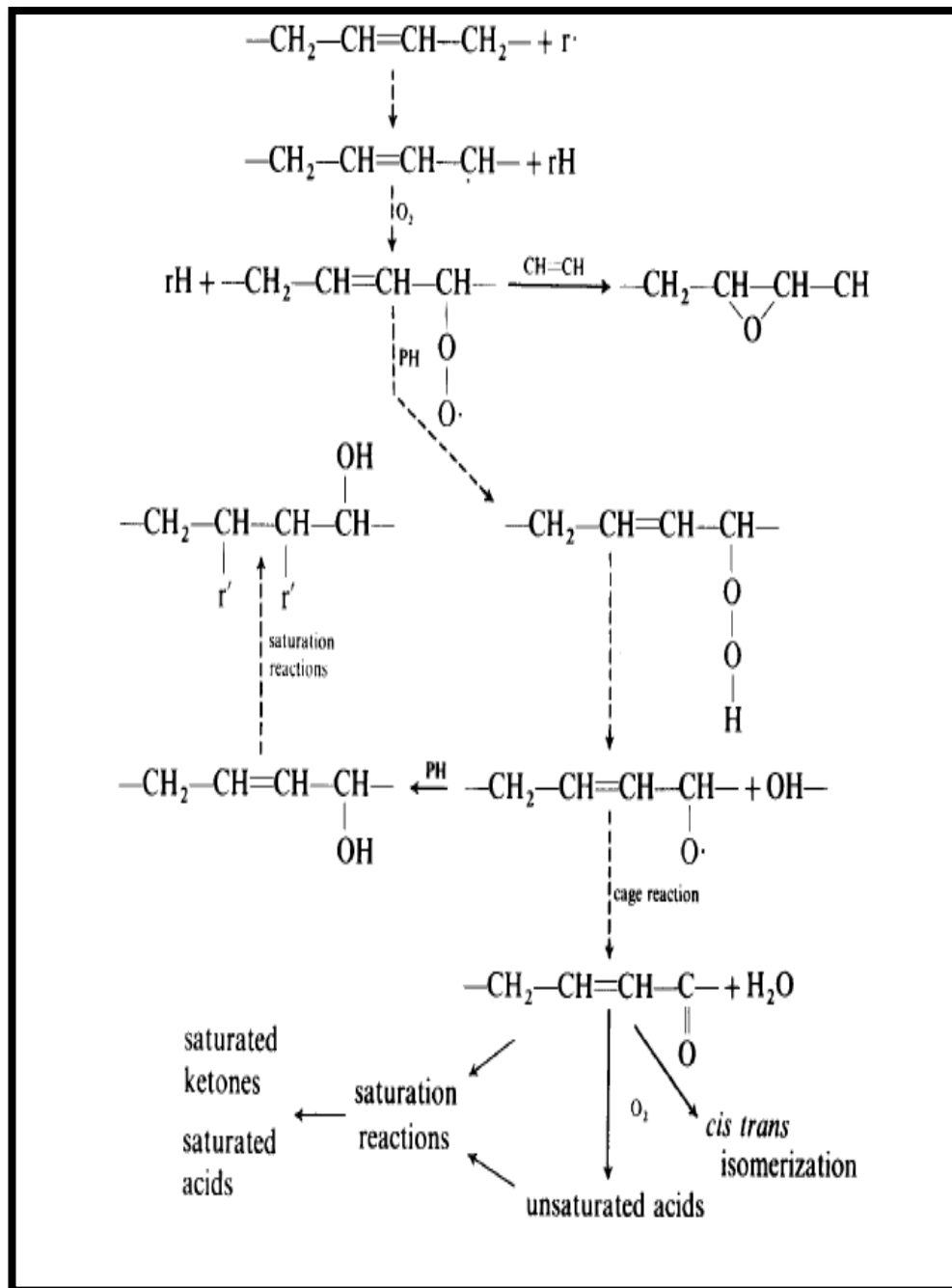


Figure 4.22: Demonstrated reaction mechanism of intermediate product and final by-product conversion pathway of XNBR under thermal-oxidation.

CHAPTER 5

CONCLUSION

Rubber ageing is an inevitable process leading to the deterioration of their properties such as reduction of the tensile strength, elasticity and elongation, wear resistance, changing in plasticity, and increases in hardness of the rubber, ultimately leading to the point where the material is no longer capable of fulfilling its function. Therefore, increasing the resistance of rubber to ageing is of great importance to increase the reliability and performance of rubber products. Various physio-mechanical tests have been carried out in this study to investigate the effect of thermal ageing on carboxylated nitrile rubber (XNBR) thin film at different temperatures using accelerated ageing. Accelerated ageing was carried out in air circulated oven at a temperature ranging from 60 °C to 100 °C and for a period ranging from 0.5 hours to 3360 hours. Real time ageing had also been carried out under fluorescent light (36 W) and in dark condition at room temperature (26 °C) with the humidity of about 65%. Results showed that thermal ageing of XNBR consists of two stages: the crosslink formation during the early stage of accelerated ageing resulting the increases in the tensile strength to a maximum due to incomplete crosslink during curing, and the latter was the breaking of the crosslink after a certain period of time causing the decrease in tensile properties. The formation of crosslinks also restricts the extensibility of XNBR and results in the decrease in swelling. At the end of the ageing treatment, XNBR turned to yellowish in colour and the changes became more pronounce at higher temperature.

Cracks were also observed under SEM as ageing was in progress. However, as compared to accelerated ageing, the effect of real time ageing on physic-mechanical properties of XNBR was in a slower rate. For lifetime prediction, tensile test were carried out on unaged and aged film specimens at ambient temperature, and the change in force at break values was chosen as characteristic indicator for ageing. A continuous decrease in force at break was observed, allowing for a reasonable application of various lifetime approaches. Arrhenius approach and Time-Temperature approach were applied to determine the activation energy and the lifetime of XNBR. In Arrhenius approach, the force at break value of the unaged specimen was used as a reference to measure the time required to reach a certain threshold. Whilst in Time-Temperature approach, a master curve was obtained by horizontally transform the ageing curve at a reference temperature along the time axes by multiplying a shift factor. Experimentally determined Arrhenius plot were extrapolated to lower temperature according to BS EN 455:4 (2009) by applying a least square linear fit method. As expected, both approaches gave a rather similar value where the time estimated for the physical properties to fall to 75% retained force at break is 25 years at 25°C and the activation energy calculated were 81.91 kJ/mol and 81.94 kJ/mol respectively. In order to understand the ageing mechanism of XNBR, characterization of XNBR thin film with and without antioxidant after accelerated ageing by FTIR were carried out. From the FTIR study, thermal ageing of XNBR showed a lot of similarity with the photo-oxidation of butadiene based polymer. Changes were mostly concentrated on hydroxyl ($3600\text{ cm}^{-1} - 3200\text{ cm}^{-1}$) and

carbonyl (1800 cm^{-1} – 1600 cm^{-1}) regions, and the reduction of butadiene characteristic peak (970 cm^{-1}) was observed.

Further investigation for a better understanding of the correlation between the film thicknesses with the changes in physico-mechanical properties of XNBR is necessary. Surface morphology changes due to crack formation during the ageing and the extent of surface damage due to cracking could be studied further. It is also important to find out the effect of different type and amount of antioxidant on thermal ageing in order to understand the role of antioxidant in protecting the XNBR film during the ageing process.

Photo degradation is also one of the interesting topic that can be discuss, as both photo degradation and thermal degradation were grouped under auto-oxidation, however the initiation step for the degradation is different for both processes. Photo degradation was initiated by the energy absorption by photon, while thermal degradation is by heat energy. It is worth to study the similarity and differences between the both degradation mechanisms which can further help in prevention of these degradations.

References

- Abadal, M., Cermak, R., Raab, M., Verney, V., Commereuc, S. and Fraisse, F., 2006. Study on photodegradation of injection moulded (beta)-polypropylene. *Polymer degradation and stability*, 91(3), pp. 459 – 463.
- Adam, C., Lacoste, J. and Lemaire, J., 1989a. Photo-oxidation of elastomeric materials: Part 1-Photo-oxidation of polybutadienes. *Polymer Degradation and Stability*, 24, pp. 185 – 200.
- Adam, C., Lacoste, J. and Lemaire, J., 1989b. Photo-oxidation of elastomeric materials: Part II-Photo-oxidation of styrene-butadiene copolymer. *Polymer Degradation and Stability*, 26, pp. 269 – 284.
- Adam, C., Lacoste, J. and Lemaire, J., 1990. Photo-oxidation of elastomeric materials: Part 3-Photo-oxidation of acrylonitrile-butadiene copolymer. *Polymer Degradation and Stability*, 27, pp. 85 – 97.
- Aguado, J. and Serrano, D.P., 1999. Catalytic cracking and reforming. In: *Feedstock Recycling of Plastic Wastes*. Cambridge: The Royal Society of Chemistry, pp. 129 – 150.
- Ain, Z.N. and Azura, A.R., 2010. Effect of different types of filler and filler loadings on the properties of carboxylated acrylonitrile- butadiene rubber latex. *Journal of Applied Polymer Science*, 119, pp. 2815 – 2823.
- Alex, R., 2009. Nanofillers in rubber-rubber blends. In: Thomas, S. and Stephen, R. (eds.). *Rubber nanocomposites: Preparation, properties and applications*. Chichester, West Sussex: John Wiley & Sons Inc., pp. 224.
- Allen, N.S. and Edge, M., 1992. Photodegradation and photooxidation of polymers. In: *Fundamentals of polymer degradation and stabilization*. Essex: Elsevier Science Publishers Ltd, pp. 75 – 101.
- Anderson, C.D. and Daniels, E.S., 2003. Industrial application. In: *Emulsion polymerization and latex applications*. Shawbury, Shrewsbury and Shropshire: iSmithers Rapra Technology, pp. 27.
- Andrady, A.L., Hamid, S.H., Hu, X. and Torikai, A., 1998. Effects of increased solar ultraviolet radiation on materials. *Journal of Photochemistry and Photobiology B: Biology*, 46, pp. 96 – 103.
- ASM International, 2003. Characterization of weathering and radiation susceptibility. In: *Characterization and failure analysis of plastics*. United states: ASM International, pp. 153.

- Batchelor, A., Loh, N.L. and Chandrasekaran, M., 2010. Mechanism of materials degradation. In: *Materials degradation and its control by surface engineering*. 3rd ed. London: Imperial College Press, pp. 165.
- Bilgic, T., 1998. Processing of PVC. In: Cheremisinoff, N.P. (ed.). In: *Advanced polymer processing operation*. United States: Noyes Publications, pp. 39 – 65.
- Biswas, T., Das, A., Debnath, S.C., Naska, N., Das, A.R. and Basu, D.K., 2004. SBR-XNBR blends: a novel approach towards compatibilization. *European Polymer Journal*, 40, pp. 847 – 854.
- Bonten C. and Berlich R., 2001. Aging mechanisms. In: *Aging and chemical resistance*. München, Germany: Carl Hanser Verlag, pp. 10 – 33.
- Bortoluzzi, J.H., Pinheiro, E.A., Carasek, E. and Soldi, V., 2006. Solid phase microextraction to concentrate volatile products from thermal degradation of polymers. *Polymer Degradation and Stability*, 89(1), pp. 33 – 37.
- Brown, R.P., 2001. *Practical guide to the assessment of the useful life of rubbers*. Shrewsbury, GBR : iSmithers Rapra, pp. 1 – 170.
- Brown, R.P., 2002. The reasons for failure. In: *Rubber product failure*. Shrewsbury, GBR : iSmithers Rapra, pp. 118.
- Brown, R.R., Forrest, M.J. and Soulagnet, G., 2000. *Long-term and accelerated ageing tests on rubbers*, Rapra Review Reports. Volume 10. Number 2. Shrewsbury, GBR: iSmithers Rapra Publishing, pp. 3.
- Brydson, J., 1999. The historical development of plastics materials. In: *Plastics materials*. 7th ed. Woburn: Butterworth-Heinemann, pp. 10.
- British Standards Institution , 2009. BS EN 455:4, Medical gloves for single use: Requirement and testing for shelf life determination. London: BSI.
- Budrugaec, P., 2000. The evaluation of the non-isothermal kinetic parameters of the thermal and thermo-oxidative degradation of polymers and polymeric materials: its use and abuse. *Polymer Degradation and Stability*, 71(1), pp. 185 – 187.
- Campo, E.A., 2008. Microbial, weather, and chemical resistance of polymeric materials. In: *Selection of polymeric materials: How to select design properties from different standards*. United States: William Andrew Inc, pp. 205 – 209.
- Cardarelli, F., 2008. Polymers and elastomers. In: *Materials handbook: A concise desktop reference*. 2nd ed. Verlag London: Springer, pp. 716 – 717.
- Cataldo, F., 1998a. Ozone interaction with conjugated polymers - I. Polyacetylene. *Polymer Degradation and Stability*, 60, pp. 223 – 231.

- Cataldo, F., 1998b. Ozone interaction with conjugated polymers - II. Polyphenylacetylene. *Polymer Degradation and Stability*, 60, pp. 233 – 237.
- Cataldo, F., Ricci, G. and Crescenzi, V., 2000. Ozonization of atactic and tactic polymers having vinyl, methylvinyl, and dimethylvinyl pendant groups. *Polymer Degradation and Stability*, 67, pp. 421 – 426.
- Chaiear, N., 2001. Skin irritation and dermatitis. In: *Health and safety in the rubber industry*. Shrewsbury, GBR: Smithers Rapra, pp. 19.
- Chaiear, N. and Saejiw, N., 2010. Rubber in the context of growing trees. In: *Update on health and safety in the rubber industries*. Shrewsbury, Shropshire, GBR: Smithers Rapra, pp. 9.
- Chaiear, N. and Saejiw, N., 2010. Health effects related to working in rubber industries. In: *Update on health and safety in the rubber industries*. Shrewsbury, Shropshire, GBR: Smithers Rapra, pp. 59 – 61.
- Chandra, R. and Rustgi, R., 1998. Biodegradable polymer. *Progress in Polymer Science*, 23(7), pp. 1273 – 1335.
- Chandrasekaran, V.C., 2009. Rubber- an overview. In: *Tank Linings for Chemical Process Industries*. Shrewsbury, Shropshire, GBR: Smithers Rapra, pp. 5 – 10.
- Choudhury, A., Bhowmick, A.K. and Soddemann, M., 2010. Effect of organo-modified clay on accelerated aging resistance of hydrogenated nitrile rubber nanocomposites and their life time prediction. *Polymer Degradation and Stability*, 95(12), pp. 2555 – 2562.
- Chronska, K. and Przepiorkowska, A., 2008. Buffing dust as a filler of carboxylated butadiene-acrylonitrile rubber and butadiene-acrylonitrile rubber. *Journal of Hazardous Materials*, 151, pp. 348 – 355.
- Ciesielski, A., 2001. Types of rubber and their essential properties. In: *Introduction to Rubber Technology*. Shrewsbury, GBR: Smithers Rapra, pp. 6 – 22.
- Colin, X., Teyssedre, G. and Fois M., 2011. Ageing and degradation of multiphase polymer systems. In: Boudenne A., Ibos L., Candau Y. and Thomas S. (eds.). *Handbook of multiphase polymer systems*. Volume 2. Weinheim, Germany: John Wiley & Sons Inc., pp. 797 – 842.
- Coran, A.Y, 2005. Vulcanization. In: James, E.M., Burak, E. and Frederick, R.E. (eds.). *The science and technology of rubber*, 3rd ed. London: Elsevier Academic Press, pp. 323.
- Cowie, J.M.G. and Arrighi, V., 2011. Physical ageing. In: Utracki L.A. and Jamieson A.M. (eds.). *Polymer physics: From suspensions to nanocomposites and beyond*. Weinheim, Germany :John Wiley & Sons Inc., pp. 8 – 26.

- Cowie, J.M.G., McEwen, I.J. and McIntyre, R., 2003. Aging and degradation of polymer blends. In: Utracki, L.A. (ed.). *Polymer blends handbook*. Volume 2. Dordrecht, Netherlands: Kluwer Academic Publishers, pp. 977 – 1022.
- Daraboina, N. and Madras, G., 2008. Thermal and photolytic degradation of poly(methyl methacrylate), poly(butyl methacrylate), and their copolymers. *Industrial and Engineering Chemistry Research*, 47(18), pp. 6828 – 6834.
- Deanin, R.D. and Mead, J.L., 2007. Synthetic resins and plastics. In: Kent J.A. (ed.). *Kent and Riegel's handbook of industrial chemistry and biotechnology*. 11th ed, Volume 1. New York: Springer, pp. 159, 630 – 709.
- Delor-Jestin, F., Barrois-Oudin, N., Cardinet, C., Lacoste, J. and Lemaire, J., 2000. Thermal ageing of acrylonitrile-butadiene copolymer. *Polymer Degradation and Stability*, 70, pp. 1 – 4.
- Drago, H., Vera, K. and Davorka, P., 1995. Thermally stimulated oxidative degradation of high impact polystyrene with nitric acid. *Polymer Engineering and Science*, 35(8), pp. 1140 – 1151.
- Dunn, D., 2002. Synthetic latex: technology and market projections. In: *Latex 2002*. Shawbury, Shrewbury, Shropshire: iSmithers Rapra Publishing, pp. 23 – 25.
- Ehrenstein G.W., 2001. Aging and stabilization. In: *Polymeric materials: structure, properties, applications*. München, Germany: Carl Hanser Verlag, pp. 229.
- Erman, B. and Mark, J.E., 2005. The molecular basis of rubberlike elasticity. In: James, E.M., Burak, E. and Frederick, R.E. (eds.). *The science and technology of rubber*. 3rd ed. London: Elsevier Academic Press, pp. 29.
- Faravelli, T., Bozzano, G., Colombo, M., Ranzi, E. and Dente, M., 2003. Kinetic modeling of the thermal degradation of polyethylene and polystyrene mixtures. *Journal of Analytical and Applied Pyrolysis*, 70(2), pp. 761 – 77.
- Feldman, D., 1990. Polymer degradation. In: *Polymer building materials*. Essex: Elsevier Science Publishers Ltd, pp. 496 – 522.
- Feldman, D. and Barbalata, A., 1996. Diene polymers. In: *Synthetic Polymers: Technology, properties, applications*. London: Chapman & Hall, pp. 153.
- Flynn, J.H., 2002. Polymer degradation. In: Gallagher, P.K. (ed.). *Handbook of thermal analysis and calorimetry: Applications to polymers and plastics*. Volume 3. The Netherlands: Elsevier Science, pp. 587 – 652.
- Fuller, T., 1999. Introduction Concepts and Definations. In: Rudin, A., (ed.). *The elements of polymer science and engineering: an introductory text and reference for engineers and chemists*, 2nd ed. New York: Johns Wiley & Sons Inc, pp. 1 – 40.

- Gatos, K.G. and Karger-Kocsis, J., 2011. Bubber-clay nanocomposites based on nitrile rubber. In: Galimberti, M. (ed.). *Rubber-Clay nanocomposites: Science, technology, and applications*. West Sussex: John Wiley & Sons Ltd., pp. 409.
- Gent, A.N., 2001. Compounding. In: *Engineering with rubber: How to design rubber components*. 2nd ed. United Kingdom: Carl Hanser Verlag, pp. 22.
- Ghaffar, A., Scott, G.A. and Scott, G., 1976. The chemical and physical changes occurring during UV degradation of high impact polystyrene. *European Polymer Journal*, 11(3), pp. 271 – 275.
- Ghosh, P., 1990. In: *Polymer science and technology of plastics and rubbers*. New Delhi: Tata McGraw-Hill Publishing Company Ltd., pp. 175 – 181.
- Gijsman, P., 2011. Polymer stabilization. In: Kutz, M. (ed.). In: *Applied plastics engineering handbook: Processing and materials*. New York: William Andrew Publishing, pp. 375 – 399.
- Gillen, K.T., Celina, M. and Keenan, M.R., 2000. Methods for predicting more confident lifetimes of seals in air environments. *Rubber Chemistry and Technology*, 73, pp. 265 – 296.
- Gillen, K.T., Celina, M. and Bernstein, R., 2003. Validation of improved methods for predicting long-term elastomeric seal lifetimes from compression stress-relaxation and oxygen consumption techniques. *Polymer Degradation and Stability*, 82, pp. 25 – 35.
- Gillen, K.T., Bernstein, R. and Celina, M., 2005a. Non-Arrhenius behavior for oxidative degradation of chlorosulfonated polyethylene materials. *Polymer Degradation and Stability*, 87, pp. 335 – 346.
- Gillen, K.T., Bernstein, R. and Derzon, D.K., 2005b. Evidence of non-Arrhenius behavior from laboratory aging and 24-year field aging of polychloroprene rubber materials. *Polymer Degradation and Stability*, 87(1), pp. 57 – 67.
- Gillen, K.T., Clough, R.L., Celina, M., Wise, J. and Malone, G.M., 1996. DOE-sponsored cable aging research at Sandia National Laboratories. In: *Proceedings of the U.S. Nuclear Regulatory Commission 23rd Water Reactor Safety Information Meeting*, NUREG/CP-0149, 3, p. 133 – 148.
- Gimouhopoulos, K., Doulia, D., Vlyssides A. and Georgiou D., 2000. Optimization studies of waste plastics/ lignite catalytic coliquefaction. *Waste Management Research*, 18, pp. 352 – 357.
- Gosh, P., 2001. Polymer characteristics and polymer characterization. In: *Polymer science and technology: Plastics, rubbers, blends and composites*. 2nd ed. New Delhi: Tata McGraw-Hill Publishing Company Ltd., pp. 203 – 256.

- Gugumus, F., 2009. Light stabilizers. In: Zweifel, H., Maier, R.D. and Schiller, M. (eds.). *Plastics additives handbook*. 5th ed. München, Germany: Carl Hanser Verlag, pp. 141 – 425.
- Gupta, A.L., 2010. Introduction; Polymer additive. In: *Polymer chemistry*. Pragati Bhawan: Pragati Publications, pp. 1 – 10; 235 – 250.
- Gupta, A.L., 2010. Basic. In: *Polymer Chemistry*. Pragati Bhawan: Pragati Publications, pp. 18 – 83.
- Ha-Anh, T. and Vu-Khanh, T., 2005. Effect of thermal ageing on fracture performance of polycholoprene. *Journal of Materials Science*, 40, pp. 5243 – 5248.
- Harvey, J.A., 2005. Lifetime predictions of plastics. In: Kutz, M. (ed.). *Handbook of environmental degradation of materials*. New York: William Andrew Publishing, pp. 65 – 77.
- Hunt, T. and Vaughan, N., 1996. Hydraulic hose. In: *Hydraulic handbook*. 9th ed. Oxford : Elsevier Advanced Technology, pp. 286.
- Huy, M.L. and Evrard, G., 1998. Methodologies for lifetime predictions of rubber using Arrhenius and WLF models. *Die Angewandte Makromolekulare Chemie*, 216/262, pp. 135 – 142.
- Jacques, B., Werth, M., Merdas, I., ThomINETTE, F. and Verdu, J., 2002. Hydrolytic ageing of polyamide 11.1. Hydrolysis kinetics in water. *Polymer*, 43(24), pp. 6439 – 6447.
- Johanson, D., 2009. Properties determining the chemical stability and breakdown of polymers. In: Krevelen, D.W. and Nijenhuis, K.T. (eds.). *Properties of polymer: Their correlation with chemical structure; their numerical estimation and prediction from additive group contribution*. 4th ed. Netherlands: Elsevier, pp. 747 – 786.
- Jones R.G, Kahovec J., Stepto R., Wilks E.S., Hess M., Kitayama T. and Metanomski W.V, 2009. *Compendium of polymer terminology and nomenclature: IUPAC recommendations 2008*. 2nd ed. Cambridge: Royal Society of Chemistry, pp. 252.
- Jong-Ryeol, K., Jong-Ho, V., Dae-Won, P. and Mi-Hye, L., 2004. Catalytic degradation of mixed plastics using natural clinoptilolite catalyst. *Reaction Kinetics and Catalysis Letters*, 81(1), pp. 73 – 81.
- Kahlen, S., Wallner, G.M. and Lang, R.W., 2010. Aging behaviour and lifetime modelling for polycarbonate. *Solar Energy*, 84, pp. 755 – 762.

Karaduman, A., Simsek, E.H., Cicek, B. and Bilgesu, A.Y., 2001. Flash pyrolysis of polystyrene waste in a free-fall reactor under vacuum. *Journal of Analytical and Applied Pyrolysis*, 60(2), pp. 179 – 186.

Kefeli, A.A., Razumovskii, S.D. and Zaikov, G.Y., 1971. Interaction of polyethylene with ozone. *Polymer Science USSR*, 13(4), pp. 904 – 911.

Khabbaz, F., Albertsson, A.C. and Karlsson, S., 1999. Chemical and morphological changes of environmentally degradable polyethylene films exposed to thermo-oxidation. *Polymer Degradation and Stability*, 63, pp. 127 – 38.

Kiran, C.N., Ekinici, E. and Srape, C.E., 2004. Pyrolysis of virgin and waste polypropylene and its mixtures with waste polyethylene and polystyrene. *Waste Management*, 24(2), pp. 173 – 81.

Li, J., Guo, S. and Li, X., 2006. Degradation kinetics of polystyrene and EPDM melts under ultrasonic irradiation. *Polymer Degradation and Stability*, 89(1), pp. 6 – 14.

Lin, Y.H. and Yen, H.Y., 2006. Fluidised bed pyrolysis of polypropylene over cracking catalysts for producing hydrocarbons. *Polymer Degradation and Stability*, 89(1), pp. 101 – 108.

Loadman, J., 2005. The battles of the giants-Thomas Hancock. In: *Tears of the tree: The story of rubber : A modern marvel*. Oxford, GBR: Oxford University Press, pp. 45 – 80.

Loadman, M.J.R., 1998. Introduction. In: *Analysis of rubber and rubber-like polymers*. 4th ed. Netherlands: Kluwer Academic Publishers, pp. 1 – 14.

Lundquist, L., Letierrier, Y., Sunderland, P. and Manson, J.A.E., 2000. The polymer life cycle. In: *Life cycle engineering of plastic: technology, economy and the environment*. Oxford: Elsevier Science Ltd, pp. 13 – 20.

Mahaling, R.N., Jana, G.K., Das, C.K., Jeong, H. and Ha, C.S., 2005. Carboxylated nitrile elastomer/filler nanocomposite: effect of silica nanofiller in thermal, dynamic mechanical behaviour, and interfacial adhesion. *Macromolecular Research*, 13, pp. 306 – 313.

Manceau, M., Rivaton, A. and Gardette, J-L., 2012. Photochemical stability of materials for OPV. In: Krebs, F.C. (ed.). *Stability and degradation of organic and polymer solar cells*. New Jersey: John Wiley & Sons Inc., pp. 71 – 108.

Marek, A., Kapralkova, L., Schimdt, P., Pflieger, J., Humlicek, J. and Pospisil, J., 2006. Polymer spatial resolution of degradation in stabilized polystyrene and polypropylene plaques exposed to accelerated photo-degradation or heat aging. *Polymer Degradation and Stability*, 91(3), pp. 444 – 458.

- Martin, J.W., Chin, J.W. and Nguyen, T., 2003. Reciprocity law experiments in polymeric photodegradation: a critical review. *Progress in Organic Coatings*, 47(3-4), pp. 292 – 311.
- McMurry, J., 2011. Synthetic Polymer. In: *Organic chemistry*. 8th ed. Stamford, Connecticut: Cengage Learning, pp. 1242 – 1250.
- Mishra, J.K., Raychowdhury, S. and Das, C.K., 2000. Effect of interchain crosslinking on the shrinkability of the blends consisting of grafted low-density polyethylene and carboxylated nitrile rubber. *Materials Letters*, 46, pp. 212 – 218.
- Mitchell, B.S., 2003. Kinetics process in materials. In: *An introduction to materials engineering and science for chemical and materials engineers*. New Jersey: John Wiley & Sons Inc, pp. 215 – 279.
- Morawets, H., 2002. The beginnings of a synthetic rubber industry. In: *Polymers: The origins and growth of a science*. New York: Courier Dover Publications, pp. 67.
- Morrell, P.R., Patel, M. and Skinner, A.R., 2003. Accelerated thermal ageing studies on nitrile rubber O-ring. *Polymr Testing*, 22, pp. 651 – 656.
- Morris, P.J.T., 2005. *Polymer pioneers: A popular history of the science and technology of large molecules*. Philadelphia, United States: Chemical Heritage Foundation, pp. 59.
- Mott, P.H. and Roland, C.M., 2001. Aging of natural rubber in air and seawater. *Rubber Chemistry and Technology*, 74, pp. 79 – 88.
- Nagai, Y., Ogawa, T., Nishimoto, Y. and Ohishi, F., 1999. Analysis of weathering of a thermoplastic polyester elastomer II. Factors affecting weathering of a polyetherepolyester elastomer. *Polymer Degradation and Stability*, 65, pp. 217 – 224.
- Naranjo, A., Noriega, M.D.P., Osswald, T., Roldan-Alzate, A. and Sierra, J.D. 2008. Environmental effects and aging. In: *Plastic testing and characterization: industrial application*. München, Germany: Carl Hanser Verlag, pp. 287.
- Nishimura, O. and Osawa, Z., 1981. Photodegradation of polyoxymethylene. *Polymer Photochemistry*, 1, pp. 191 – 204.
- Odian, G.G., 2004. Introduction. In: *Principles of Polymerization*. 4th ed. New Jersey: John Wiley & Sons Inc., pp. 1 – 38.
- Osswald, T.A. and Menges, G., 2003. Introduction to processing. In: *Materials science of polymer for engineerings*. 2nd ed. München, Germany: Carl Hanser Verlag, pp. 229.

Pal, K., Pal, S.K., Das, C.K. and Kim, J.K., 2011. Effect of fillers on morphological properties and wear characteristic of XNBR/NR blends. *Journal of Applied Polymer Science*, 120, pp. 710 – 718.

Pallardy, S.G., 2008. Lipids terpenes and related substances. In: *Physiology of woody plants*. 3rd ed. London: Academic Press, pp. 229.

Palmer, J.D., 2011. Durability of Nonstructural Adhesive. In: Silva, L.F.M., Öchsner, A. and Adams, R.D. (eds.). *Handbook of adhesion technology*, Volume 2. New York: Springer-Verlag Berlin Heidelberg, pp. 903 – 920.

Palmisano, A.C. and Pettigrew, C.A., 1992. Biodegradability of plastics. *Bioscience*, 42(9), pp. 680 – 685.

Peacock, A.J. and Calhoun, A.R., 2006. Polymer degradation and stability. In: *Polymer chemistry: properties and applications*. München, Germany: Carl Hanser Verlag, pp. 171 – 183.

Peter, A.C. and Norman, H., 1999. Introduction. In: *The rubber formulary*. Illustrated. United States: Noyes Publications, pp. 1 – 5.

Pielichowski, K. and Njuguna, J., 2005. Introduction and mechanisms in thermal degradation of polymer. In: *Thermal degradation of polymeric materials*. Shrewsbury, GBR: Smithers Rapra, pp. 1 – 2; 31 – 36.

Pinprayon, O., Groves, R. and Saunders, B.R., 2008. A study of poly(butadiene/methacrylic acid) dispersions: Form pH-responsive behaviour to the effects of added Ca^{2+} . *Journal of colloid and Interface Science*, 321, pp. 315 – 322.

Piton, M. and Rivaton, A., 1996a. Photooxidation of ABS at long wavelength ($\lambda > 300$ nm). *Polymer Degradation and Stability*, 55, pp. 147 – 157.

Piton, M. and Rivaton, A., 1996b. Photooxidation of polybutadiene at long wavelength ($\lambda > 300$ nm). *Polymer Degradation and Stability*, 53, pp. 343 – 359.

Pospisil, J., Filar, J., Billingham, N.C., Marek, A., Horek, Z. and Nespurek, S., 2006. Factor affecting accelerated testing of polymer photostability. *Polymer Degradation and Stability*, 91(3), pp. 417 – 422.

Potter, B., 2006. Estimating shelf life of medical products made from natural & synthetic rubber latex. In: *Latex 2006*. Germany: Rapra Technology Ltd., pp. 93 – 103.

Quirk, R.P. and Pickel, D.L.G., 2005. Polymerization: elastomer synthesis. In: James, E.M., Burak, E. and Frederick, R.E. (eds.), *The science and technology of rubber*. 3rd ed. London: Elsevier Academic Press, pp. 29.

- Ranby, B., 1989. Photodegradation and photo-oxidation of synthetic polymers. *Journal of Analytical and Applied Pyrolysis*, 15, pp. 237 – 247.
- Rakovsky, S.K. and Zaikov, G.E., 2004. Ozone degradation and stabilization of conventional rubbers. In: Monakov, Y.B. and Zaikov, G.E. (eds.). *Focus on polymer research*. New York: Nova Science Publishers, pp. 43 – 122.
- Ramis, X., Cadenato, A., Salla, J.M., Morancho, J.M., Valles, A., Contat, L. and Ribes, A., 2004. Thermal degradation of polypropylene/starch-based materials with enhanced biodegradability. *Polymer Degradation and Stability*, 86, pp. 483 – 491.
- Ratnam, Chantara Thevy, and Mohd Saiful Ahmad, (2006) *Stress-strain, morphological and rheological properties of radiation-crosslinked PVC/ENR blend*. Malaysian Polymer Journal, 1 (1). pp. 1-10.
- Rauwendaal, C. 2002. Troubleshooting extruders. In: *Polymer extrusion*. 4th ed. Munchen: Carl Hanser Verlag, pp. 634 – 705.
- Rawe, A., 2000. Degradation of polymer. In: *Principle of polymer chemistry*. 2nd ed. New York: Kluwer Academic/Plenum Publishers, pp. 581 – 616.
- Robert, L., Hastie, Jr. and Morris, D.H., 1993. The effects of physical aging on the creep response of a thermoplastic composite. In: Harris, C.H. and Gates, T.S. (eds.). *High temperature and environmental effects on polymeric composites*, Volume 1. Virginia: American society for testing and materials International, pp. 163 – 186.
- Roland, C.M., 2009. Vagaries of elastomer service life predictions. *Plastic, Rubber and Composites*, 38(8), pp. 349 – 354.
- Rosu, D., Rosu, L. and Cascaval, C.N., 2009. IR-change and yellowing of polyurethane as a result of UV irradiation. *Polymer Degradation and Stability*, 94, pp. 591 – 596.
- Routh A.F. and Keddie J., 2010. An introduction to latex and the principle of colloidal stability. In: *Fundamentals of latex film formation: Processes and properties*. New York: Springer, pp. 1 – 26.
- Schaefer, R.J., 2002. Mechanical properties of rubber. In: Harris C.M. and Piersol A.G. (eds.). *Harris' shock and vibration handbook: Mechanical properties of rubber*. 5th ed. New York: McGraw-Hill, pp. 1108.
- Scheirs, J., 2000. Problems related to additives in polymers. In: *Composition and failure analysis of polymers: a practical approach*. New York: Johns Wiley & Sons Inc, pp. 482 – 517.

- Scheirs, J., 2009. Specialty geomembranes and liners. In: *A guide to polymeric geomembranes: A practical approach*. West Sussex: John Wiley & Sons Ltd., pp. 173 – 175.
- Shah, V., 2002. Plastic testing. In: Kutz, M. (ed.). In: *Handbook of materials selection*. New York: John Wiley & Sons Inc., pp. 545 – 590.
- Simpson, R., 2002. Rubber. In: *Rubber basics*. Shrewsbury, GBR: Smithers Rapra, pp. 77.
- Singh, B. and Sharma, N., 2008. Mechanistic implications of plastic degradation. *Polymer Degradation and Stability*, 93, pp. 561 – 584.
- Skypala, I. and Venter, C., 2009. Management of allergic disease. In: *Food hypersensitivity : Diagnosing and managing food allergies and intolerance*. Hoboken, NJ, USA: Wiley-Blackwell, pp. 326.
- Slobodian, P., 2010. Synthesis of vinyl polymer/carbon nanotube nanocomposites prepared by suspension polymerization and their properties. In: Mittal, V. (ed.). *Polymer nanotube nanocomposites: Synthesis, properties, and applications*. New Jersey: John Wiley & Sons Inc., pp. 225.
- Speight, J.G., 2010. Monomers, polymers, and plastics. In: *Handbook of industrial hydrocarbon processes*. Burlington: Gulf Professional Publishing, pp. 499 – 538.
- Sperling, L.H., 2006. Introduction to polymer science. In: *Introduction to physical polymer science*. 4th ed. New Jersey: John Wiley & Sons Inc., pp. 10 – 14.
- Starnes, W.H., 2002. Structural and mechanistic aspects of the thermal degradation of poly(vinyl chloride). *Progress in Polymer Science*, 27(10), pp. 2133 – 2170.
- Stein, R.S., Krogh, L.C., Soga, D.Y., Brinker, C.J., Dill, K.A., Grubbs, R.H., Karger, E.J., Krause, S., Mark, J.E., McCall, D.W., McGrath, J.E., Paul, D.R., Petrie, S.E., Tirrell, D.A. and Willson, C.G., 1994. Manufacturing: materials and processing. In: *Polymer science and engineering: the shifting research frontiers*. Washington: National Academies, pp. 65 – 115.
- Tung Ha- Anh, 2007. *Influence of thermo-oxidative aging on the mechanical behaviours of polychloroprene*. Thesis of Doctorate Degree, University Sherbrooke (Quebec), Canada.
- Wei, X.W., Guo, G., Gong, C.Y., Guo, M.L. and Qian, Z.Y., 2011. Biodegradable polymer: research and application. In: Sharma, S. K. and Mudhoo, A. (eds.). *A handbook of applied biopolymer technology: Synthesis, degradation and application*. Cambridge: Royal Society of Chemistry, pp. 365 – 387.

- White, J.L., 1995. Natural and Synthetic Rubber. In: *Rubber processing: Technology- materials- principles*. United Kingdom: Carl Hanser Verlag, pp. 3 – 12.
- White, J.R., 2006. Polymer ageing: Physics, chemistry or engineering? Time to reflect. *Comptes Rendus Chimie*, 9(11), pp. 1396 – 1408.
- White, J.L. and Kim, K.J., 2008. Multicomponent compounds. In: *Thermoplastic and rubber compounds: Technology and physical chemistry*. München, Germany :Hanser Verlag, pp. 222.
- White, J.R. and De, S.K., 2001. Natural Rubber. In: *Rubber technologist's handbook*. Illustrated. Shawbury, Shrewsbury and Shropshire: iSmithers Rapra Technology, pp. 1 – 39.
- Wicks, Z.W., Jones, F.N., Pappas, S.P. and Wicks, D.A., 2007. Latexes. In: *Organic coatings: science and technology*, 3rd ed. Weinheim, Germany: John Wiley & Sons Inc., pp. 176.
- Williams, P.T. and Bagri, R., 2003. Hydrocarbon gases and oils from the recycling of polystyrene waste by catalytic pyrolysis. *International Journal of Energy Research*, 28(1), pp. 31 – 44.
- Wirth, H.O. and Andreas, H., 1977. The stabilization of pvc against heat and light. *Pure and Applied Chemistry*, 49, pp. 62 – 648.
- Wise, J., Gillen, K.T. and Clough, R.L., 1995. An ultrasensitive technique for testing the Arrhenius extrapolation assumption for thermally aged elastomers. *Polymer Degradation and Stability*, 49, pp. 403 – 418.
- Woo, C.S. and Park, H.S., 2011. Useful lifetime prediction of rubber component. *Engineering Failure Analysis*, 18(7), pp. 1645 – 1651.
- Wolf, H. and Wol, R., 2009. Genesis. In: *Rubber: A story of glory and greed*. Shrewsbury, Shropshire, GBR: Smithers Rapra, pp. 9.
- Woodard and Curran Inc., 2006. Wastes from industries (case studies). In: *Industrial waste treatment handbook*. 2nd ed. Burlington: Butterworth-Heinemann, pp. 460.
- Yamada-Onodera, K., Mukumoto, H., Katsuyaya, Y., Saiganji, A. and Tani, Y., 2001. Degradation of polyethylene by a fungus, *Penicillium simplicissimum* YK. *Polymer Degradation and Stability*, 72, pp. 323 – 327.
- Yahya, Y. S. R., Azura, A. R. and Ahmad, Z. (2011). Effect of curing system on thermal degradation behaviour of natural rubber (SMR CV 60). *Journal of Physical Science*, 22, 1-14.

Yoshioka, T. and Grause, G., 2008. Hydrolysis of polyesters and polycarbonates. In: Moeller, H.W. (ed.). *Progress in polymer degradation and stability research*. New York: Nova Science Publishers Inc, pp. 1 – 32.

Zhang, S.W., 2004. Introduction. In: *Tribology of elastomers*. Volume 47. Amsterdam: Elsevier, pp. 1 – 5.

Zuev, V.V., Bertini, F. and Audisio, G., 2006. Investigation on the thermal degradation of acrylic polymers with fluorinated side-chains. *Polymer Degradation and Stability*, 91(3), pp. 512 – 516.

Appendix A

Accelerated ageing

Table: Mechanical properties of sample under accelerated ageing at 60 °C.

Ageing Time	Tensile	Max Force	Elong at Max	Stress at Break	Force at Break	Elongation	Thickness	Width
Day	MPa	N	%	MPa	N	%	mm	mm
0	31.75	16.64	399.3	31.74	16.64	399.4	0.087	6
7	31.50	16.41	395.1	31.48	16.41	395.2	0.087	6
14	31.93	16.65	379.2	31.83	16.60	379.6	0.087	6
21	32.87	16.93	379.2	32.85	16.92	379.3	0.086	6
42	34.79	18.30	372.0	34.76	18.28	372.1	0.088	6
56	34.58	17.92	370.4	34.56	17.91	370.6	0.086	6
70	35.62	18.38	362.4	35.58	18.35	362.6	0.086	6
105	33.37	17.79	353.8	33.34	17.77	353.9	0.089	6
140	31.86	17.13	342.8	31.86	17.13	342.8	0.090	6

Table: Mechanical properties of sample under accelerated ageing at 70 °C.

Ageing Time	Tensile	Max Force	Elong at Max	Stress at Break	Force at Break	Elongation	Thickness	Width
Day	MPa	N	%	MPa	N	%	mm	mm
0	28.57	15.72	351.4	28.56	15.72	351.4	0.092	6
2	25.77	15.51	353.9	25.77	15.51	353.9	0.100	6
7	25.44	14.88	350.5	25.44	14.88	350.5	0.098	6
14	27.27	15.67	343.5	27.27	15.67	343.5	0.096	6
28	27.86	16.16	329.0	27.86	16.16	329.0	0.097	6
42	25.50	15.36	328.0	25.50	15.36	328.0	0.100	6
70	23.82	14.19	323.6	23.78	14.16	323.7	0.099	6
98	22.93	13.33	328.6	22.93	13.33	328.6	0.097	6
126	22.87	13.08	324.5	22.86	13.07	324.6	0.095	6

Table: Mechanical properties of sample under accelerated ageing at 80 °C.

Ageing Time	Tensile	Max Force	Elong at Max	Stress at Break	Force at Break	Elongation	Thick	Width
Day	MPa	N	%	MPa	N	%	mm	mm
0	30.28	16.22	375.1	30.27	16.22	375.1	0.089	6
0.167	30.45	16.39	364.0	30.44	16.38	364	0.090	6
0.333	30.17	15.99	363.3	30.14	15.98	363.4	0.089	6
2	30.73	15.95	357.8	30.72	15.95	357.9	0.086	6
7	31.19	16.63	353.7	31.16	16.61	353.9	0.089	6
14	33.26	17.78	356.2	33.17	17.73	356.7	0.089	6
28	31.97	17.01	353.7	31.96	17.01	353.7	0.089	6
42	26.74	15.59	355.0	26.74	15.58	355.0	0.097	6
56	21.64	11.74	348.6	21.63	11.73	348.7	0.090	6
70	19.80	11.40	342.7	19.77	11.38	342.8	0.096	6

Table: Mechanical properties of sample under accelerated ageing at 90 °C.

Ageing Time	Tensile	Max Force	Elong at Max	Stress at Break	Force at Break	Elongation	Thick	Width
Day	MPa	N	%	MPa	N	%	mm	mm
0	26.40	15.16	347.7	26.38	15.15	347.8	0.096	6
0.021	25.91	14.85	351.2	25.91	14.84	351.3	0.096	6
0.083	29.47	16.34	354.0	29.46	16.33	354.1	0.093	6
0.167	27.32	15.49	348.4	27.31	15.48	348.5	0.095	6
0.333	25.82	15.13	342.4	25.82	15.13	342.4	0.098	6
1	23.97	14.45	340.7	23.96	14.44	340.7	0.101	6
7	24.78	14.76	332.2	24.77	14.76	332.2	0.099	6
14	26.29	15.40	327.5	26.28	15.39	327.6	0.098	6
21	22.27	13.30	323.2	22.27	13.30	323.2	0.100	6

Table: Mechanical properties of sample under accelerated ageing at 100 °C.

Ageing Time	Tensile	Max Force	Elong at Max	Stress at Break	Force at Break	Elongation	Thick	Width
Day	MPa	N	%	MPa	N	%	mm	mm
0	34.16	17.90	363.8	34.14	17.89	363.9	0.087	6
0.021	34.60	18.14	363.1	34.58	18.12	363.1	0.087	6
0.042	35.06	18.06	356.9	35.06	18.06	357.0	0.086	6
0.083	35.43	18.48	358.6	35.10	18.31	358.7	0.087	6
0.167	33.47	17.16	349.2	33.43	17.14	349.3	0.086	6
0.333	35.67	18.29	348.0	35.64	18.27	348.2	0.086	6
1	37.13	19.31	349.2	37.13	19.31	349.2	0.087	6
2	38.11	19.88	344.5	38.09	19.87	344.6	0.087	6
4	37.88	20.32	342.6	37.47	20.11	342.7	0.089	6
7	36.13	19.09	339.8	35.94	18.99	340.0	0.088	6

Table: Linear swell properties of sample under accelerated ageing at various temperatures.

Ageing Time (days)	Diameter (cm)				
	Temperature (°C)				
	60	70	80	90	100
0	45.00	45.00	45.00	45.00	45.00
0.021	-	-	-	43.50	43.50
0.042	-	-	-	-	44.00
0.083	-	-	-	43.00	42.50
0.167	-	-	44.00	42.50	42.00
0.333	-	-	44.00	42.50	42.00
1	-	-	-	42.00	40.50
2	-	43.50	43.00	-	40.50
4	-	-	-	-	40.50
7	44.50	43.00	42.50	41.00	40.00
14	42.00	42.00	42.00	40.50	-
21	42.00	-	-	41.00	-
28	-	42.00	41.50	-	-
42	42.00	41.00	42.00	-	-
56	41.00	-	41.00	-	-
70	40.00	40.00	40.50	-	-
98	-	40.00	-	-	-
105	40.50	-	-	-	-
126	-	-	-	-	-
140	40.0	-	-	-	-

Table: Colour properties of sample under accelerated ageing at various temperatures.

Ageing Time (days)	Total colour change (ΔE)				
	Temperature($^{\circ}$ C)				
	60	70	80	90	100
0	0	0	0	0	0
0.021	-	-	-	0.413	0.917
0.042	-	-	-	-	1.078
0.083	-	-	-	0.592	0.355
0.167	-	-	0.890	0.364	6.377
0.333	-	-	1.230	0.220	15.870
1	-	-	-	1.370	4.862
2	-	1.206	1.35	-	12.428
4	-	-	-	-	32.267
7	1.093	0.806	2.419	5.383	33.877
14	0.885	1.955	3.598	10.016	-
21	1.315	-	-	10.836	-
28	-	3.076	6.043	-	-
42	2.268	5.622	11.787	-	-
56	2.806	-	13.102	-	-
70	3.645	7.917	16.860	-	-
98	-	10.779	-	-	-
105	4.882	-	-	-	-
126	-	11.456	-	-	-
140	6.085	-	-	-	-

Appendix B

Real time ageing

Table: Mechanical properties of sample under fluorescent light

Ageing Time	Tensile	Max Force	Elong at Max	Stress at Break	Force at Break	Elongation	Thickness	Width
Day	MPa	N	%	MPa	N	%	mm	mm
0	33.33	16.88	397.2	33.32	16.87	397.3	0.084	6
1	34.84	17.71	406	34.66	17.63	406.3	0.085	6
2	33.62	17.66	397.3	33.56	17.62	397.6	0.088	6
3	34.25	17.79	375.4	34.17	17.75	375.6	0.087	6
6	32.75	17.08	367.7	32.72	17.06	367.8	0.087	6
9	30.44	15.67	359.3	30.43	15.67	359.3	0.086	6
12	29.19	15.78	360.3	29.18	15.78	360.3	0.090	6
15	27.22	15.19	361.1	27.22	15.19	361.1	0.093	6

Table: Mechanical properties of sample under dark condition

Ageing Time	Tensile	Max Force	Elong at Max	Stress at Break	Force at Break	Elongation	Thickness	Width
Day	MPa	N	%	MPa	N	%	mm	mm
0	30.52	15.75	396.7	30.32	15.64	396.9	0.086	6
1	29.85	15.54	402.3	29.85	15.54	402.3	0.087	6
2	31.12	16.16	387.9	30.94	16.07	388.5	0.087	6
3	33.02	17.32	365.6	33.01	17.31	365.7	0.087	6
6	30.92	16.93	341	30.92	16.93	341	0.091	6
9	29.45	15.89	354.4	29.45	15.89	354.4	0.090	6
12	28.78	15.19	348.3	28.76	15.18	348.3	0.088	6
15	27.26	15.01	343.7	27.26	15.01	343.7	0.092	6

Table: Linear swell properties of sample under real time ageing.

Ageing Time (months)	Diameter (cm)	
	Under fluorescent light	Under dark condition
0	45.00	45.00
1	43.00	43.00
2	43.00	43.00
3	42.00	42.00
6	42.00	42.00
9	42.00	42.00
12	41.50	41.00
15	41.50	41.50

Table: Colour properties of sample under real time ageing.

Ageing Time (months)	Diameter (cm)	
	Under fluorescent light	Under dark condition
0	0	0
1	0.772	0.639
2	0.986	0.547
3	0.865	0.398
6	1.282	0.622
9	0.779	0.925
12	1.032	0.696
15	0.406	0.628

Appendix C

Lifetime prediction

Table: Retained force at break of the samples after accelerated ageing at various temperature.

Ageing Time (days)	Retained force at break (N)				
	Temperature (°C)				
	60	70	80	90	100
0	16.52	15.66	15.98	14.88	17.92
0.021	-	-	-	14.75	18.04
0.042	-	-	-	-	17.94
0.083	-	-	-	16.14	17.80
0.167	-	-	16.54	15.44	17.28
0.333	-	-	15.80	15.24	18.36
1	-	-	-	14.49	19.48
2	-	15.64	15.68	-	19.74
4	-	-	-	-	20.08
7	16.18	14.96	16.76	15.06	18.72
14	16.66	15.74	17.76	15.14	-
21	17.16	-	-	13.25	-
28	-	16.18	16.84	-	-
42	17.96	15.36	15.44	-	-
56	17.64	-	11.56	-	-
70	18.54	14.25	11.55	-	-
98	-	13.32	-	-	-
105	17.92	-	-	-	-
126	-	13.2	-	-	-
140	17.14	-	-	-	-